UNIVERSIDAD COMPLUTENSE DE MADRID
FACULTAD DE FARMACIA

TESIS DOCTORAL

Nuevos tratamientos de infecciones protésicas: Micropartículas e implantes impresos 3D personalizados

New treatments for Prosthetic Infections: Microparticles and personalised 3D printed Implants

MEMORIA PARA OPTAR AL GRADO DE DOCTOR

PRESENTADA POR

Francis Cristina Luciano De León

DIRIGIDA POR

María de la Paloma Ballesteros Papantonakis
Dolores Remedios Serrano López
Pablo Sanz Ruiz

Madrid

UNIVERSIDAD COMPLUTENSE DE MADRID

FACULTAD DE FARMACIA

TESIS DOCTORAL

Nuevos tratamientos de infecciones protésicas:
Micropartículas e implantes impresos 3D personalizados

New treatments for Prosthetic Infections:
Microparticles and personalised 3D printed Implants

MEMORIA PARA OPTAR AL GRADO DE DOCTOR

PRESENTADA POR

Francis Cristina Luciano De León

DIRECTORES

María de la Paloma Ballesteros Papantonakis
Dolores Remedios Serrano López
Pablo Sanz Ruiz

UNIVERSIDAD COMPLUTENSE DE MADRID

FACULTAD DE FARMACIA

TESIS DOCTORAL

Nuevos tratamientos de infecciones protésicas:
Micropartículas e implantes impresos 3D personalizados

New treatments for Prosthetic Infections:
Microparticles and personalized 3D printed Implants

MEMORIA PARA OPTAR AL GRADO DE DOCTOR, DOCTORADO EN FARMACIA D9BI

PRESENTADA POR

Francis Cristina Luciano De León

DIRECTORES

María de la Paloma Ballesteros Papantonakis
Dolores Remedios Serrano López
Pablo Sanz Ruiz

Madrid, 2025

Cuando pase lo nublado contaremos las estrellas…

Agradecimientos

Quiero dar las gracias a Dios por su infinita bondad conmigo, por haberme permitido llegar hasta aquí y que gracias a su amor esta tesis es posible. Gracias a mis directores de tesis Paloma por ser como una madre, Pablo por toda su ayuda y dirección, a Loli por ser el ángel que llegó en este camino y me ayudo a recorrerlo, por acompañarme en cada momento y en creer en mi por encima de todo.

Agradezco al Departamento de Farmacia Galénica y Tecnología Alimentaria, a cada uno de sus profesores y al resto del personal por su ayuda. También quiero agradecer su ayuda y apoyo a la Dra. Carmina Rodríguez Fernández, del Departamento de Microbiología y Parasitología, y la Dra. Almudena Ribed Sánchez, del Hospital Gregorio Marañón de Madrid, cuyo conocimiento y trabajo han sido fundamentales para el desarrollo de este trabajo. Al Dr. Luca Cassetari y a la Università degli Urbino Carlo Bo, por la realización de mi estancia, colaborando a que esta tesis doctoral sea mención internacional y ampliar mis conocimientos. GRACIAS MIL a Maca por toda su paciencia en cada uno de los trámites, con el mismo buen humor y disposición.

Gracias a mi familia, mami gracias por ser una madre 5x5 por creer en mí, por hacerme la mujer que soy y no permitir que desmaye en mis sueños, esta tesis es tuya y gracias a ti, A mi tía Tury por ser mi segunda madre, mi bastón, mi soporte, por recordarme lo fuerte que soy y que hay que luchar por lo que se quiere siempre hasta el final y a Chanchi por darme su admiración y amor, a Daniel mi ahijado porque ser un ejemplo para ti me ha impulsado a ser mejor. Gracias papi por tus risas y tu entusiasmo, por mostrarme con orgullo como tu niña estrella. Mi hermana Alba por decirme en los momentos más duros ¨voy a ti¨. Gracias a mis hermanos, a mis tías y tíos, por estar ahí honrados de mí desde la distancia.

Gracias a mi compañero fiel y entregado de tesis Ivan (Graciaaaaas Ivan) sin tí no habría sido posible, gracias por tu paciencia, dedicación y complicidad. A mis partners incondicionales Brayan, Zaid, Gracia, Amadeo, chicos ustedes saben todo lo que significan para mí, gracias por estar y por haberme ayudado a ser. A todo mi team del labo Bianca, Irving, Baris, Aytug por las risas, los cafés y los amigos invisibles. A Anaís por haber sido más que una amiga, convertirse en familia, por las charlas interminables y los abrazos en los días duros.

A Ariana por convertirse en mi hermana de la vida, acompañarme con certeza y celebrar cada uno de mis logros como si fuesen de ella. A doña Susi por adoptarme, llenarme de

consejos (comida y vino jajaj) y darme el calor de una madre en los días fríos. A Andrea por recibirme desde el primer día como si fuese su hija y mantenerse con el mismo amor y el apoyo hasta hoy. Rosa Alba, Francis varón y Marlen mis hermanos de la vida porque han sido mi aliento de positividad y de entereza cuando sentí flaquear. Gerlin, Alberto y Adrián por ser mi familia granadina y confiar siempre en mí.

Grazie mille a mi mafia rubia Rita e Irene adoro le mie ponteti bionde anche al mio favorito il più bellissimo Marco. A los que llegaron por poco tiempo en el labo pero se quedaron con un lugar especial en mi corazón Iliana, Chrisy, Andreina, Narella, Rebeca, Greta, Felipe.

Grazie alla mia famiglia di Urbino per avermi fatto sentire parte di voi, aiutandomi e rendendomi magico il soggiorno, Matti, Giorgia, Sofi, Francesca ¨un bicchiere de vino con un panino la felicitá¨.

To my Falling Walls Lab family, for all the support, good vibes and love you guys shared with me, one of the best experiences on my thesis was this amazing opportunity and you. You guys rock!!

A todos mis amigos de RD en Madrid y los que aún siguen allá, que, aunque están lejos se hacen sentir cerca, gracias por hacerme entender lo alto que he llegado y la fuerza que me ha dado para poner mi país en alto. Eva y Francis Gómez dos seres de luz, especiales y a los que agradezco el estar aquí.

Gracias al Ministerio de Educación Superior Ciencia y Tecnología de la República Dominicana, por concederme la beca para iniciar mis estudios de doctorado.

Finalmente, las gracias más especiales, a quién le dedico esta tesis, mi trabajo de todo este tiempo, a mi abuelo ¨Don Negro¨ que me está esperando desde que me fui y quién me enseñó que ¨Cuando pase lo nublado contaremos las estrellas¨.

I want to thank God for his infinite goodness to me, for having allowed me to get this far and that thanks to his love this thesis is possible. Thanks to my thesis directors Paloma for being like a mother, Pablo for all his help and guidance, Loli for being the angel that came along this path and helped me to walk it, for accompanying me at every moment and for believing in me above all.

I thank the Department of Galenical Pharmacy and Food Technology, each of its professors and the rest of the staff for their help. I would also like to thank Dr. Carmina Rodríguez Fernández, from the Department of Microbiology and Parasitology, and Dr. Almudena Ribed Sánchez, from the Hospital Gregorio Marañón in Madrid, whose knowledge and work have been fundamental for the development of this work, for their help and support. To Dr. Luca Cassetari and the Università degli Urbino Carlo Bo, for the realization of my stay, collaborating to make this doctoral thesis an international mention and to broaden my knowledge.

Thanks to my family, mommy thanks for being a 5x5 mother for believing in me, for making me the woman I am and not allowing me to faint in my dreams, this thesis is yours and thanks to you, To my you Tury for being my second mother, my cane, my support, for reminding me how strong I am and that you have to fight for what you want always until the end and to Chanchi for giving me your admiration and love, to Daniel my godson because being an example for you has pushed me to be better. Thank you daddy for your laughter and enthusiasm, for proudly showing me as your star child. My sister Alba for telling me in the hardest moments ¨I come to you¨. Thanks to my siblings, my aunts and uncles, for being there honoring me from a distance.

Thanks to my faithful and dedicated thesis partner Ivan (Graciaaaaas Ivan) without you it would not have been possible, thanks for your patience, dedication and complicity. To my unconditional partners Brayan, Zaid, Gracia, Amadeo, you guys know how much you mean to me, thank you for being there and for helping me to be. To all my labo team Bianca, Irving, Baris, Aytug for the laughs, the coffees and the invisible friends. To Anaís for being more than a friend, for becoming family, for the endless talks and hugs on hard days.

To Ariana for becoming my sister in life, accompanying me with certainty and celebrating each of my achievements as if they were hers. To Doña Susi for adopting me, filling me with advice (food and wine hahahah) and giving me the warmth of a mother on cold days.

To Andrea for receiving me from the first day as if I were her daughter and for maintaining the same love and support until today. To Rosa Alba, Francis and Marlen, my brothers and sisters in life because they have been my encouragement of positivity and strength when I felt like I was weakening. Gerlin, Alberto and Adrián for being my Grenadian family and always trusting me.

Thank you very much to mi mafia rubia Rita and Irene I adore my blonde pontets also to my favorite the most beautiful Marco. A los que llegaron por poco tiempo en el labo pero se quedaron con un lugar especial en mi corazón Andreina, Iliana, Chrisy, Narella, Rebeca, Greta,Felipe.

Thank you to my family in Urbino for making me feel part of you, helping me and making my stay magical, Matti, Giorgia, Sofi, Francesca ¨un bicchiere de vino con un panino la felicitá¨.

To my Falling Walls Lab family, for all the support, good vibes and love you guys shared with me, one of the best experiences on my thesis was this amazing opportunity and you. You guys rock!

To my friends from the DR in Madrid and those who are still there, who, although so far away, feel close, thank you for making me understand how high I have come and the strength you have given me to put my country on high.

Thanks to the Ministry of Higher Education, Science and Technology of the Dominican Republic, for granting me the scholarship to start my doctoral studies.

Finally, the most special thanks, to whom I dedicate this thesis, my work of all this time, to my grandfather ¨Don Negro¨ who has been waiting for me since I left and who taught me that ¨When the clouds pass we will count the stars¨.

Índice

Resumen/ Summary

Resumen

En la actualidad, las cirugías de prótesis articulares o artroplastias aumentan cada vez más y conllevan un alto riesgo de infecciones, también conocidas como PJI (*periprosthetic joint infections*) causadas por las bacterias propias de la piel del paciente o las del medio quirúrgico, adhiriéndose a los componentes de la prótesis y formando una comunidad microbiana llamada *biofilm*, desencadenando infecciones que llevan a dolor, pérdida de la movilidad e incluso la muerte del paciente, traduciéndose en un alto coste para el sistema de salud. Actualmente la solución más utilizada, es someter al paciente a un nuevo procedimiento quirúrgico, retirar la prótesis infectada y sustituirla por un cemento óseo cargado con antibiótico durante varias semanas y luego una nueva intervención para colocar una nueva prótesis. No obstante, la liberación de antibióticos a partir del cemento óseo resulta insuficiente, y su uso puede comprometer las propiedades biomecánicas de la articulación. Además, tanto este enfoque como otros tratamientos convencionales carecen de eficacia frente a la totalidad de los patógenos responsables de las infecciones protésicas articulares. En respuesta a esta limitación, se están desarrollando nuevos enfoques terapéuticos para el manejo de las PJIs. Sin embargo, debido a que estas estrategias aún se encuentran en etapas preliminares de investigación, su aplicación clínica no es previsible en un futuro inmediato. Una alternativa a esta problemática seria crear soluciones para prevenir las PJI en lugar de tratar la prótesis infectada, utilizando tecnologías como la microencapsulación o la impresión 3D para desarrollar formulaciones y sistemas que actúen directamente sobre la prótesis evitando la formación del biofilm y consecuentemente la infección. De esta manera, se podrían prevenir todas las consecuencias que traen las PJI, sobretodo nuevas cirugías y el coste sanitario que implican las soluciones actuales.

La tecnología de microencapsulación es una alternativa prometedora ya que podrían desarrollarse formulaciones con principios activos de naturaleza compleja y /o la combinación de fármacos para elaborar otras formas farmacéuticas y siendo una gran opción en la industria farmacéutica para su producción a gran escala. Por otra parte, la impresión 3D como tecnología cada vez toma más auge en medicina y desarrollo de sistemas farmacéuticos; ya existen distintos tipos de implantes en 3D para la administración de fármacos por vía parenteral. Basado~~s~~ en esto, el objetivo principal de

este trabajo ha sido formular, desarrollar y caracterizar unas micropartículas, que formen un gel bioadhesivo, cargadas con agentes antimicrobianos que liberen los principios activos y puedan prevenir o tratar la infección en las artroplastias de cadera y, por otro lado, con la impresión 3D diseñar, desarrollar y optimizar unos implantes impresos en 3D con los antimicrobianos con la misma finalidad. Ambas formulaciones, para su aplicación in situ en el momento de la cirugía de reemplazo articular.

Las micropartículas fueron obtenidas mediante la técnica de spray-drying o secado por atomización, utilizando la anfotericina B (AmB) como antifúngico y la vancomicina como antibiótico de amplio espectro, encapsulando cada fármaco por separado y otra formulación con la combinación de ambos, utilizando Eudragit, Soluplus y Kollicoat IR como excipientes, para el control de su liberación y coadyuvantes para su solubilidad en la formula. Finalmente se mezclan con ácido hialurónico y H_2O para formar el gel bioadhesivo, mostrando una rápida adhesión y secado, y extendiéndose con facilidad por toda la superficie de la prótesis. Las micropartículas exhibieron un perfil de liberación dual, combinando una fase inicial inmediata con una liberación sostenida a lo largo del tiempo. La dosis máxima de principios activos incorporada en las micropartículas no generó toxicidad hemolítica, no obstante, mostraron un efecto antibacteriano y antifúngico significativo frente a diversas especies de *Staphylococcus spp. y Candida spp.*, que son las principales causantes de las infecciones protésicas. Otro punto importante para destacar es que las formulaciones fueron estables en las condiciones de almacenamiento con presencia de humedad y temperatura manteniendo un 90% de su actividad al menos durante los primeros 100 días. Las formulaciones tanto con los principios activos por separado como en combinación mostraron una capacidad protectora con menor toxicidad para las líneas celulares utilizadas hFOB 1.19, Saos-2 y BJ, que los fármacos sin encapsular.

Por otra parte, en esta tesis doctoral los implantes en 3D han sido impresos mediante la técnica de modelo por deposición fundida (FDM), basada en la extrusión directa de pellets formulados con una combinación de los polímeros EVA (etil-vinil acetato) y PEG (polieltilenglicol), utilizando la anfotericina B (AmB) como antifúngico. Previo a la extrusión de pellets de EVA-PEG, la AmB se impregnó en la superficie de estos. La red impresa en 3D mostró un efecto antifúngico significativo frente a *C. albicans*, aunque menor en otras especies de *Candidas spp.*

Summary

Currently, joint replacement surgeries, or arthroplasties, are becoming increasingly common, but they are associated with a high risk of infection, resulting in periprosthetic joint infections (PJIs). These infections are typically caused by bacteria from the patient's skin or the surgical environment, which can adhere to the prosthetic components and form a microbial community called biofilm. This can trigger infections that result in pain, loss of mobility, and even death, translating into a significant economic burden for healthcare systems. The most used solution involves a new surgery to remove the infected prosthesis, replacing it temporarily with antibiotic-loaded bone cement for several weeks, followed by a second procedure to implant a new prosthesis. However, antibiotic release from bone cement is often insufficient, and its use can compromise the biomechanical properties of the joint. Additionally, this approach, like other conventional treatments, is ineffective against all pathogens responsible for PJIs. In response to this limitation, new therapeutic approaches are being developed to manage PJIs, though these strategies are still in the early stages of research and are unlikely to be clinically available soon.

An alternative to this problem would be to develop preventive solutions for PJIs rather than treating infections afterwards. Technologies such as microencapsulation and 3D printing could be used to create formulations that act directly on the area where microorganisms adhere, preventing biofilm formation and, subsequently, infection. This approach could prevent the complications associated with PJIs, particularly the need for additional surgeries and the financial burden imposed by current treatments.

Microencapsulation technology is a promising alternative, as it enables the development of formulations with complex active ingredients and/or drug combinations, allowing for the manufacture of various pharmaceutical forms, making it a viable option for large-scale production in the pharmaceutical industry. Additionally, 3D printing technology is gaining traction in medicine and the development of pharmaceutical systems, with different types of 3D-printed implants already available for parenteral drug delivery. Based on this, the main objective of this work was to formulate, develop, and characterize microparticles capable of forming a bioadhesive gel loaded with antimicrobial agents that release active ingredients to prevent or treat infections in hip arthroplasties. Furthermore, 3D printing was used to design, develop, and optimize implants loaded with antimicrobials for the same purpose. Both formulations are intended for *in situ* application

during joint replacement surgery.

Microparticles were obtained using spray-drying technique, with amphotericin B (AmB) as an antifungal agent and vancomycin as a broad-spectrum antibiotic. Each drug was encapsulated separately, and another formulation combined both, using Eudragit RL100, Soluplus, and Kollicoat IR as excipients to control release and enhance solubility. The final formulation was mixed with hyaluronic acid and water to create a bioadhesive gel, which demonstrated rapid adhesion, quick drying, and easy spreading over the prosthesis surface. The microparticles exhibited a dual release profile, combining an immediate release phase with sustained release over time. The maximum dose of active ingredients incorporated into microparticles did not cause hemolytic toxicity but showed significant antibacterial and antifungal activity against various species of *Staphylococcus spp.* and *Candida spp.,* the main pathogens responsible for prosthetic infections. Another important point is that the formulations remained stable under storage conditions with humidity and temperature, retaining 90% stability for at least the first 100 days.Both formulations, whether with separate active ingredients or in combination, exhibited protective capacity for cell viability, with lower toxicity for the cell lines hFOB 1.19, Saos-2, and BJ compared to the unencapsulated drugs.

In addition, in this doctoral thesis, 3D-printed implants were produced using fused deposition modeling (FDM), with direct extrusion of pellets formulated from a combination of the polymers EVA (ethyl-vinyl acetate) and PEG (polyethylene glycol) loaded with amphotericin B (AmB) as an antifungal agent. The drug was incorporated through direct adhesion of the solid drug to the pellets. These implants demonstrated significant antifungal activity against *C. albicans,* though to a lesser extent against other *Candida spp.* species.

Introducción

La introducción de esta Tesis Doctoral está estructurada en el formato de una publicación de tipo revisión, con el objetivo de proporcionar un marco teórico sólido y actualizado sobre el principal tema que conforma la investigación. Esta sección, pretende sintetizar y analizar los avances más relevantes en el área de estudio, estableciendo las bases conceptuales que sustentan el desarrollo de este trabajo.

Las infecciones articulares periprotésicas o periprosthetic joint infections (PJI), son un tipo de infección distintiva en el área clínica y diferente de las infecciones que involucran hueso u articulaciones nativas. Esta condición se caracteriza por la interacción entre la respuesta inmunitaria del huésped y diversos agentes patógenos, entre ellos predominando las bacterias, pero ocasionalmente microorganismos fúngicos forman parte de esta. La principal problemática de este tipo de infecciones es que los microorganismos son capaces de adherirse y agruparse formando una biopelícula o biofilm alrededor de la superficie de los componentes de las prótesis. Estas biopelículas tienen una alta capacidad de resistencia a los recursos terapéuticos convencionales y a las propias defensas del organismo [1-3]. Desafortunadamente la carga de microorganismos patógenos que se requiere para la formación de esta biopelícula es muy baja, incluso menor que la de una infección de articulación nativa, por ello pueden producirse con mucha facilidad [4].

Las infecciones articulares periprotésicas representan un desafío clínico significativo, ya que contribuyen de manera considerable al aumento de la morbilidad y mortalidad asociadas a los procedimientos de artroplastia. Incluso, han desplazado al desgaste del polietileno o las luxaciones de los implantes como la principal indicación para realizar artroplastias de revisión, subrayando su impacto crítico en el manejo y la evolución de los pacientes sometidos a estas [5, 6]. Las PJIs están causadas por microorganismos propios de la piel o del medio quirúrgico, principalmente *Staphylococcus aureus*, y/u hongos, siendo los más comunes *Candida spp*. Estos patógenos en el momento del procedimiento quirúrgico son capaces de atravesar al medio interno y adherirse a las prótesis articulares formando posteriormente la biopelícula [7-9].

Existen comorbilidades que representan factores de riesgo para que se produzcan las infecciones periprotésicas como el consumo de tabaco, obesidad, desnutrición, consumo excesivo de alcohol, entre otros. Existen otros factores no modificables relacionados con

la cirugía, incluyendo el tiempo del procedimiento quirúrgico prolongado cuando se extiende más de 90 minutos, la posible complicación del procedimiento en sí y los postoperatorios [10]. En la actualidad, la incidencia de las PJIs en países desarrollados es de entre 1-4%, aumentando en países en vía de desarrollo hasta más del 30% [6, 11-15].

Estas infecciones obligan a la realización de procedimientos quirúrgicos adicionales, prolongan los periodos de hospitalización y aumentan el riesgo de desarrollar complicaciones secundarias, lo que agrava aún más el pronóstico clínico y la carga socioeconómica de la enfermedad. Se estima que el incremento del coste sanitario puede llegar al 300% para los tratamientos asociados a las PJIs suponiendo un impacto considerable para la calidad de vida del paciente, ya que dentro de sus posibles consecuencias pueden encontrarse dolor, pérdida de la función física de la extremidad e incluso la muerte [16].

La terapéutica convencional para las infecciones periprotésicas se basa en la combinación de fármacos antibióticos e intervenciones quirúrgicas; no obstante, cada tratamiento debe ser personalizado de acuerdo con las condiciones del paciente. En los procedimientos que conllevan cirugía se retira la biopelícula manualmente o bien se realiza una revisión protésica, la cual puede llevarse a cabo en uno o dos tiempos. En el método de revisión en dos tiempos, que es el más común, se procede a retirar la prótesis infectada y se implanta un espaciador temporal elaborado con cemento óseo de polimetilmetacrilato impregnado con antibióticos. Posteriormente, tras un período de varias semanas, se reemplaza el espaciador por una nueva prótesis definitiva [15, 17, 18].

No obstante, la liberación de antibióticos desde los cementos óseos utilizados en los tratamientos no siempre es suficiente para prevenir de manera efectiva la formación de biopelículas en las superficies protésicas y tiene el riesgo de que los microorganismos generen resistencias. Las biopelículas, debido a su alta resistencia a los agentes antimicrobianos, pueden persistir y facilitar la reinfección; sobre la superficie de los cementos óseos complicando significativamente el tratamiento. Además, el uso de espaciadores de cemento cargados con antibióticos puede estar asociado a la aparición de otras complicaciones clínicas, entre las que destaca la dislocación de la articulación tratada. Este problema no solo agrava el estado del paciente, sino que también puede

requerir intervenciones adicionales para corregir el daño y restablecer la funcionalidad articular, aumentando aún más los riesgos y los costes sobre el sistema de salud [19-23].

La elevada incidencia de las PJIs, combinada con las alarmantes tasas de mortalidad asociadas a los tratamientos actuales, que pueden alcanzar hasta un 40% tras la revisión quirúrgica en dos tiempos, subraya la urgencia de avanzar en la investigación y desarrollo de nuevas alternativas terapéuticas. Esta necesidad se vuelve aún más crítica considerando el impacto negativo que estas infecciones tienen tanto en la calidad de vida de los pacientes como en los recursos de los sistemas de salud a nivel global [6].

En la actualidad, se están explorando estrategias innovadoras para el tratamiento de las infecciones articulares periprotésicas, entre las que se incluyen el empleo de anticuerpos monoclonales, hidrogeles, nanopartículas con antibióticos, nanotubos de titanio implantes en 3D y otras terapias. Estas aproximaciones prometen abordar las limitaciones de los tratamientos convencionales, como la eliminación ineficaz de biopelículas o la resistencia microbiana. Sin embargo, la mayoría de estas estrategias aún se encuentran en etapas iniciales de desarrollo, principalmente en fases preclínicas, lo que implica un largo tiempo para su aprobación regulatoria y su aplicación clínica [24-32].

En la **publicación 1** se describe con más detalle la prevalencia de las infecciones periprotésicas, comorbilidades, costes para el sistema sanitario, las terapias convencionales y las soluciones innovadoras que se están desarrollando en la actualidad.

Referencias

1. Wagenaar, F.B.M., et al., Persistent Wound Drainage After Total Joint Arthroplasty: A Narrative Review. J Arthroplasty, 2019. 34(1): p. 175-182.
2. Beam, E. and D. Osmon, Prosthetic Joint Infection Update. Infect Dis Clin North Am, 2018. 32(4): p. 843-859.
3. Nair, R., M.L. Schweizer, and N. Singh, Septic Arthritis and Prosthetic Joint Infections in Older Adults. Infect Dis Clin North Am, 2017. 31(4): p. 715-729.
4. Premkumar, A., et al., Periprosthetic Joint Infection in Patients with Inflammatory Joint Disease: Prevention and Diagnosis. Curr Rheumatol Rep, 2018. 20(11): p. 68.
5. Tai, D.B.G., et al., Microbiology of hip and knee periprosthetic joint infections: a database study. Clin Microbiol Infect, 2022. 28(2): p. 255-259.
6. Izakovicova, P., O. Borens, and A. Trampuz, Periprosthetic joint infection: current concepts and outlook. EFORT Open Rev, 2019. 4(7): p. 482-494.
7. Li, C., N. Renz, and A. Trampuz, Management of Periprosthetic Joint Infection. Hip Pelvis, 2018. 30(3): p. 138-146.
8. Chisari, E., et al., Fungal periprosthetic joint infection: Rare but challenging problem. Chin J Traumatol, 2022. 25(2): p. 63-66.
9. Lu, J., et al., Infection after total knee arthroplasty and its gold standard surgical treatment: Spacers used in two-stage revision arthroplasty. Intractable Rare Dis Res, 2017. 6(4): p. 256-261.
10. Christensen, D.D., et al., Perioperative Antibiotic Prophylaxis: Single and 24-Hour Antibiotic Dosages are Equally Effective at Preventing Periprosthetic Joint Infection in Total Joint Arthroplasty. J Arthroplasty, 2021. 36(7s): p. S308-s313.
11. McNally, M., et al., The EBJIS definition of periprosthetic joint infection. Bone Joint J, 2021. 103-b(1): p. 18-25.
12. Blanco, J.F., et al., Risk factors for periprosthetic joint infection after total knee arthroplasty. Arch Orthop Trauma Surg, 2020. 140(2): p. 239-245.
13. Premkumar, A., et al., Projected Economic Burden of Periprosthetic Joint Infection of the Hip and Knee in the United States. J Arthroplasty, 2021. 36(5): p. 1484-1489.e3.
14. Hossain, F., S. Patel, and F.S. Haddad, Midterm assessment of causes and results of revision total knee arthroplasty. Clin Orthop Relat Res, 2010. 468(5): p. 1221-8.

15. Koh, I.J., et al., Causes, risk factors, and trends in failures after TKA in Korea over the past 5 years: a multicenter study. Clin Orthop Relat Res, 2014. 472(1): p. 316-26.
16. Tansey, R., et al., Definition of Periprosthetic Hip and Knee Joint Infections and the Economic Burden. Open Orthop J, 2016. 10: p. 662-668.
17. Natsuhara, K.M., et al., Mortality During Total Hip Periprosthetic Joint Infection. J Arthroplasty, 2019. 34(7s): p. S337-s342.
18. Xu, C., et al., Is Treatment of Periprosthetic Joint Infection Improving Over Time? J Arthroplasty, 2020. 35(6): p. 1696-1702.e1.
19. Edelstein, A.I., et al., Nephrotoxicity After the Treatment of Periprosthetic Joint Infection With Antibiotic-Loaded Cement Spacers. J Arthroplasty, 2018. 33(7): p. 2225-2229.
20. Chaudhry, Y.P., et al., Acute kidney injury in the context of staged revision arthroplasty and the use of antibiotic-laden cement spacers: a systematic review. J Orthop Surg Res, 2023. 18(1): p. 340.
21. Nelson, C.L., et al., Sonication of antibiotic spacers predicts failure during two-stage revision for prosthetic knee and hip infections. Clin Orthop Relat Res, 2014. 472(7): p. 2208-14.
22. Schmolders, J., et al., Evidence of MRSE on a gentamicin and vancomycin impregnated polymethyl-methacrylate (PMMA) bone cement spacer after two-stage exchange arthroplasty due to periprosthetic joint infection of the knee. BMC Infect Dis, 2014. 14: p. 144.
23. Anagnostakos, K., O. Fürst, and J. Kelm, Antibiotic-impregnated PMMA hip spacers: Current status. Acta Orthop, 2006. 77(4): p. 628-37.
24. Yang, Y., et al., Monoclonal Antibody Targeting Staphylococcus aureus Surface Protein A (SasA) Protect Against Staphylococcus aureus Sepsis and Peritonitis in Mice. PLOS ONE, 2016. 11: p. e0149460.
25. Yuste, I., et al., Engineering 3D-Printed Advanced Healthcare Materials for Periprosthetic Joint Infections. 2023. 12(8): p. 1229.
26. Li, Y.J., et al., Synthesis of Self-Assembled Spermidine-Carbon Quantum Dots Effective against Multidrug-Resistant Bacteria. Adv Healthc Mater, 2016. 5(19): p. 2545-2554.
27. Kulshrestha, S., S. Qayyum, and A.U. Khan, Antibiofilm efficacy of green synthesized graphene oxide-silver nanocomposite using Lagerstroemia speciosa floral

extract: A comparative study on inhibition of gram-positive and gram-negative biofilms. Microb Pathog, 2017. 103: p. 167-177.

28. Getzlaf, M.A., et al., Multi-disciplinary antimicrobial strategies for improving orthopaedic implants to prevent prosthetic joint infections in hip and knee. J Orthop Res, 2016. 34(2): p. 177-86.

29. Sangeetha, K. and E.K. Girija, Tailor made alginate hydrogel for local infection prophylaxis in orthopedic applications. Mater Sci Eng C Mater Biol Appl, 2017. 78: p. 1046-1053.

30. Gulati, K., M.S. Aw, and D. Losic, Drug-eluting Ti wires with titania nanotube arrays for bone fixation and reduced bone infection. Nanoscale Research Letters, 2011. 6(1): p. 571.

31. Levack, A.E., et al., Current Options and Emerging Biomaterials for Periprosthetic Joint Infection. Curr Rheumatol Rep, 2018. 20(6): p. 33.

32. Bácskay, I., et al., The Evolution of the 3D-Printed Drug Delivery Systems: A Review. Pharmaceutics, 2022. 14(7).

PUBLICACIÓN 1:

Understanding periprosthetic joint infections: prevalence, treatment, prophylaxis and novel agents

F.C. Luciano, I. Yuste, B. J. Anaya, P. Sanz-Ruiz, A. Ribed, M.P. Ballesteros, D.R. Serrano

Pendiente de publicación

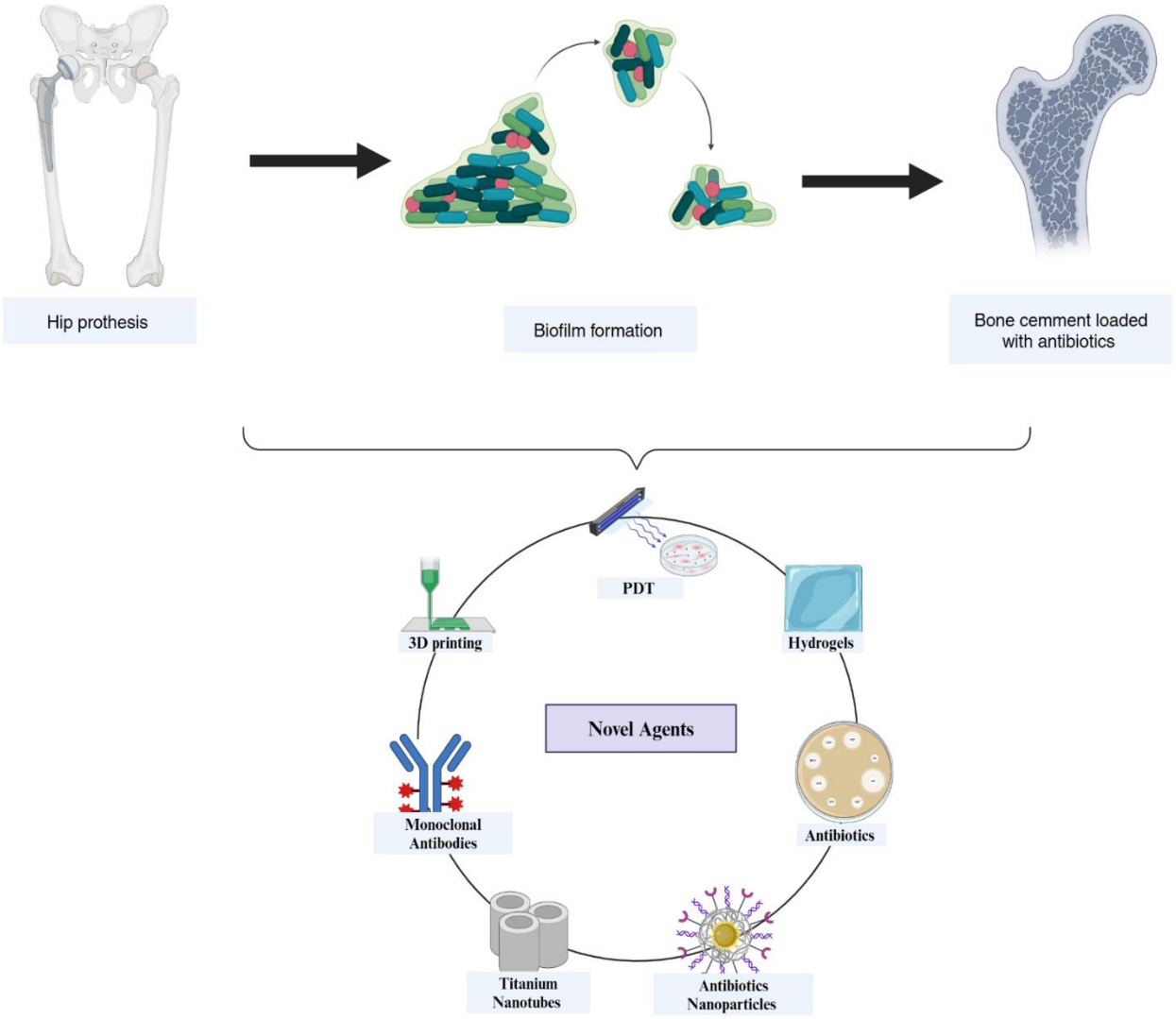

Abstract

Periprosthetic joint infections (PJIs) are a significant and increasingly prevalent complication following hip or knee arthroplasty, with an estimated prevalence ranging from 1% to 4% of patients undergoing these procedures. This incidence has been rising steadily over time. The primary etiological factor contributing to PJIs is the formation of biofilm around the prosthetic components. Biofilms represent a major challenge as they confer protection on bacteria, making infections difficult to treat with standard antimicrobial therapies. This issue imposes a substantial burden on healthcare systems, both in terms of economic cost and increased patient morbidity and mortality, with mortality rates reaching up to 30%. Currently, there is no definitive treatment that completely addresses both the prevention and eradication of biofilm-related infections. However, numerous novel therapeutic strategies are under development to combat PJIs. These include a combination of surgical intervention, antimicrobial treatments, and the use of modified prosthetic surfaces with antimicrobial properties to reduce biofilm formation. Effective management of PJIs requires a personalized approach, tailored to each patient's specific condition. An ideal treatment would utilize biodegradable and biocompatible components, thereby minimizing the need for repeat surgeries and mitigating the risk of microbial resistance. Although these innovative treatments have demonstrated promising results in preclinical studies, further *in vivo* research and clinical trials are necessary for their successful translation from the laboratory to clinical practice. This review aims to provide a comprehensive overview of the current strategies, challenges, and future directions in the prevention and treatment of PJIs.

Keywords:

Prothesis, arthroplasty, PJIs, infections, antimicrobial, biofilm,

1. Prevalence of periprosthetic joint infections (PJI) and economic burden

Orthopedic surgical procedures often involve the placement of a foreign body, such as a prosthetic joint, joint components, or other parts to stabilize bone structures or repair fractures. Unfortunately, in knee and hip arthroplasties, the main unwanted consequences are infections and dislocations or loosening of the prosthesis that has been implanted. The infection can result either from direct contamination of the implanted device, by hematogenous spread of the patient's microorganisms, or from the surgical environment. Total hip and knee arthroplasty is a cost-effective intervention to decrease pain, improve motor function, and enhance a patient’s quality of life with degenerative or inflammatory hip and knee pathologies [1]. In total hip and knee arthroplasty, a damaged and painful joint is replaced by metallic components (such as chromium, cobalt, titanium, and oxylium), ceramics, and polyethylene. All these components are usually combined in different ways to extend the prosthesis's life, for example, by reducing friction between the different parts. (Fig. 1 y Fig.2)

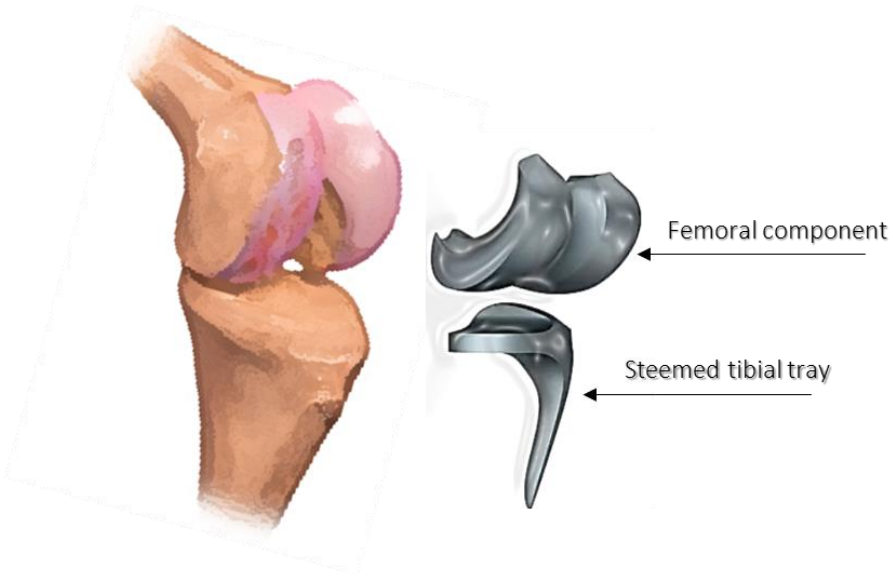

Fig. 1. Components of a knee replacement.

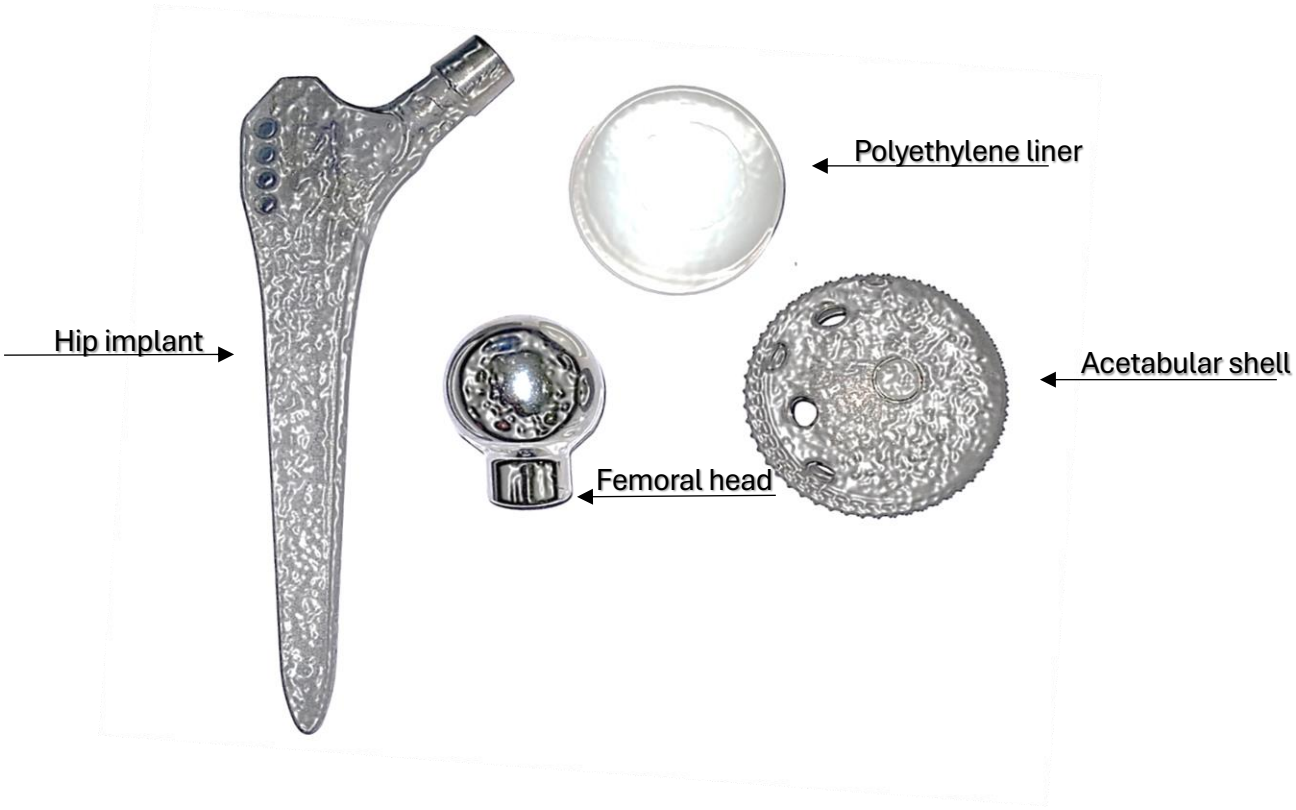

Fig.2. Components of a hip replacement.

The cost-effectiveness of hip and knee replacement surgeries is comparable to other types of procedures such as bypass or renal dialysis[2].

At an international level, the number of hip and knee replacements has also increased rapidly since 2000 in most OECD (Organization for Economic Co-operation and Development) countries. On average, the rate of hip replacement increased by 30% between 2000 and 2015 (166 operations over 100,000 population) while the rate of knee replacement nearly doubled (126 operations over 100,000 population), exhibiting Switzerland, Germany, Austria, and Belgium the highest rates for both of hip and knee replacement (> 250 surgeries/ 100.000 population) [3].

In Spain, the incidence of hip fractures is estimated at 40,000 to 45,000 per year, with an annual cost of 1,591 million € and a loss of quality-adjusted years of life of 7,218. Similar incidence is estimated for knee replacement surgery [4], which are both expected to rise shortly, especially among the population over 80 years [5]. PJIs following hip and knee replacements are an important complication causing major concern for patients, operating surgeons, and healthcare systems having a substantial economic impact [6]. Although its

incidence over the years has dwindled due to modern theater facilities and aseptic measures, currently, its prevalence varies from 1-4% in developed countries [7, 8] and can be much greater in developing countries (>30%) [9, 10].
Unfortunately, by 2011 in Spain, the infection rate for these surgeries hovers at 1.5% for the hip and 2.5% for the knee resulting in a significant economic cost, a drop in the quality of life of patients, and the risk of mortality that becomes up to 18% [2].
The cost associated with ARI involves direct costs both intrahospital (surgery, antibiotherapy.) and extra hospital costs (rehabilitation, pharmacy, follow-up of patients…) but also indirect costs such as low productivity and work absenteeism. It has been estimated that the overall cost of a hip replacement surgery without infection is 22.927€ [12.148-43.453€] while ARI can increase the cost up to 79.188€ [39.354-141.359€]. Even though there are major differences in the overall cost related to hip and knee replacement surgery, depending on the country and the health system, it can be considered that PJIs can increase the cost by 2-4 folds [4, 11].

Standard treatment of PJI is usually a two-stage process: i) the existing joint is removed and surrounding soft tissues are cleaned out and ii) an acrylic bone cement spacer loaded with antibiotics is placed to maintain normal joint space and alignment while the infection is treated. This procedure is followed by at least six weeks of intravenous antibiotics and the reimplantation of a new total joint arthroplasty later. Each time a joint replacement is removed, bone is lost, and tissues are damaged. Apart from the impact on patients' quality of life and prolonged antibiotic toxicity, the economic burden for public health systems is very high. For this reason, there is an important clinical need to minimize the risk of PJIs and to find solutions for treating adequately those produced. This review will discuss how PJI takes place and how it can be prevented and treated when it occurs.

Due to the high incidence of knee and hip osteoarthritis, and the cost of surgical procedures related to them, Western countries have found the need for cost-effectiveness studies of these interventions, both before and after surgery [12].

Some articles have been earmarked on the cost-effectiveness impact of hip and knee prostheses in the USA according to data for 2007 and 2005, around 515,400 knee replacements and 572,000 hips were performed respectively, it is estimated that by 2030 an increase in total hip replacement of 174% and in the case of knee around 16 million people needed this surgical procedure. Counting on this surgery to influence an estimated

$16 trillion in expenditure by 2007 [13].

According to a study by the Hospital Clinic San Pablo de Coquimbo in Chile, the approximate cost of a patient in an incident-free hip replacement is US$2,354 however, for patients with infection the cost is about US$6,174.8, without leaving aside the fact that it implies an increase in the stay of the patient admitted to the hospital in an average of 13 days to the patient with infection to 54 days the patient with infection. However, in addition to the increase in cost, it is worth mentioning the psychological, physical, economic, and social impact on the patient as well as on health entities, taking into account that the limb is at stake and even the life of the affected by the infection [2].

As we explained above the main cause of infection in hip replacement surgery is skin bacteria, however, the same surgical environment and bacteria that could release medical equipment are potential causes of a PJI. However, other factors could be predisposing the patient to a higher chance of developing a PJI. (Fig. 3) [14].

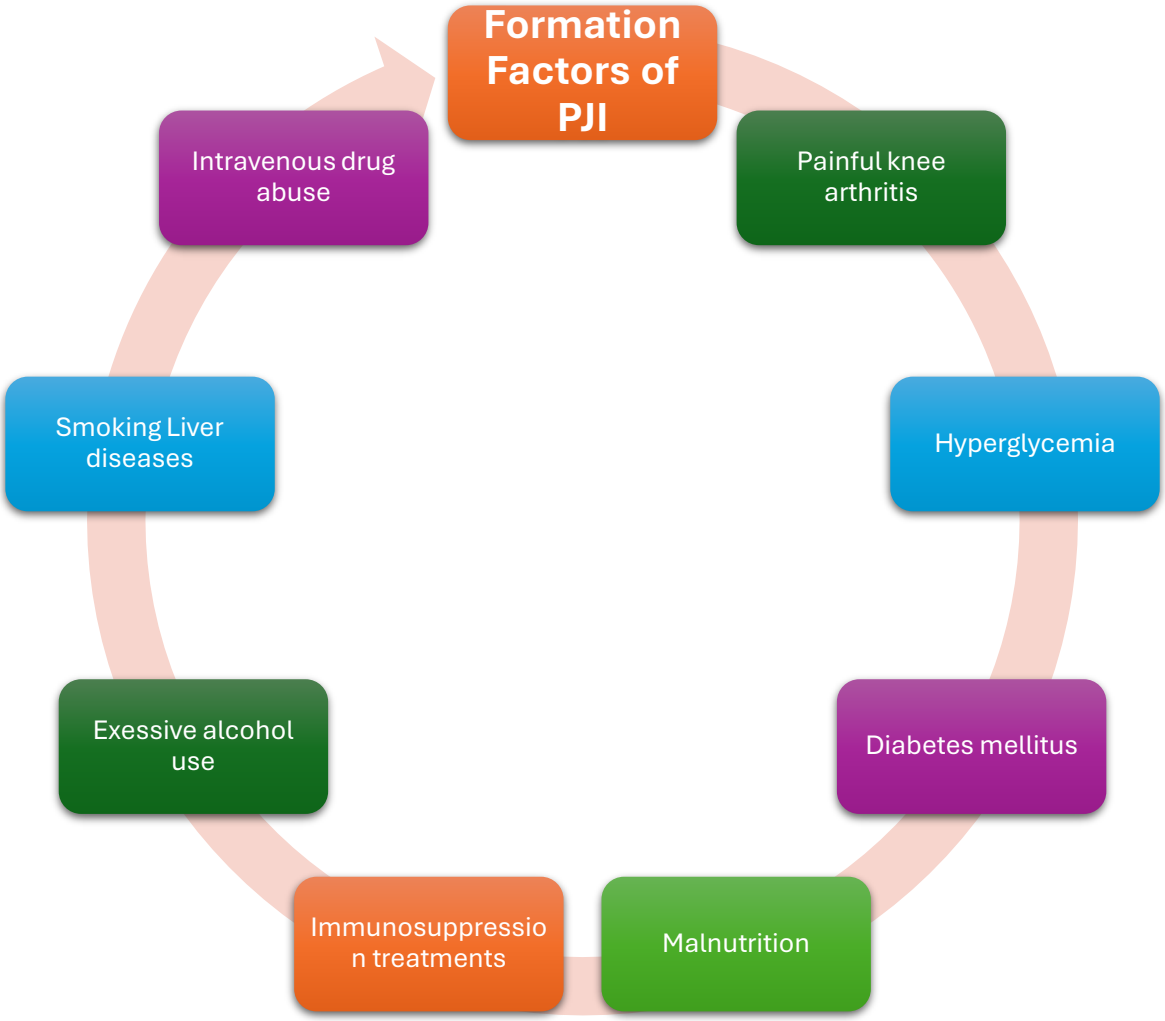

Fig.3 Formation factors of a PJI.

2. Biofilm formation associated with PJIs

It has been proved that bacterial biofilms appear on a bunch of infected implants, including prosthetic hip and knee joints and internal fixation devices, surrounding metal orthopedic prosthetics components [15]. Some study shows that bacteria such as *Pseudomonas aeruginosa, S. epidermis, and S. aureus* can easily produce biofilms on materials like stainless steel and titanium orthopedic screws [16].

During surgery, bacteria localized on the surface of the skin can penetrate and adhere to the surface of joint prosthesis forming a biofilm leading to a very difficult infection. A bacteria biofilm consists of a group of bacteria or microorganisms capable of adhering to a regularly inert or living surface, producing a matrix or layer also called *polymeric extracellular substance* that is composed of extracellular DNA, proteins, and polysaccharides, which is difficult to permeate, hampering the access of antibiotics and immune cells, and thus, being very difficult to treat [17].

Apart from the type of surface is an important feature in the formation of the biofilm and its fixation process, according to Characklis and col. They were able to identify an increase in the extent of microbial colonization as surface roughness increases because shear forces decrease and on rougher surfaces, the surface area is larger. Other important characteristics of the aqueous environment, such as nutrient levels, ion strength, pH, and temperature could influence the binding of bacteria to a surface [18].

Bacterial biofilms can be monomicrobial or polymicrobial, being able to have these latter sub-populations and respond differently to antibiotic agents, since these sub-populations even though they are of the same organism could have phenotypic and genotypically different characteristics. We could say, the biofilm formation cycle has three fundamental parts: adhesion (where bacteria adhere to the implant surface and compete with the individual's defense mechanisms), growth or maturation (where the attached bacteria replicate or divide), and the detachment or separation phase (the bacteria already mature, isolate them or in fragments of biofilm and colonize other surfaces) (Fig.4).

The formation of a biofilm begins when the bacteria adhere to the inert surface (in this case of the implant) and begin to produce the polymeric extracellular substance (Fig. 1). At this time, the bacteria are not fully protected, and antibiotics are more accessible to the region, and hence, an intravenous anti biotherapy can be successful without requiring implant removal. Wolcott et al. showed that biofilms can be effectively treated during the

first 24 h post-infection when bacteria are still sensitive to the action of antibacterial while after 48 hours, they became increasingly resistant to treatment. The reason behind this fact is that the biofilm begins to mature, making antibiotic access negligible [19].

When the biofilm is already mature can tolerate antibiotic agents at concentrations of 10-1000 times that needed to kill a normal bacterium and can be resistant to phagocytosis, making them very difficult to eliminate from their hosts. Unfortunately, surgical removal and replacement of the infected tissue or medical device is a frequent necessity when biofilms appear [20].

It is important to know, that over 65% of all human infections are biofilm-related (BRIs), in the U.S. these types of infections that go into surgery cost about $6 trillion annually. BRIs are of high impact in orthopedic replacement surgeries, because of the sequelae they leave in the bone, hip, and knee. As mentioned earlier in this review, due to the nature of the materials of joint replacement surgeries are highly susceptible to colonization and eventual formation of bacterial biofilm [21]

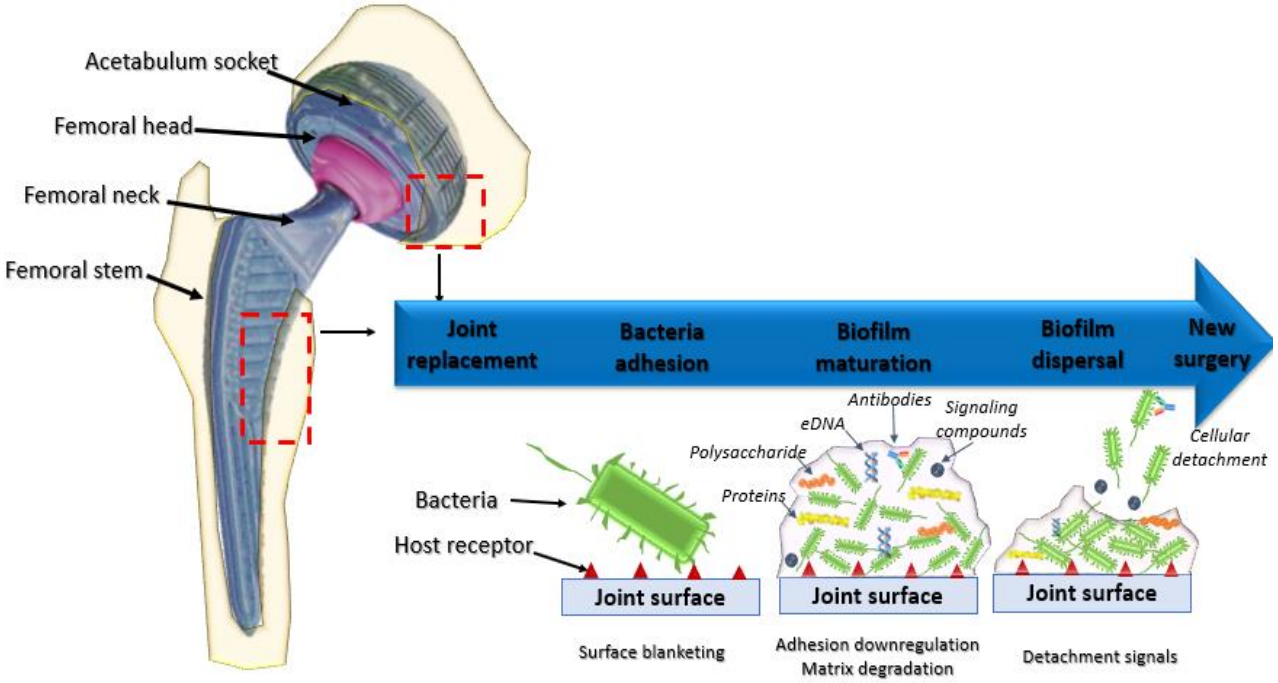

Fig 4. Biofilm formation

Hip arthroplasty infections are closely related to the formation or existence of bacterial biofilm. Infections are divided into biofilm-related infections and implant-related infections. The need of whether to remove the implant or not to treat the infection will be dependent on the presence or absence of a functional or mature bacterial biofilm [17]. Taking this into account and according to Tsukayama and Zimmerli [ref], PJIs can be classified into the following categories:

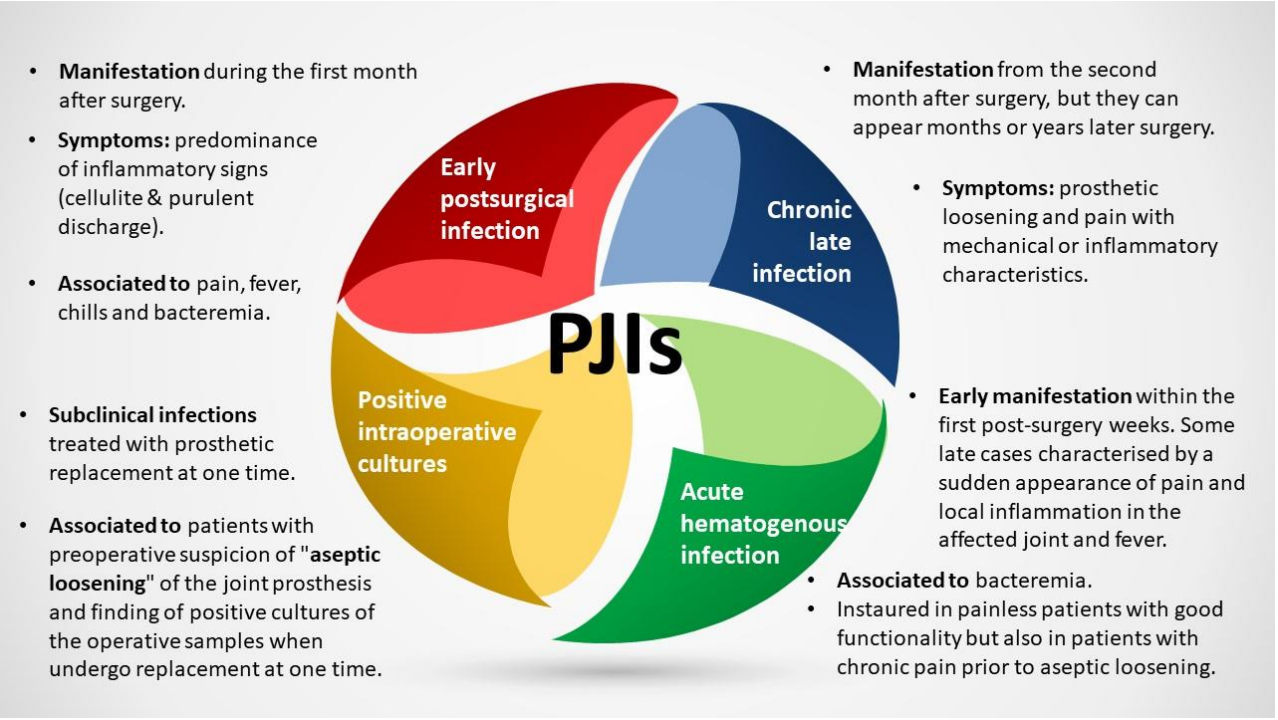

Fig. 5. PJI classification according *Tsuyama* et al [22, 23]

There is another classification of PJI according to Coventry et al, where the infections could be classified in three stages, based on the time they show the symptoms; within the first 30 days after the surgery (Type I); after the 30 days post-procedure (Type II) and, past 2 years or more after the surgical procedure (Type III). Table 2. [24-26].

Table 1. PJI classification according to *Coventry* et al [24-26].

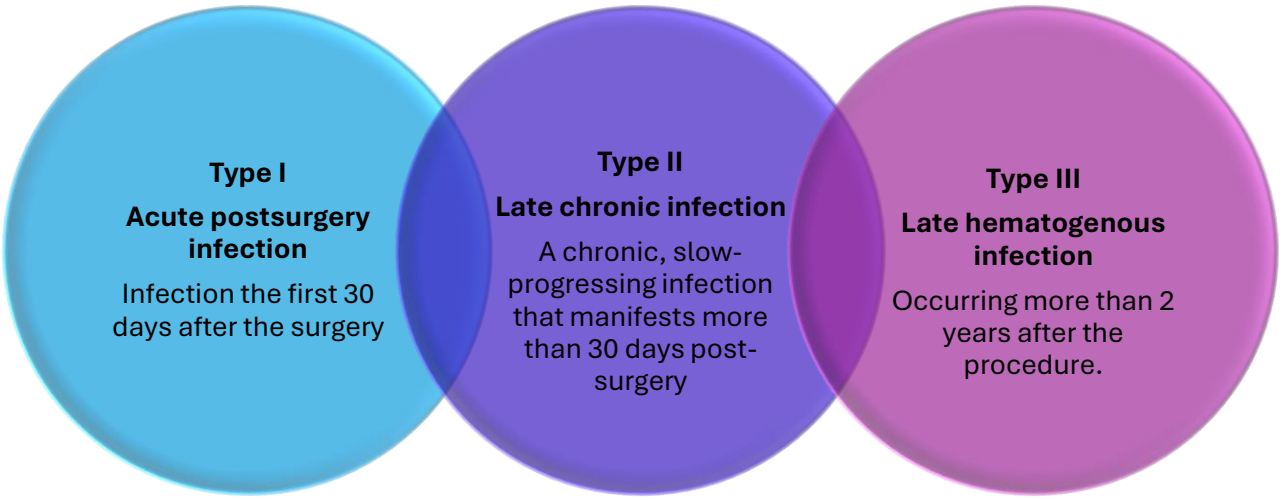

3. Treatments

The treatment for PJI would depend on the type of infection, the patient's state, the comorbidities related to it, and other factors. However, eradicating prosthetic joint infections requires both medical and surgical interventions, antibiotic therapies are essential in all cases and involve the administration of one or a combination of antimicrobial agents [27, 28]. The most common treatments will be described in the following sections.

3.1 Surgical treatment

PJI therapies aim to eliminate the infection and restore the joint function and, the quality of life of the patients, requiring a multidisciplinary team for the right treatment and, individualized solutions for each patient [29-32]. The prosthetic joint infection solutions can be separated into different options, the most used are the surgical therapy that could be: i) Debridement, antibiotic, and implant retention ii) One-stage implant replacement, and, iii) Two-stage implant replacement [33-36].

DAIR

Debridement, antibiotic, and implant retention are techniques used for the treatment of PJIs and could involve the removal of fibrous membranes, soft tissues, and even damaged bone [27, 37]. This technique is characterized by being less invasive and requiring less technical expertise, resulting in reduced morbidity, shorter hospital stays, improved preservation of bone stock, and a decreased economic impact; but, is limited, because it is appropriate only for select cases [38-40]. To keep the implant or not, depends on multiple factors including the ability to contain biofilm within a brief timeframe, the no immunocompromised patient or comorbidities attached and, the involvement of low virulence microorganisms [38, 41-44].

Two-stage implant replacement

The two-stage implant replacement method is considered so far, the most successful option for PJIs, named the ¨gold standard¨ treatment having approximately a 91% success rate against infections [45-51] consisting of removing all possible devitalized or infected tissue, membranes and, soft tissue and all the prothesis material and replacing with the stabilizer spacer for the joint and with a cement loaded with antibiotic [52]. However, the interval between the two stages, which can range from 6 weeks to several months, notably affects mobility and often leads to increased patient dependency. Additional significant adverse effects reported include the challenges of systemic antibiotic therapy, alterations in family dynamics, and a considerable psychological impact [53, 54]. The surgeons have many issues with this kind of technique such as the risk of bone loss, difficulties removing the cement with antibiotics, and the fact that requires more surgical procedures, increasing medical costs and perioperative morbidity [55-59].

One-stage implant replacement

One-stage revision surgery for prosthetic joint infection (PJI) was developed as an alternative to two-stage revision surgery for chronic PJI. It has been reported to achieve comparable rates of infection-free success to two-stage revision, while also demonstrating lower mortality and morbidity, reduced hospital stays, shorter durations of antibiotic treatment, and decreased overall healthcare costs [45, 60, 61]. The method involves the removal of all biofilm-infected tissues, followed by definitive reconstruction using antibiotic-loaded cement and antibiotic-loaded calcium sulfate hemihydrate pellets. In this case, the pellets can destroy the biofilm exposed to the surface [48]. The biofilm eradication rates of this method ranging between 67% to 100% [62-64]. However, the microbiological profile of the pathogen can influence the one-stage revision method also, poor local tissue and bone stock could be contraindications for this procedure [65].

There is a dilemma about which one is the best procedure between one or two-stage implant replacement techniques for PJI treatment. Klouche et al. did not show significant differences between the two procedures [66]. Other researchers like Zhao et al. and Lazic et al. found no differences between the stages in the reoperation and reinfection rates, and it will be taken into consideration the treatment, the patient, and PJIs associated factors [67, 68].

3.2 Local antibiotic therapies

The system used for local antibiotic release includes bone cement loaded with antibiotics called PMMA (polymethylmethacrylate) and others such as biodegradable sponges and beads. The principal aim of local antibiotic treatments is to achieve the highest drug concentration in a localized area, eradicating the pathogen microorganisms while minimizing or eliminating the antibiotic side effects on the rest of the organisms [69, 70]. Another local therapy for PJI is beads usually loaded with vancomycin, gentamycin, and tobramycin. Beads have a very high concentration of the drugs and effective release; however, there are significant challenges associated with the use of antibiotic-loaded beads. One of the main drawbacks is the need for an additional surgical procedure to remove the beads once they have released their antibiotic content. This requires another operation, which increases the overall burden on the patient, both in terms of recovery time and the risks inherent in any surgical procedure, such as infection, anesthesia complications, or damage to surrounding tissues. Furthermore, the beads themselves can

become a foreign body within the infected joint or surrounding tissues. This presents a risk, as foreign bodies can serve as a surface for the formation of biofilms, which are microbial communities that adhere to surfaces and are encased in a protective matrix. Biofilm formation can complicate the treatment of infection, as bacteria within biofilms are often more resistant to antibiotics and the immune system, making it difficult to completely eradicate the infection.[70-73].

Local continuous irrigation with a catheter or antibiotic pump is another option for localized treatment methods. Success rates with this technique have been reported between 18 and 85%. The primary advantage of this approach is the ability to adjust the antibiotic agent as necessary and facilitate intra-articular fluid drainage. Nevertheless, it imposes a significant burden on the patient, this treatment often requires the patient to manage an implanted device (such as a catheter or pump), which may be uncomfortable and carry risks of complications, such as catheter-related infections, mechanical failure, or discomfort associated with the continuous infusion [70, 74-77].

Another strategy based on the use of local antibiotics is the gentamicin-loaded collagen sponges which are biodegradable and do not require surgical removal. The mechanism consists of when the water is added the collagen rapidly expands, allowing a very fast release to the gentamicin achieving a high local concentration in the initial hours up to 40 hours. However, one of the disadvantages of this method is the prolonged and increased wound secretion [72, 78, 79].

One of "the gold standard solutions" is the bone cement spacer impregnated with high concentrations of antibiotics, inserted inside the articulation, replacing the prosthesis and allowing the drug release *in situ* on the target place after the surgical procedure. However, this method is very limited because the antibiotics released at convenient concentrations are only 24-48h after inserting the spacer [80-82]. Other issues have been reported, including the presence of bacterial biofilm on the cement surface during revision surgeries and the occurrence of renal injury [83-87]. Furthermore, due to the temporary nature of these cement spacers, which are intentionally designed with reduced structural stability to allow for subsequent removal, they have been linked to a higher incidence of complications, such as spacer fracture, fractures of the adjacent bone and joint dislocation [80, 88].

4. Novel Agents

Despite the advancements in current medical treatments, existing therapeutic strategies remain insufficient to provide an effective solution for the management of periprosthetic joint infections. In this work, we aim to explore innovative approaches that could offer improved solutions for both the prophylaxis and treatment of PJIs. These emerging strategies hold promise for addressing the challenges associated with the prevention and management of these complex and often debilitating infections, which continue to pose significant clinical challenges (Fig.5).

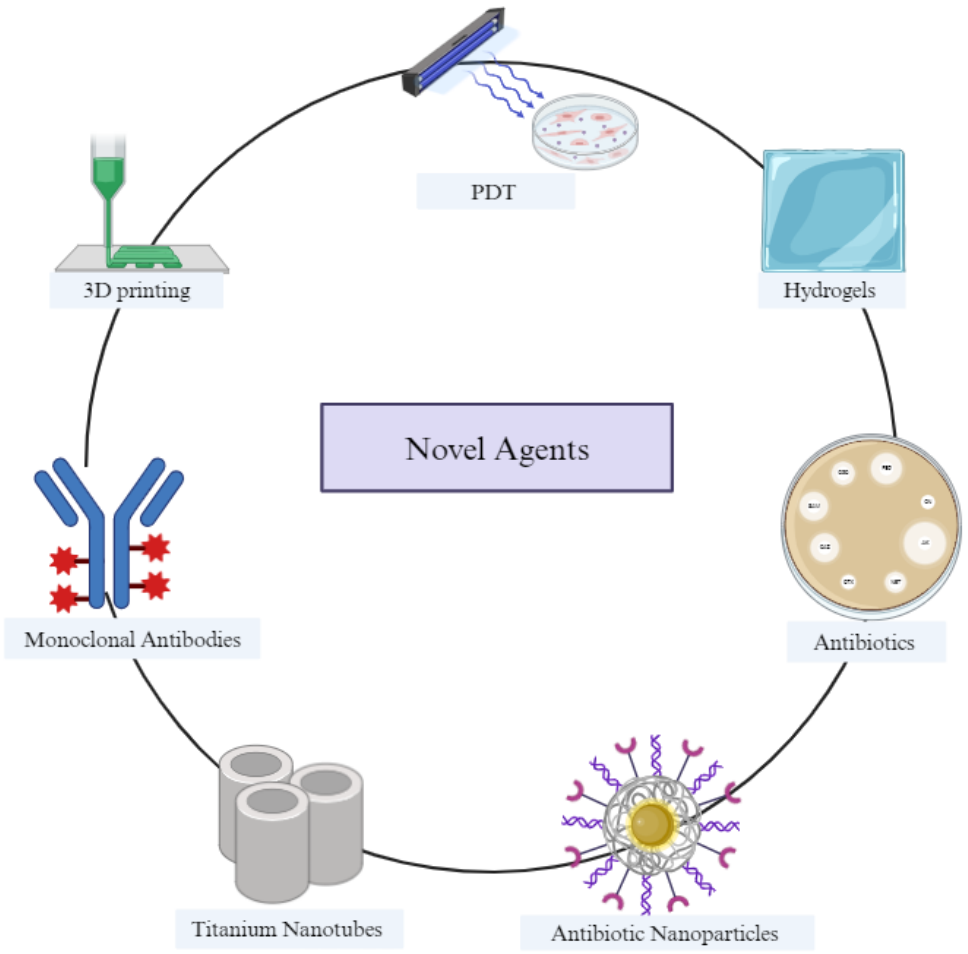

Fig 6. Novel Agents for PJI

Antibiotic Nanoparticles

Nanoparticles (NPs) can contribute to the generation and accumulation of reactive oxygen species (ROS), which disrupts the integrity of bacterial cell membranes. Several NPs have been demonstrated to have antibacterial properties because of their nature including zinc oxide, copper, silver, and quantum dots (which include a semiconductor material such as zinc or cadmium as a core). Furthermore, the nanoparticles can interact with the cell's walls interfering with the proteins involved in the cell's metabolism. As the NPs deliver a combination of antibacterial mechanisms, it becomes more difficult for bacterial cells to develop resistance against them [80, 89]. It has been reported different *in vitro* studies of the efficacy of NPs loaded with graphene oxide-silver composites, spermidine-carbon quantum dots, and silver against bacteria Gram-negative (e.g. *Pseudomonas aeruginosa*, *Klebsiella pneumoniae, Escherichia coli*) and Gram-positive (e.g. *Staphylococcus aureus, Streptococcus mutans*). The nanoparticles demonstrated high biocompatibility and low toxicity effects on the cells. However, it must be tested *in vivo* infection models [90-92]

Monoclonal Antibodies

Yang et al. developed an anti-SasA monoclonal antibody (2H7), which binds to a highly conserved region of SasA (*S. aureus* surface protein A) wich recognizes the adhesive matrix molecules (MSCRAMMs) and has been described as a target for mAbs (monoclonal antibodies). It has been evaluated its efficacy in a mouse model of sepsis induced by methicillin-resistant *Staphylococcus aureus* (MRSA). After 1-hour administration the antibody could protect the mice from 40% mortality, showing its potential therapeutical value. Another potential novel solution would be 5143G monoclonal antibody that targets the *S. aureus* cell wall component protein A (SpA). The latter has demonstrated successful *in vitro* opsonization of both methicillin-resistant Staphylococcus aureus (MRSA) and methicillin-sensitive *S. aureus* (MSSA), enhancing their clearance by immune cells. *In vivo*, intravenous administration of 514G3 effectively rescued mice with MRSA bacteremia, both when used alone and in combination with vancomycin, highlighting its potential as a therapeutic agent for bacterial infections [93, 94].

PDT

An innovative approach for treating PJIs is Photodynamic Therapy (PDT). This method utilizes phenothiazine dyes such as methylene blue and light. Upon exposure to light at a specific wavelength and in the presence of oxygen, the absorbed dye is activated, leading to the production of reactive oxygen species (ROS). These ROS cause damage to the bacterial plasma membrane and DNA, ultimately resulting in cell death. Studies demonstrated that this technique using methylene blue and laser can eradicate *MRSA*, *MSSA*, *S. epidermidis*, and *P. aeruginosa* mature biofilm grown on different titanium surfaces. The fast action and the low possibility of bacteria resistance make this method a promising strategy for treating prosthetic joint infections, particularly during revision surgery to sterilize the infected area following implant removal [95-97].

Hydrogels

One innovative option for PJI treatment is that some researchers developed implants coated with rapidly resorbable hydrogels that incorporate one or more antibiotics, facilitating localized drug delivery without interfering with osseointegration. These studies have compared hydroxyapatite and composed gelatin matrices and alginate-based hydrogels for drug delivery. The *in vitro* studies results have shown a sustained release of the drug for 5 hours in the composite matrix and 10 days in the alginate matrix. These hydrogel membranes not only offer extended drug release but also possess intrinsic antimicrobial properties, providing dual functionality for infection prevention and treatment [98, 99].

Antibiotics

A new line of antibiotics has been approved by the FDA such as dalbavancin and oritavancin both have action on Gram-positive bacteria. Dalbavancin is a semisynthetic lipoglycopeptide antibiotic with a prolonged half-life that functions by inhibiting bacterial cell wall synthesis. It can distribute and penetrate the joint tissues and bone. *In vitro* studies have demonstrated that dalbavancin retains antibiofilm activity against clinical isolates of *S. epidermidis* and *S. aureus* from prosthetic joint infections. Moreover, dalbavancin was effective in controlling the systemic dissemination of MRSA [100-103]. On the other hand, oritavancin has been shown to possess bactericidal activity against methicillin-sensitive *Staphylococcus aureus* (MSSA), methicillin-resistant *S.*

aureus (MRSA), vancomycin-resistant *S. aureus*, and methicillin-resistant coagulase-negative *Staphylococci*. Bone penetration and concentration of oritavancin were evaluated *in vivo* following intravenous administration. The results demonstrated that oritavancin was rapidly absorbed into the bones, maintaining stable concentrations for over 165 h [104-106]. Unfortunately, these antibiotics are only approved by the FDA for skin infections, but they could be a potential treatment for PJIs. However, the cost of the drugs might be a limitation, and yet it has been tested in more *in vivo* studies.

Titanium Nanotubes

Another innovative strategy to prevent periprosthetic joint infections (PJI) is local antibiotic delivery using nanotube arrays fabricated with titanium. Titanium alloys coated with nanotube arrays can provide sustained release of gentamicin for up to 11 days. Similarly, non-antibiotic antimicrobial peptides with broad-spectrum activity have also been released from titanium nanotubes for 7 days. While this technology shows promise for multi-drug delivery applications, further research is needed to assess its impact on osseointegration with titanium surfaces and to ensure that the nanotube arrays do not hinder the process of bone bonding to the implant [107, 108].

3D printing

The 3D printing technology could be a potential treatment for PJIs. The integration of this technology into drug delivery provides several benefits, including the creation of customized drug delivery systems such as implants with determined biocompatible raw materials, the design of intricate drug release profiles and geometries, with adaptable internal and external structures, as well as overcoming limitations associated with prolonged stability profiles. Currently, this technique is advancing in the development of individualized drug delivery systems (IDD, although none of the systems outlined have yet been implemented in clinical settings. Despite promising results from 3D-printed scaffolds and implants in the treatment of periprosthetic joint infections, however, *in vitro* and *in vivo* studies and clinical trials are necessary for approval by regulatory bodies such as the FDA and EMA [109-114].

5. Conclusions and Future perspective

Periprosthetic joint infections (PJI) remain a significant complication following joint replacement surgeries, contributing to increased patient morbidity, prolonged hospital stays, and substantial healthcare costs. These infections are particularly challenging to diagnose and treat due to the complex nature of the infection, which often involves microbial biofilms on the prosthetic surface, making bacteria less susceptible to both the immune system and antibiotics. Early identification is critical to prevent irreversible damage to the joint and surrounding tissues, and current diagnostic strategies rely on clinical evaluation, laboratory markers, microbiological cultures, and imaging. However, diagnosing PJI is still difficult due to the variability in clinical presentation and the lack of a single, definitive diagnostic test.

The treatment of PJI generally involves a combination of surgical and medical interventions. Surgical options include debridement with or without implant retention, one- or two-stage revision arthroplasty, or even complete removal of the infected prosthesis. The choice of surgical approach depends on factors like the severity of the infection, the infecting organism, and the patient's overall health. Antibiotic therapy is a critical component, often requiring prolonged courses of intravenous antibiotics followed by oral therapy, based on the organism's susceptibility. In more complex cases, prolonged antibiotic suppression or customized regimens may be necessary to control the infection, especially with resistant organisms like methicillin-resistant *Staphylococcus aureus* (MRSA) or *Pseudomonas aeruginosa*.

Despite these treatment strategies, PJI remains a leading cause of joint failure, particularly with the growing incidence of resistant pathogens and the challenges posed by chronic infections. In this context, ongoing advancements in medical research are crucial to improve PJI management. Future perspectives include the development of more advanced and rapid diagnostic techniques, such as PCR-based methods or the use of novel biomarkers, which could enable quicker identification of pathogens and more precise treatment. Additionally, there is a growing interest in exploring antimicrobial coatings for prosthetic devices, which could prevent biofilm formation and reduce the incidence of infections.

The use of personalized medicine, where treatment strategies are tailored to the patient's

specific infection profile and underlying conditions, is also likely to become a key aspect of future PJI management. Moreover, advances in immunomodulation therapies may offer new avenues to boost the patient's immune response, helping to combat infections more effectively.

In summary, while significant progress has been made in understanding and managing PJI, the condition remains a challenging issue. Ongoing research into better diagnostic methods, more effective antibiotics, novel surgical techniques, and preventative measures holds promise for improving patient outcomes and reducing the burden of this complication in joint replacement surgeries.

References

1. Pagès, E.I., J.; Cuxart, A. , *Artroplastia de cadera.* Sociedad Española de rehabilitación y Medicina Física, 2007. **41**: p. 280-289.
2. Garcia, E.G., *Evaluacion de estancia hospitalaria en protesis de cadera* in *Departamento de Ciencias Sanitarias y Medico-Sociales*. 2011, Universidad de Alcalá: España. p. 233.
3. *OECD "Hip and knee replacement", in Health at a Glance 2017: OECD Indicators, OECD Publishing, Paris. Retrieved the 7 March 2020 from: https://doi.org/10.1787/health_glance-2017-65-en.* 2017.
4. Franco, M., *Tesis doctoral: Epidemiología de la infección de prótesis articular en España en la última década. Análisis de la evolución de la etiología en el tiempo. Retrieved the 24 February from: file:///D:/FEB%202020/Caixa%20impulse/references/prevnalcecia%20de%20artroplastia%20de%20cadera%20en%20espama.pdf.* 2017.
5. *Registro nacional de fracturas decadera pro fragilidad. Retrieved the 24 February from: https://sogacot.org/wp-content/uploads/2018/05/INFORME_ANUAL_RNFC_2017.pdf.* 2017.
6. Tansey, R., et al., *Definition of Periprosthetic Hip and Knee Joint Infections and the Economic Burden.* Open Orthop J, 2016. **10**: p. 662-668.
7. Gupta, A., et al., *Multifunctional Nanohydroxyapatite-Promoted Toughened High-Molecular-Weight Stereocomplex Poly(lactic acid)-Based Bionanocomposite for Both 3D-Printed Orthopedic Implants and High-Temperature Engineering Applications.* ACS Omega, 2017. **2**(7): p. 4039-4052.
8. Garrote-Garrote, M., et al., *Antibioterapia profiláctica en la artroplastia de cadera. Estudio de cohortes.* Rev Esp Quimioter., 2018. **31**(2): p. 118-122.
9. Hossain, F., S. Patel, and F.S. Haddad, *Midterm Assessment of Causes and Results of Revision Total Knee Arthroplasty.* Clin Orthop Relat Res, 2010. **468**: p. 1221-1228.
10. Koh, I.J., et al., *Causes, Risk Factors, and Trends in Failures After TKA in Korea Over the Past 5 Years: A Multicenter Study.* Clin Orthop Relat Res, 2014. **472**: p. 316-326.
11. Kapadia, B.H., et al., *The Economic Impact of Periprosthetic Infections After Total Hip Arthroplasty at a Specialized Tertiary-Care Center.* J Arthroplasty, 2016. **31**(7): p. 1422-6.

12. Herrera-Espiñeira Carmen, E.A., Navarro-Espigares Jose Luis, Luna del Castillo Juan de Dios, Garcia-Perez Lidia, Godoy-Montijano Amparo *Prótesis total de rodilla y cadera: variables asociadas al costo.* Cir Cir 2013. **81**: p. 207-213.
13. Carlos Rabago, C.A.W., María Florencia Marengo,Julia Martínez, Mario Menón, Bruno Ivernizzi, Pedro Abatte, Maximiliano Zuliani, German Augusto Caputo, Juan Ignacio Chamorro, Néstor Fabián Pugliese, Nicolás Pietropaolo, Fernando Eberle, *Eficacia y costo-utilidad de primer reemplazo total de cadera y rodilla en pacientes con osteoartritis.* Revista Argentina de Reumatologia 2017. **28**(4): p. 9-17.
14. González, A.D., *Infección en prótesis total de rodilla: Factores de riesgo, relación con el recambio patelar*. 2022, Universidad de Burgos.
15. Rabih o. Darouiche, A.D., Andrew J. Miller, and I.I.R. Glenn C. Landon, and Daniel M. Musher, *Vancomycin Penetration into Biofilm Covering Infected Prostheses and Effect on*

Bacteria. The Journal of Infectious Diseases, 1994. **170**(3): p. 720-3.
16. Zhijun Song, L.B., Niels Høiby, Hong Wu,Torben Sandberg Sørensen, Arne Borgwardt, *Prosthesis infections after orthopedic joint replacement: the possible role of bacterial biofilms.* Page Press, 2013. **5**(14): p. 65-71.
17. P., C.P.-C., *Diagnóstico microbiologico en las infecciones peripótesicas de cadera y rodilla: Implicaciones en el tratamiento quirúrgico de las prótesis infectadas.*, in *Departamento de cirugía*. 2015, Universidad Autonoma de Barcelona: Barcelona, España. p. 150.
18. RM., D., *Biofilms: microbial life on surfaces.* Emerg Infect Dis, 2002. **8**(9): p. 881-890.
19. Wolcott, R.D., Rumbaugh, K. P., James, G., Schultz, G., Phillips, P., Yang, Q., Watters, C., Stewart, P. S., & Dowd, S. E, *Biofilm maturity studies indicate sharp debridement opens a time- dependent therapeutic window.* Journal of wound care, 2010. **19 (8)**: p. 320-328.
20. Jefferson, K.K., *What drives bacteria to produce a biofilm?* FEMS Microbiology Letters, 2004. **236**(2): p. 163-173.
21. Herbert O Gbejuade, A.M.L., Jason C Webb, *The role of microbial biofilms in prosthetic joint infections.* Acta Orthopaedica, 2014. **85**(6): p. 147-158.
22. Ariza J., E.G., Murillo O., *Infecciones relacionadas con las prótesis articulares.* Elsevier España, S.L., 2008. **26 (6)**: p. 380-390.
23. Gomes, L., *Early Diagnosis of Periprosthetic Joint Infection of the Hip—Current Status, Advances, and Perspectives.* 2019.

24. Pellegrini, A., V. Suardi, and C. Legnani, *Classification and management options for prosthetic joint infection.* Ann Jt, 2022. **7**: p. 3.
25. Rahardja, R., et al., *Success of Debridement, Antibiotics, and Implant Retention in Prosthetic Joint Infection Following Primary Total Knee Arthroplasty: Results From a Prospective Multicenter Study of 189 Cases.* The Journal of Arthroplasty, 2023. **38**(7, Supplement 2): p. S399-S404.
26. Bernard, L., et al., *Value of Preoperative Investigations in Diagnosing Prosthetic Joint Infection: Retrospective Cohort Study and Literature Review.* Scandinavian Journal of Infectious Diseases, 2004. **36**(6-7): p. 410-416.
27. Zimmerli, W., A. Trampuz, and P.E. Ochsner, *Prosthetic-joint infections.* New England journal of medicine, 2004. **351**(16): p. 1645-1654.
28. Osmon, D.R., et al., *Executive summary: diagnosis and management of prosthetic joint infection: clinical practice guidelines by the Infectious Diseases Society of America.* Clinical infectious diseases, 2013. **56**(1): p. 1-10.
29. Li, C., N. Renz, and A. Trampuz, *Management of Periprosthetic Joint Infection.* Hip Pelvis, 2018. **30**(3): p. 138-146.
30. Wang, K., et al., *Progress in Prevention, Diagnosis, and Treatment of Periprosthetic Joint Infection.* Evid Based Complement Alternat Med, 2021. **2021**: p. 3023047.
31. Bjerke-Kroll, B.T., et al., *Periprosthetic Joint Infections Treated with Two-Stage Revision over 14Years: An Evolving Microbiology Profile.* The Journal of Arthroplasty, 2014. **29**(5): p. 877-882.
32. Sandiford, N.A. and K. Wronka, *The multidisciplinary approach to managing prosthetic joint infection: could this lead to improved outcomes?* Annals of Joint, 2020. **7**.
33. Brivio, A., et al., *Debridement, antibiotics and implant retention (DAIR) is successful in the management of acutely infected unicompartmental knee arthroplasty: a case series.* Ann Med, 2023. **55**(1): p. 680-688.
34. Osmon, D.R., et al., *Diagnosis and management of prosthetic joint infection: clinical practice guidelines by the Infectious Diseases Society of America.* Clin Infect Dis, 2013. **56**(1): p. e1-e25.
35. Achermann, Y., et al., *Characteristics and outcome of 27 elbow periprosthetic joint infections: results from a 14-year cohort study of 358 elbow prostheses.* Clin Microbiol Infect, 2011. **17**(3): p. 432-8.
36. Alrayes, M.M. and M. Sukeik, *Two-stage revision in periprosthetic knee joint infections.* World J Orthop, 2023. **14**(3): p. 113-122.

37. Longo, U.G., et al., *Debridement, antibiotics, and implant retention (DAIR) for the early prosthetic joint infection of total knee and hip arthroplasties: a systematic review.* Journal of ISAKOS, 2024. **9**(1): p. 62-70.
38. Choi, H.-R., et al., *Can implant retention be recommended for treatment of infected TKA?* Clinical Orthopaedics and Related Research®, 2011. **469**(4): p. 961-969.
39. Koyonos, L., et al., *Infection control rate of irrigation and débridement for periprosthetic joint infection.* Clinical Orthopaedics and Related Research®, 2011. **469**(11): p. 3043-3048.
40. Gardner, J., T.J. Gioe, and P. Tatman, *Can this prosthesis be saved?: implant salvage attempts in infected primary TKA.* Clinical Orthopaedics and Related Research®, 2011. **469**: p. 970-976.
41. Qasim, S.N., A. Swann, and R. Ashford, *The DAIR (debridement, antibiotics and implant retention) procedure for infected total knee replacement–a literature review.* SICOT-J, 2017. **3**.
42. Gehrke, T., P. Alijanipour, and J. Parvizi, *The management of an infected total knee arthroplasty.* The bone & joint journal, 2015. **97**(10_Supple_A): p. 20-29.
43. Moran, E., et al., *Guiding empirical antibiotic therapy in orthopaedics: the microbiology of prosthetic joint infection managed by debridement, irrigation and prosthesis retention.* Journal of Infection, 2007. **55**(1): p. 1-7.
44. Van Kleunen, J.P., et al., *Irrigation and débridement and prosthesis retention for treating acute periprosthetic infections.* Clinical Orthopaedics and Related Research®, 2010. **468**(8): p. 2024-2028.
45. Kalore, N.V., T.J. Gioe, and J.A. Singh, *Diagnosis and management of infected total knee arthroplasty.* The open orthopaedics journal, 2011. **5**: p. 86.
46. Maale, G.E., et al., *The evolution from the two stage to the one stage procedure for biofilm based periprosthetic joint infections (PJI).* Biofilm, 2020. **2**: p. 100033.
47. Cadambi, A., R. Jones, and G. Maale, *A protocol for staged revision of infected total hip and knee arthroplasties: the use of antibiotic-cement-implant composites.* Orthop Int Ed, 1995. **3**: p. 133-145.
48. Maale, G.E., *Debridement for orthopaedic infections.* Let's discuss surgical site infections. Rosemont, IL: American Academy of Orthopaedic Surgeons, 2015: p. 121-156.

49. Haddad, F.S., et al., *The PROSTALAC functional spacer in two-stage revision for infected knee replacements.* The Journal of Bone & Joint Surgery British Volume, 2000. **82**(6): p. 807-812.
50. Maale, G., H. Pascoe, and E. Piercy, *A standardized approach for the treatment of infected total joint arthroplasties by the DFW sarcoma group osteomyelitis protocol; Staged revisions at 2 weeks using antibiotic-cement-implant composites as spacers.* The Journal of Arthroplasty, 1993. **8**(1): p. 102.
51. Cuckler, J.M., et al., *Diagnosis and management of the infected total joint arthroplasty.* Orthopedic Clinics of North America, 1991. **22**(3): p. 523-530.
52. Iorio, R., et al., *A Modified Technique for Two-Stage Revision in Knee PJI Treatment.* Journal of Clinical Medicine, 2023. **12**(23): p. 7323.
53. Moore, A.J., et al., *Deep prosthetic joint infection: a qualitative study of the impact on patients and their experiences of revision surgery.* BMJ open, 2015. **5**(12): p. e009495.
54. Anis, H.K., et al., *Greater prevalence of mental health conditions in septic revision total knee arthroplasty: a call to action.* The Journal of Knee Surgery, 2022. **35**(02): p. 190-197.
55. Longo, U.G., et al., *Outcomes of posterior-stabilized compared with cruciate-retaining total knee arthroplasty.* The journal of knee surgery, 2018. **31**(04): p. 321-340.
56. Cui, Q., et al., *Antibiotic-impregnated cement spacers for the treatment of infection associated with total hip or knee arthroplasty.* JBJS, 2007. **89**(4): p. 871-882.
57. Hebert, C.K., et al., *Cost of treating an infected total knee replacement.* Clinical Orthopaedics and Related Research (1976-2007), 1996. **331**: p. 140-145.
58. Simmons, T.D. and S.H. Stern, *Diagnosis and management of the infected total knee arthroplasty.* The American journal of knee surgery, 1996. **9**(2): p. 99-106.
59. Simpson, A., M. Deakin, and J. Latham, *Chronic osteomyelitis: the effect of the extent of surgical resection on infection-free survival.* The Journal of Bone & Joint Surgery British Volume, 2001. **83**(3): p. 403-407.
60. Haddad, F.S., M. Sukeik, and S. Alazzawi, *Is single-stage revision according to a strict protocol effective in treatment of chronic knee arthroplasty infections?* Clinical Orthopaedics and Related Research®, 2015. **473**(1): p. 8-14.
61. Srivastava, K., et al., *Reconsidering strategies for managing chronic periprosthetic joint infection in total knee arthroplasty: using decision analytics to find the optimal strategy between one-stage and two-stage total knee revision.* JBJS, 2019. **101**(1): p. 14-24.

62. Ehrlich, G., et al., *Culture-negative infections in orthopedic surgery.* Culture negative orthopedic biofilm infections, 2012: p. 17-27.
63. Tande, A.J. and R. Patel, *Prosthetic joint infection.* Clinical microbiology reviews, 2014. **27**(2): p. 302-345.
64. Thakrar, R., et al., *Indications for a single-stage exchange arthroplasty for chronic prosthetic joint infection: a systematic review.* The Bone & Joint Journal, 2019. **101**(1_Supple_A): p. 19-24.
65. Rowan, F.E., et al., *The Role of One-Stage Exchange for Prosthetic Joint Infection.* Current Reviews in Musculoskeletal Medicine, 2018. **11**(3): p. 370-379.
66. Kurtz, S.M., et al., *Future young patient demand for primary and revision joint replacement: national projections from 2010 to 2030.* Clinical Orthopaedics and Related Research®, 2009. **467**: p. 2606-2612.
67. Zhao, Y., et al., *Systematic review and meta-analysis of single-stage vs two-stage revision for periprosthetic joint infection: a call for a prospective randomized trial.* BMC Musculoskelet Disord, 2024. **25**(1): p. 153.
68. Lazic, I., et al., *Treatment options in PJI – is two-stage still gold standard?* Journal of Orthopaedics, 2021. **23**: p. 180-184.
69. Diefenbeck, M., T. Mückley, and G.O. Hofmann, *Prophylaxis and treatment of implant-related infections by local application of antibiotics.* Injury, 2006. **37**(2): p. S95-S104.
70. Kuiper, J.W., et al., *Treatment of acute periprosthetic infections with prosthesis retention: Review of current concepts.* World J Orthop, 2014. **5**(5): p. 667-76.
71. Barth, R.E., et al., *'To bead or not to bead?'Treatment of osteomyelitis and prosthetic joint-associated infections with gentamicin bead chains.* International journal of antimicrobial agents, 2011. **38**(5): p. 371-375.
72. Geurts, J.A., et al., *Good results in postoperative and hematogenous deep infections of 89 stable total hip and knee replacements with retention of prosthesis and local antibiotics.* Acta Orthopaedica, 2013. **84**(6): p. 509-516.
73. Tintle, L.S.M., et al., *Prosthesis retention, serial debridement, and antibiotic bead use for the treatment of infection following total joint arthroplasty.* Orthopedics, 2009. **32**(2): p. 87-93.
74. Fukagawa, S., et al., *High-dose antibiotic infusion for infected knee prosthesis without implant removal.* Journal of Orthopaedic Science, 2010. **15**: p. 470-476.

75. PERRY, C.R., et al., *Treatment of acutely infected arthroplasties with incision, drainage, and local antibiotics delivered via an implantable pump.* Clinical Orthopaedics and Related Research®, 1992. **281**: p. 216-223.
76. BURGER, R.R., T. BASCH, and C.N. HOPSON, *Implant salvage in infected total knee arthroplasty.* Clinical Orthopaedics and Related Research®, 1991. **273**: p. 105-112.
77. Davenport, K., S. Traina, and C. Perry, *Treatment of acutely infected arthroplasty with local antibiotics.* The Journal of Arthroplasty, 1991. **6**(2): p. 179-183.
78. Swieringa, A.J., et al., *In vivo pharmacokinetics of a gentamicin-loaded collagen sponge in acute periprosthetic infection: serum values in 19 patients.* Acta orthopaedica, 2008. **79**(5): p. 637-642.
79. Kuiper, J.W., et al., *Implantation of resorbable gentamicin sponges in addition to irrigation and debridement in 34 patients with infection complicating total hip arthroplasty.* Hip International, 2013. **23**(2): p. 173-180.
80. Taha, M., et al., *New Innovations in the Treatment of PJI and Biofilms-Clinical and Preclinical Topics.* Curr Rev Musculoskelet Med, 2018. **11**(3): p. 380-388.
81. Anagnostakos, K., et al., *Elution of gentamicin and vancomycin from polymethylmethacrylate beads and hip spacers in vivo.* Acta Orthop, 2009. **80**(2): p. 193-7.
82. Bertazzoni Minelli, E., et al., *Antimicrobial activity of gentamicin and vancomycin combination in joint fluids after antibiotic-loaded cement spacer implantation in two-stage revision surgery.* J Chemother, 2015. **27**(1): p. 17-24.
83. Edelstein, A.I., et al., *Nephrotoxicity After the Treatment of Periprosthetic Joint Infection With Antibiotic-Loaded Cement Spacers.* J Arthroplasty, 2018. **33**(7): p. 2225-2229.
84. Chaudhry, Y.P., et al., *Acute kidney injury in the context of staged revision arthroplasty and the use of antibiotic-laden cement spacers: a systematic review.* J Orthop Surg Res, 2023. **18**(1): p. 340.
85. Nelson, C.L., et al., *Sonication of antibiotic spacers predicts failure during two-stage revision for prosthetic knee and hip infections.* Clin Orthop Relat Res, 2014. **472**(7): p. 2208-14.
86. Schmolders, J., et al., *Evidence of MRSE on a gentamicin and vancomycin impregnated polymethyl-methacrylate (PMMA) bone cement spacer after two-stage exchange arthroplasty due to periprosthetic joint infection of the knee.* BMC Infect Dis, 2014. **14**: p. 144.

87. Anagnostakos, K., O. Fürst, and J. Kelm, *Antibiotic-impregnated PMMA hip spacers: Current status.* Acta Orthop, 2006. **77**(4): p. 628-37.
88. Erivan, R., et al., *Complications with cement spacers in 2-stage treatment of periprosthetic joint infection on total hip replacement.* Orthop Traumatol Surg Res, 2018. **104**(3): p. 333-339.
89. Zaidi, S., L. Misba, and A.U. Khan, *Nano-therapeutics: A revolution in infection control in post antibiotic era.* Nanomedicine, 2017. **13**(7): p. 2281-2301.
90. Li, Y.J., et al., *Synthesis of Self-Assembled Spermidine-Carbon Quantum Dots Effective against Multidrug-Resistant Bacteria.* Adv Healthc Mater, 2016. **5**(19): p. 2545-2554.
91. Qayyum, S. and A.U. Khan, *Biofabrication of broad range antibacterial and antibiofilm silver nanoparticles.* IET Nanobiotechnol, 2016. **10**(5): p. 349-357.
92. Kulshrestha, S., S. Qayyum, and A.U. Khan, *Antibiofilm efficacy of green synthesized graphene oxide-silver nanocomposite using Lagerstroemia speciosa floral extract: A comparative study on inhibition of gram-positive and gram-negative biofilms.* Microb Pathog, 2017. **103**: p. 167-177.
93. Yang, Y., et al., *Monoclonal Antibody Targeting Staphylococcus aureus Surface Protein A (SasA) Protect Against Staphylococcus aureus Sepsis and Peritonitis in Mice.* PLoS One, 2016. **11**(2): p. e0149460.
94. Varshney, A.K., et al., *A natural human monoclonal antibody targeting Staphylococcus Protein A protects against Staphylococcus aureus bacteremia.* PLoS One, 2018. **13**(1): p. e0190537.
95. Castano, A.P., T.N. Demidova, and M.R. Hamblin, *Mechanisms in photodynamic therapy: part two-cellular signaling, cell metabolism and modes of cell death.* Photodiagnosis Photodyn Ther, 2005. **2**(1): p. 1-23.
96. Briggs, T., et al., *Antimicrobial photodynamic therapy-a promising treatment for prosthetic joint infections.* Lasers Med Sci, 2018. **33**(3): p. 523-532.
97. Giannelli, M., et al., *Effects of photodynamic laser and violet-blue led irradiation on Staphylococcus aureus biofilm and Escherichia coli lipopolysaccharide attached to moderately rough titanium surface: in vitro study.* Lasers Med Sci, 2017. **32**(4): p. 857-864.
98. Getzlaf, M.A., et al., *Multi-disciplinary antimicrobial strategies for improving orthopaedic implants to prevent prosthetic joint infections in hip and knee.* J Orthop Res, 2016. **34**(2): p. 177-86.

99. Sangeetha, K. and E.K. Girija, *Tailor made alginate hydrogel for local infection prophylaxis in orthopedic applications.* Mater Sci Eng C Mater Biol Appl, 2017. **78**: p. 1046-1053.

100. Crotty, M.P., et al., *New Gram-Positive Agents: the Next Generation of Oxazolidinones and Lipoglycopeptides.* J Clin Microbiol, 2016. **54**(9): p. 2225-32.

101. Dunne, M.W., et al., *Extended-duration dosing and distribution of dalbavancin into bone and articular tissue.* Antimicrob Agents Chemother, 2015. **59**(4): p. 1849-55.

102. Fernández, J., K.E. Greenwood-Quaintance, and R. Patel, *In vitro activity of dalbavancin against biofilms of staphylococci isolated from prosthetic joint infections.* Diagn Microbiol Infect Dis, 2016. **85**(4): p. 449-51.

103. Barnea, Y., et al., *Efficacy of dalbavancin in the treatment of MRSA rat sternal osteomyelitis with mediastinitis.* J Antimicrob Chemother, 2016. **71**(2): p. 460-3.

104. Brade, K.D., J.M. Rybak, and M.J. Rybak, *Oritavancin: A New Lipoglycopeptide Antibiotic in the Treatment of Gram-Positive Infections.* Infect Dis Ther, 2016. **5**(1): p. 1-15.

105. Zhanel, G.G., F. Schweizer, and J.A. Karlowsky, *Oritavancin: mechanism of action.* Clin Infect Dis, 2012. **54 Suppl 3**: p. S214-9.

106. Lehoux, D., et al., *Oritavancin Pharmacokinetics and Bone Penetration in Rabbits.* Antimicrob Agents Chemother, 2015. **59**(10): p. 6501-5.

107. Gulati, K., M.S. Aw, and D. Losic, *Drug-eluting Ti wires with titania nanotube arrays for bone fixation and reduced bone infection.* Nanoscale Research Letters, 2011. **6**(1): p. 571.

108. Levack, A.E., et al., *Current Options and Emerging Biomaterials for Periprosthetic Joint Infection.* Curr Rheumatol Rep, 2018. **20**(6): p. 33.

109. Yuste, I., et al., *Engineering 3D-Printed Advanced Healthcare Materials for Periprosthetic Joint Infections.* Antibiotics, 2023. **12**: p. 1229.

110. Bácskay, I., et al., *The Evolution of the 3D-Printed Drug Delivery Systems: A Review.* Pharmaceutics, 2022. **14**(7).

111. Mathew, E., et al., *3D Printing of Pharmaceuticals and Drug Delivery Devices.* Pharmaceutics, 2020. **12**(3): p. 266.

112. Domsta, V. and A. Seidlitz, *3D-Printing of Drug-Eluting Implants: An Overview of the Current Developments Described in the Literature.* Molecules, 2021. **26**(13).

113. Wong, K.C., *3D-printed patient-specific applications in orthopedics.* Orthop Res Rev, 2016. **8**: p. 57-66.

114. Yuste, I., et al., *Mimicking bone microenvironment: 2D and 3D in vitro models of human osteoblasts.* Pharmacol Res, 2021. **169**: p. 105626.

Hipótesis y objetivos

Hipótesis

La profilaxis y el tratamiento de las infecciones protésicas (PJI) en la actualidad son muy limitados, ya que existen factores críticos para su efectividad tales como; i) la poca vascularización en el sitio de acción; ii) los fármacos y concentraciones exactas para la eliminación o prevención del biofilm; iii) el riesgo de producir resistencias en los microorganismos causando problemas mayores; iv) posibles problemas a futuro de las propiedades biomecánicas de la articulación y v) el coste asociado que implica para el sistema de salud. Considerando la complejidad clínica de estas infecciones y las limitaciones de los tratamientos actuales, lo ideal sería disponer de una terapia que cumpla con las siguientes características:

1. Formulaciones con fármacos de amplio espectro que eviten la formación de biofilm por los principales microorganismos causantes de PJI.
2. Componentes biocompatibles y biodegradables, para prevenir una nueva intervención quirúrgica.
3. Liberación controlada y/o sostenida en el tiempo, para que no exista riesgo de resistencias y la terapia sea eficaz.
4. Personalización del tratamiento para que sea fácilmente adaptable al espacio intraarticular de la prótesis y no interponga la osteointegración.
5. Terapias que impliquen bajo coste para el sistema de salud.

Aunque se esté trabajando para desarrollar nuevos tratamientos, muchos de ellos carecen de precisión en su aplicación, o requieren aún más tiempo para su investigación y realización en fase clínica. Las soluciones actuales traen muchos riesgos asociados para la vida del paciente y alto costes para el sistema médico. Los cementos óseos cargados con antibióticos son muy inexactos en sus dosis y concentración de fármaco necesitándose un tratamiento personalizado para las PJI.

Objetivos

El objetivo principal de esta Tesis Doctoral ha sido diseñar, desarrollar y optimizar formulaciones para la prevención y tratamiento de PJI, por un lado, basadas en micropartículas cargadas con agentes antimicrobianos de amplio espectro capaces de formar un gel bioadhesivo para aplicar sobre la prótesis, y por otro lado desarrollar implantes impresos en 3D adaptados a la morfología convexa del componente acetabular de la prótesis de cadera. En base a esto, se establecieron los siguientes objetivos específicos:

1. Formular, desarrollar, optimizar y caracterizar micropartículas cargadas con antimicrobianos para prevenir las infecciones de prótesis articulares.
2. Diseñar, producir y caracterizar implantes impresos en 3D para prevenir infecciones fúngicas asociadas a las artroplastias articulares.

Resultados

PUBLICACIÓN 2:

Unraveling the potential of bioadhesive antimicrobial microparticles for the treatment of prosthetic joint infections

F.C. Luciano, I. Yuste, P. Sanz-Ruiz, A. Ribed-Sánchez, M.P. Ballesteros, C. Rodríguez , B.J. Anaya, M. Tiboni, G. Maurizzi, L. Casettari, E. González-Burgos, D.R. Serrano

Pendiente de publicación: Enviado a: Journal of Drug Delivery Science and Technology (IF: 4.5, Q1)

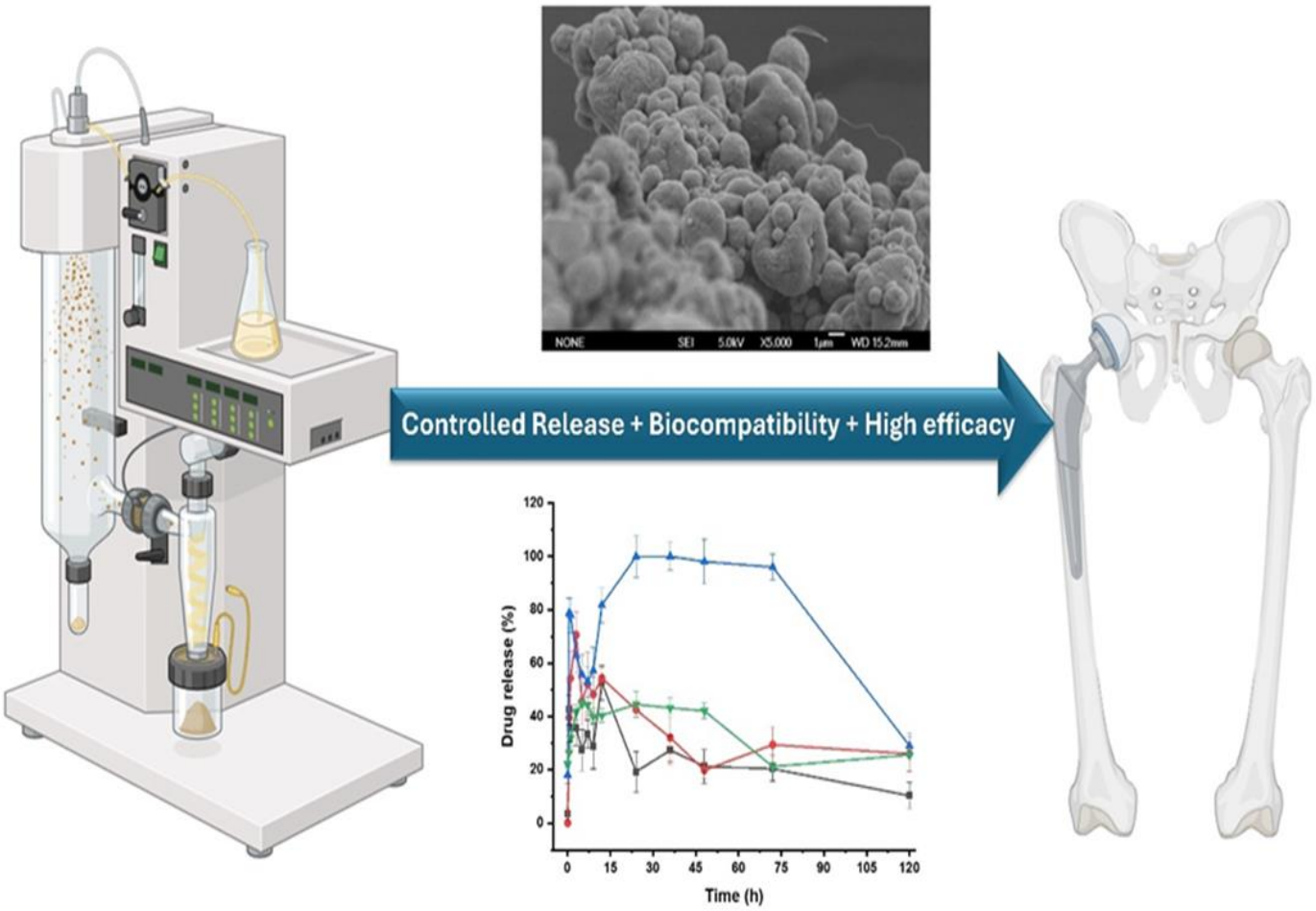

Abstract

Periprosthetic joint infections (PJIs) are severe complications occurring after a hip or knee arthroplasty, causing devasting healthcare problems and increasing significantly the economic burden. Current therapies to prevent and treat bacterial PJIs are far from ideal providing a deficient antimicrobial efficacy and may also alter the biomechanical properties of the prosthesis. Alternatives available against fungal infections are negligible, and even though they have a lower incidence (about 2 %), they lead to major health issues in patients. PJIs are associated with biofilms, which consist of a tridimensional cluster of different microorganisms surrounded by an extracellular matrix evading the immunological system of the patient and blocking access to antibiotics. In this work, a novel approach to prevent and treat bacterial and fungal PJIs has been assessed consisting of smart bioadhesive microparticles loaded with a combination of broad spectra antibacterial (vancomycin) and antifungal (amphotericin B) drugs. Solid dry microparticles were redispersed into a hyaluronic gel before adhesion to the prosthesis. The excipients (Soluplus, Eudragit RL100, Kollicoat IR) were carefully selected to ensure biodegradability and biocompatibility. The microparticles showed a sustained release profile marked by a burst release ranging from 40 % to 80 % depending on the drug over the first 10 h followed by a prolonged sustained release over 7 days. A range of different microbiological species including *Staphylococcus* spp. (*S. epidermidis* and *S. aureus*) and *Candida* spp. (*C. albicans*, *C. parapsilopsis*, *C. glabrata* and *C. krusei*) were susceptible to the microparticulate formulation. The microparticles showed reduced haemolytic toxicity and a protective effect in mammalian cell lines (Saos-2, BJ, hFOB).

Keywords: microparticles, amphotericin B, vancomycin, periprosthetic joint infections, bone, controlled release, infection, prosthesis

1. Introduction

In recent years, prosthetic joint replacement has significantly improved patients' quality of life suffering from joint injuries. However, the success of this surgery can be undermined by the increasing risk of periprosthetic joint infections (PJI), specially PJI associated with antimicrobial resistance [1]. Considering population aging, the increasing levels of obesity, and the growth in sport-related injuries, the incidence of knee and hip arthroplasties is growing exponentially, being underestimated the true incidence rate of (PJIs) which are one of the most devastating and costly complications following arthroplasty surgery [2].

Periprosthetic joint infections often require long and complex treatments, representing high morbidity associated with implant removal and even death. Most surgical infections associated with arthroplasties have their origin at the time of surgery because of the bacterial flora of the patient's skin, which is difficult to fully eradicate with conventional antiseptics. The suppression status due to surgery and the easier bacterial colonization due to the use of metal implants. Moreover, infections can also occur later by the hematogenous route [3, 4]. More than two-thirds of PJIs are caused by intraoperative microorganisms [5]. Bacterial PJIs have a higher incidence compared to fungal ones (10 % *vs* 1 % of the cases) [6, 7]. The major bacteria responsible for PJIs are Gram-positive bacteria such as *Staphylococcus (S.) aureus* and *S. epidermidis* in 70 % of all cases [8]. However, Gram-negative bacteria, such as *Pseudomonas aeruginos*a can also occur, in less percentage, but cause devastating problems [9, 10]. It´s important to note that in 15% of cases these infections are caused by multiple bacteria.

Conventional PJI treatments rely on the administration of antimicrobial therapy along with a new surgical procedure which can focus just on the debridement of the infected area but with retention of the prosthesis with a success rate varying from 16 % - 83 % or in a one or two-stage implant replacement with a success rate between 85 % - 90 %, and 66 % - 95 % respectively [11, 12]. In the one-stage replacement surgery, the infected prosthesis is replaced with a new one, while in the two-stage revision, a polymethyl methacrylate cement spacer loaded with antimicrobials is placed in the joint followed by the insertion of a new prosthesis several weeks later.

Biofilm formation is associated with PJIs, which consists of the formation of tridimensional clusters of different microorganisms surrounded by an extracellular matrix

evading the immunological system of patients and limiting access to antibiotics [11, 13, 14]. Biofilm formation takes place in four phases starting with the adhesion of the microorganism to the surface of the implant followed by proliferation, maturation, cellular detachment, and invasion to other regions, the latter triggering the symptoms of PJIs due to the activation of the immune system such as inflammation, oedema, pain, and implant loosening [11, 14]. The difficulty in eradicating this biofilm is the main reason for the difficulty in treating these infections.

Current therapies to prevent and treat PJIs are far from ideal. In the case of irrigation of the prosthesis with antibiotics, the latter are washed away rapidly from the joint providing short antibacterial protection and can alter the biomechanical properties of the prosthesis. In the case of the use of cement spacers, they can lead to joint dislocations and risk of fractures as they are intended for temporary use in the body but also, the antimicrobials loaded in the cement only elute in suitable concentrations for 24 h - 48 h after insertion, followed by a very slow release pattern that can even trigger the appearance of resistance [11-16].

Regarding fungal PJIs, the incidence is lower than bacterial infection, but the alternatives are very limited and can cause devastating effects on patients [11, 14, 17-19]. Hence, there is an urgent clinical need to develop novel therapies that allow the prevention and treatment of bacterial and fungal PJIs. The hypothesis underpinning this work is that the administration of broad-spectrum antimicrobials encapsulated within bioadhesive microparticles could provide a longer sustained release to prevent and treat PJIs. Based on this premise, this work aimed to develop bioadhesive sustained-released microparticles combining vancomycin and amphotericin B (AmB) to prevent and treat both bacterial and fungal PJIs. Microparticles were adhered to the surface of the metallic hip prosthesis to assess drug release. Optimization studies along with an extensive particle characterization and evaluation of biological performance were carried out.

2. Materials and methods

2.1 Materials

Soluplus® and Kollicoat IR were donated from Basf (Ludwigshafen, Germany). Eudragit® RL 100 was provided by Evonik (Darmstadt, Germany) as a gift. Hyaluronic Acid was purchased from Merk (Madrid, Spain). Vancomycin (purity > 90 %) was supplied by the Gregorio Marañón Hospital (Madrid, Spain) and AmB (purity > 90 %) was purchased from Kemprotec Limited (Cumbria, UK). Commercial disks of vancomycin and AmB were purchased from Neo-Sensitabs (Rosco, Denmark). Salts and solvents (HPLC-grade) were purchased from Proquinorte (Madrid, Spain). All other chemicals and solvents were at least of ACS reagent grade and were used without further purification.

2.1 Design of Experiment (DoE)

Two DoEs were carried out using the Software Design Expert® version 8.04 (Stat-Ease, Minneapolis, United States) to optimize the fabrication of microparticles containing AmB using spray drying. The combination of Soluplus®, Eudragit® RL100, and Kolicoat® IR was evaluated to target a sustained-drug release profile microparticles by spray drying.

2.1.1. Pre-screening DoE: Taguchi design

Seven variables with two levels with only eight experiments (L8 = 2^7) were established to determine which variables were most critical in the atomization process. Both the components of the formulation and the process parameters of the atomizer were taken into consideration including the amount of AmB (1 % or 5 %), the amount of Soluplus® (35 or 65 %), airflow (600 NL/h or 800 NL/h), inlet temperature (65 ºC or 72 ºC), vacuum aspiration (90 % or 100 %), liquid inlet velocity (5 mL/min or 15 mL/min) and time of sonication of the suspension before spray drying in a water bath at 10 W (5 min or 10 min).

In each experiment, the batch size was kept constant at 1g. Depending on the amount of AmB and Soluplus®, the remaining up to 1 g (100 %) was completed with Eudragit® RL100. In 100 mL of ethanol, Eudragit® was first dissolved under continuous magnetic stirring. Afterwards, AmB was dispersed in the mixture followed by the corresponding amount of Soluplus®. The mixture was kept under stirring for at least 15 min and then it was transferred to the water bath ultrasound for either 5 min or 10 min at 10 W. The obtained suspension was spray-dried in a Buchi Spray drier B-190 (Labortechnik AG,

Flawil, Switzerland) using the corresponding parameters from the DoE. After the process, the powder was immediately collected from the collector's vessel and stored in a desiccator under refrigerated conditions.

The responses evaluated were the yield of the process (%), the encapsulation of the AmB (%), the AmB aggregation state, and the antifungal activity. The matrix design of Taguchi DoE is shown in **Table S1**.

2.3 Surface response DoE: Box-Behnken design

Three variables were studied at three levels with a total of seventeen experiments (L17=3^3) to optimize the final formulation including the amount of AmB (5 % - 7.5 % - 10 %), the amount of Soluplus® (50 % - 65 % - 80 %) and the liquid inlet velocity (10 mL/min - 15 mL/min - 20 mL/min). Based on the results obtained in the Taguchi design, several factors were kept constant in the Box-Behnken design such as 700 NL/h airflow, 100 % aspiration, 10 min water bath sonication, and 70 ºC inlet temperature. As previously, the batch size was 1 g of total mass dispersed in 100 mL of ethanol. Eudragit® RL100 was added in sufficient quantity to complete 100 % of the formulation. Each sample was prepared as described in the previous section. The responses studied were yield (%), AmB encapsulation efficiency (%), and AmB aggregation state.

2.4 Formulation optimization and validation

The formulation was optimized aiming for the highest yield and AmB encapsulation efficiency. After optimization studies, the suggested formulation consisted of AmB as an API, Eudragit® RL100 as a controlled release excipient, and Soluplus® as a solubilizer.

After the optimization, preliminary drug release studies showed a too-prolonged release in aqueous media. Kollicoat® IR was incorporated into the mixture to counteract this effect. The resulting formulation included 27.5 % Eudragit® RL100, 50 % Soluplus®, 17.5 % Kollicoat® IR, and 5 % AmB. Excipients and drug (1 g in total) were dispersed in methanol (100 mL) and the mixture was sonicated (10 min in a water bath) and then spray dried at 700 NL/h airflow, 100 % aspiration, 70 ºC inlet temperature, and 12 mL/min liquid inlet velocity. Microparticles (50 mg) were mixed with hyaluronic acid (15 mg) and then dispersed in deionized water (0.7 mL) to form a gel-like structure to enhance the adhesive properties of the microparticulate formulation onto the metallic surface of the

hip prosthesis. The same process parameters and formulation composition were utilized to encapsulate vancomycin within polymeric microparticles. A third combined formulation was prepared incorporating 5 % AmB and 5 % vancomycin. The combined formulation was consisting of 5 % AmB, 5 % vancomycin, 50 % Soluplus®, 22.5 % Eudragit® RL100 and 17.5 % Kollicoat® IR.

2.5 Yield quantification

To determine the yield, the amount of product collected at the end of the atomization process compared to the initial mass was calculated with the following **Equation 1**:

$$Yield\ (\%) = \frac{Amount\ collected}{Total\ mass\ atomized} x\ 100 \qquad \text{(Equation 1)}$$

2.6 Quantification of AmB encapsulation by HPLC

10 mg of each spray-dried formulation were weighed and dissolved in 5 mL of methanol. The solution was diluted (1:5, *v:v*) with mobile phase before HPCL analysis using a previously validated method with a Hypersil BDS column (200 mm × 4.6 mm, 5µm), a mobile phase consisting of acetonitrile (AcN), acetic acid (AcOH) and water (52: 4.3: 43.7, *v:v:v*) at 1 mL/min flow rate, 50 µL injection volume and 406 nm wavelength [20]. A calibration curve was performed between 50 µg/m - 0.08 µg/mL to determine the slope value and the coefficient of determination (R^2). The encapsulation efficiency was calculated using **Equation 2**:

$$Encapsulation\ (\%) = \frac{Experimental\ amount\ of\ AmB}{Theoretical\ amount\ of\ AmB}\ x\ 100 \qquad \text{(Equation 2)}$$

2.7 Aggregation of AmB

Formulations were reconstituted and diluted as necessary with deionized water up to a theoretically 10 µg/mL AmB concentration. The resulting dilutions were scanned between 300 nm – 450 nm (Shimadzu UV-1700 spectrophotometer) as previously described [20, 21]. To calculate the AmB aggregation state, the ratio between the peak at 328 and 406 nm was taken into consideration according to **Equation 3**:

$$Aggregation\ ratio = \frac{Abs\ \lambda\ 328\ nm}{Abs\ \lambda\ 406\ nm} \quad \text{(Equation 3)}$$

The wavelengths at 328 nm and 406 nm were chosen since they correlate with the AmB aggregation state, being the absorption at 328 nm characteristic of the dimeric state (oligomeric state) and the absorption at 406 nm of the monomeric state. If the aggregation ratio was greater than 1, this indicated a more aggregated AmB state while the opposite was indicative of a monomeric AmB predominance [22].

2.8 Physicochemical and solid-state characterization

Particle morphology

The morphology of the optimized microparticles containing AmB, vancomycin, or a mixture of both drugs was characterized by Scanning Electron Microscopy (SEM) using a JEOL6335F (Mussashime, Japan) with a voltage of 20 kV. A thin layer coating with gold was sputtered for 120 seconds on microparticles mounted on carbon-coated tubs using a QUORUM Q150R S (Mussashime, Japan) to help conductivity. Also, SEM analysis was carried out on the combined AmB/vancomycin microparticles reconstituted with hyaluronic acid and deionized water. The gel was spread over a stub and left overnight to dry at room temperature before analysis.

Powder X Ray Diffraction (PRXD)

Powder X-ray analysis was carried out using a Philips®X'Pert-MPD X-ray diffractometer (Malvern Panalytical®; Almelo, The Netherlands) equipped with Ni-filtered Cu K radiation (1.54). A 40 kV voltage and 40 mA current were used to perform the study. PXRD patterns were recorded at a step scan rate of 0.05° per second from 5° to 40° on

the 2-theta scale (n = 3) [23]. Physical mixtures of raw powder materials between API and excipients were carried out in an agate mortar and pestle for comparison purposes.

Differential Scanning Calorimetry (DSC) and thermogravimetric analysis (TGA)

DSC and TGA analysis were performed simultaneously on an SDT Q600 instrument (TA Instruments, Elstree, UK) with nitrogen as the purge gas. The samples (4-6 mg) were weighted and heated at a rate of 10 °C/min, ranging from 25 °C to 500 °C. The instrument was calibrated with indium as the reference standard (n = 3). TA Universal analysis software v 4.5A (Waters, USA) was used for data collection and analysis.

Fourier-Transform Infrared (FT-IR) Spectroscopy

FT-IR analyses were conducted using a Nicolet Nexus 670–870 (Thermofisher®, Madrid, Spain). Infrared spectra were recorded in the range of 400 cm^{-1} – 4000 cm^{-1} with a 1 nm step scan. The data were interpreted using Spectragryph (version 1.2.9, Oberstdorf, Germany) software, and data normalization was carried out.

2.9 Haemolysis studies

Venous blood was obtained from a healthy 27-year-old male volunteer (5.48 x 10^6 RBC/mL) and collected into a K2-EDTA-coated Vacutainer tube to prevent coagulation. Haemolysis studies were performed as previously described [24, 25]. Briefly, blood was centrifuged (5 min at 1000 g) and the haematocrit and plasma levels were marked on the tube. The supernatant was discarded, and the tube was refilled with 150 mM NaCl solution. The RBCs were washed twice. After the last wash, the supernatant was discarded, and the RBCs were diluted to 4 % concentration using PBS at pH 7.4. The diluted RBCs were added to a 96-well plate (180 µL/well). Stock solutions of the three microparticulate formulations (AmB, vancomycin, and AmB-vancomycin-loaded formulations) were prepared with a drug concentration ranging from 50 mg/mL – 0.5 mg/mL using deionized water. As a comparison, a standard solution of each drug in DMSO at the same concentrations was tested. Samples (20 µL) from each concentration were loaded into the wells in triplicate. For positive control wells, a 20 % solution of Triton X-100 (20 µL) was utilized. For negative control wells, PBS at pH 7.4 (20 µL) was

incorporated. Plates were incubated at 37 ºC for 1 h. Afterward, plates were centrifuged at 2,500 rpm for 5 min to pellet intact RBCs, and 50 µL of the supernatant from each well was transferred into a clear, flat-bottomed 96-well plate. The absorbance of the supernatants was measured using a plate reader (BioTek, ELx808) at 570 nm. The percentage of haemolysis was calculated using the **Equation 4**:

$$\text{Haemolysis (\%)} = \frac{(\text{ABS}_{\text{sample}} - \text{ABS}_{\text{PBS}})}{(\text{ABS}_{\text{Triton}} - \text{ABS}_{\text{PBS}})} \qquad \text{(Equation 4)}$$

Where ABS sample is the absorbance value of each sample, ABS PBS is the absorbance value of PBS and ABS Triton is the absorbance value of Triton [24].

2.10 Adhesion studies

Fifty milligrams of the microparticles were mixed with 15 mg of hyaluronic acid followed by the addition of 0.7 mL of deionized water. The mixture was stirred until a homogenous bioadhesive gel was formed. The gel (1 g quantity) was spread over the surface of a femoral stem (10 cm^2) and the time needed for full dryness was quantified.

2.11 Rheological characterization

Flow viscosity of the bioadhesive gels was evaluated in triplicate using a Rheometer Brookfield (Middleborough, MA, USA) Model DV-III fitted with a temperature control probe. A 5-cm cone–plate measuring geometry was used (Spindle CP-42). The temperature of all the measurements was maintained at 25 °C. Viscosity (cP) and shear stress (D × cm^{-2}) were determined over a speed rate ramping from 0 rpm to 0.5 rpm and from 0.5 rpm to 0 rpm, and a shear rate from 0 (1/s) to 1.92 (1/s). Before measurements, a standard was analyzed. The fluidity parameter was calculated using linear regression from the slope of the shear stress versus shear rate plot.

2.12 Drug release

The microparticles (50 mg) containing AmB, vancomycin, or both drugs were mixed in a mortar and pestle with 15 mg of hyaluronic acid and were dispersed in 700 µL of deionized water. The mixture was manually mixed until a homogenous gel was obtained which immediately was spread over a 10 cm^2 over the surface of a femoral stem. The femoral stem prosthesis with the bioadhesive gel adhered and dried on the surface was immersed in a 3D printed container with similar dimensions to the prosthesis to mimic the bone microenvironment, with a capacity for 20 mL of liquid that consisted of a

mixture of PBS buffer pH 7.4 with human albumin (Grifols®, Barcelona, UK) (80:20, *v: v*). The addition of albumin to the medium was crucial, considering the high plasma protein binding of AmB and vancomycin. The experiment was performed in triplicate. The container was covered with parafilm to prevent evaporation of the medium and was kept at 37°C for 120 h. Samples (750 µL) were withdrawn at different times (0, 0.5 h, 1 h, 3 h, 5 h, 7 h, 9 h, 12 h, 24 h, 48 h, 36 h, 72 h and 120 h) and then were further diluted with methanol (1:1, *v:v*). The volume was replaced with a fresh 750 µL medium to maintain sink conditions. Collected samples were frozen for 24 h at -20 °C to precipitate proteins before HPLC analysis. Subsequently, samples were centrifuged at 10,000 rpm for 15 min and the supernatant (300 µL) was analyzed by HPLC. For the analysis of vancomycin, the mobile phase consisted of 50 mM ammonium phosphate: acetonitrile (92:8, *v: v*), with a final pH of 2.2, using a Nucleosil C18 column (250 mm × 4.6 mm, 5µm) with a 0.7 mL/min flow rate and the injection volume of 40 µL. The detector was set at 205 nm [26, 27]. A calibration curve between 50 µg/mL - 0.08 µg/mL was performed.

2.13. Long-term and accelerated stability studies

The optimized microparticles containing either AmB or vancomycin (10 mg) were placed in uncapped HPLC vials and introduced into test Cuspor stability chambers exposed to different conditions of temperature and humidity (**Table 1**). The desired humidity was achieved by using Cuspor humidity capsules (Cuspor Ltd., Ireland) which were placed into the chamber, which in turn were put inside ovens at the selected temperature to ensure that the RH equilibrium was reached before the aging of the formulations [28, 29]. A sensor cap was introduced to the test chamber to collect the temperature and humidity test conditions wirelessly. At different time points, samples were collected and analyzed by HPLC for chemical degradation. A humidity-corrected Arrhenius equation was used to estimate the effect of temperature and RH on degradation rates (**Equation 5**) [30]:

$$LnK = LnA - \frac{Ea}{RT} B(RH) \qquad \text{(Equation 5)}$$

Where K is the degradation constant, A is the collision frequency, Ea is the activation energy, B(RH) is the humidity sensitivity factor, T is the absolute temperature and R is the gas constant. Different fitting methods/models were assessed: Avrami, diffusion, first order, second order, and zero order. The model with the highest R^2 was selected for shelf-

life prediction at a mean kinetic temperature of 25 °C and 60 % relative humidity and under refrigerated conditions [31].

Table 1. Storage conditions of the long-term and accelerated stability studies (RH, relative humidity).

Group	Storage conditions	Time points
Accelerated	40 ± 2 °C/75% RH ± 5% RH 50 ± 2 °C/75% RH ± 5% RH 50 ± 2 °C/10% RH ± 5% RH 60 ± 2 °C/10% RH ± 5% RH 70 ± 2 °C/10% RH ± 5% RH 60 ± 2 °C/50% RH ± 5% RH	3, 8, 16, 22 days
Long-term	25 ± 2 °C/60% RH ± 5% RH 4± 3 °C/10% RH ± 5% RH	3, 6, 9, 12 months

2.14 Antibacterial *in vitro* assay

The antibacterial effect of the loaded microparticles was tested against *Staphylococcus epidermidis* (ATCC 12228) and *Staphylococcus aureus* (ATCC 23235). The antimicrobial activity was tested by diffusion assay in Kirby-Bauer agar [25]. Microparticles with vancomycin and the combination of both APIs dissolved in deionized water were loaded onto 6 mm in diameter paper discs and placed in the center of agar plates. Commercial discs of vancomycin (30 µg, Neo-Sensitabs, Rosco, Denmark) were used as a positive control. A vancomycin raw material in the same concentrations as in the formulation (10 µg) was used also as a control. Inhibition zone diameters were measured at points where there was complete inhibition of bacterial growth after 24 h of incubation. Isolates were classified as vancomycin susceptible (S) when the zone of inhibition was greater than 15 mm according to the CLSI guidelines.

Minimum Inhibitory Concentration (MIC) was evaluated as previously described (28). Cultures were prepared by picking a single colony from a 24-h Mueller-Hinton agar (MHA) plate and re-suspending it in 5 mL of Mueller Hinton Broth (MHB). Afterward, cultures were grown aerobically for 20 h at 37 ºC with shaking at 200 rpm. The cultures were diluted with fresh MHB with a 0.1 absorbance at 600 nm, corresponding to 10^6

colony forming units (CFU)/mL based on 0.5 McFarland standard. The suspension was further diluted with MHB up to a concentration of 4 x 10^5 CFU/mL.

Microparticles with vancomycin and a combination of both drugs were dissolved in 6 different volumes of MHB to obtain concentrations ranging from 2 µg/mL to 64 µg/mL respectively. The inoculum (50 µL) containing 2 x 10^4 CFU was added to the solution, except in medium growth for the control tubes. As a positive control for bacterial growth, the bacteria were grown in MHB. Tubes were incubated at 37 ºC with shaking at 180 rpm for 24 h. The turbidity of the tubes was visually checked. Additionally, to calculate the MIC, 10 µL from each tube was cultured on MHA plates and was further incubated for 24 h at 37 ºC (drop plate method). The MIC was determined as the lowest concentration with an absence of colony growth [32].

2.16 Antifungal *in vitro* assay

The antifungal activity was evaluated by agar diffusion assay with different species of *Candida* sp. (*Candida albicans* CECT 1394, *Candida parapsilosis* 57744, *Candida glabrata* 60750, and *Candida krusei* 1068) [21, 33]. Microparticles with AmB and the combination of both drugs (AmB and vancomycin) were dissolved in deionized water and loaded onto 6 mm in diameter paper discs and placed in the center of the agar plate. Discs loaded with AmB dissolved in DMSO (10 µg) and commercial discs of AmB (10 µg, Neo-Sensitabs, Rosco, Denmark) were used as a positive control. After 48 h, inhibition zone diameters were measured at points where complete inhibition of fungal growth was observed. Isolates were classified according to the Clinical & Laboratory Standards Institute (CLSI) as AmB susceptible (S) when the zone of inhibition was greater than 15 mm; resistant (R), if the zone of inhibition was greater than 10 mm; and intermediate (or dose-dependent) (I) if the zone of inhibition was between 11 and 14 mm.

The MIC was also evaluated. Cultures were prepared by picking a single colony from a 24-h MHB plate and resuspending with 0.9 % sterile physiological saline solution to achieve 0.1 absorbance at 600 nm, corresponding to 10^6 CFU/mL based on the 0.5 McFarland standard. The suspension was further diluted with MHB up to a concentration of 4 x 10^5 CFU/mL.

Microparticles with AmB and a combination of both drugs were dispersed in MHB in 6 different concentrations from 2 µg/mL to 64 µg/mL. The inoculum (50 µL) containing 2 x 10^4 CFU was added to the solution (2 mL), except in the medium growth that was used

as a control tube. As a positive control for bacterial growth, a tube just containing MHB, and bacteria inoculum was prepared. Tubes were incubated at 37 ºC with shaking at 180 rpm for 24 h. The turbidity of the tubes was visually checked. Additionally, to calculate the MIC, 10 µL from each tube was cultured on MHA plates and was further incubated for 24 h at 37 ºC (drop plate method) [32]. The MIC was determined as the lowest concentration with an absence of colony growth.

2.17. Cytotoxicity studies

Cell culture

The human osteosarcoma cell line Saos-2 (HTB - 85™), the human fibroblast cell line BJ (CR-2522™), and the human fetal osteoblastic cell line hFOB 1.19 (CRL - 11372™) were obtained from the American Type Culture Collection (ATCC®). The Saos-2 cells were cultured in Dulbecco's Modified Eagle Medium (DMEM) (Lonza, Basel, Switzerland) containing 10 % fetal bovine serum (FBS) (Linus) and 1 % penicillin/streptomycin (HyClone Cytiva, Austria). The BJ cells were grown in Eagle's Minimum Essential Medium (HyClone Cytiva, Austria) supplemented with 10 % FBS and 1 % penicillin/streptomycin. The hFOB cells were cultured in a 1:1 mixture of Ham's F12 and DMEM without phenol red (HyClone Cytiva, Austria) containing 10 % FBS and 1 % geneticin. These cell lines were maintained in a humidified atmosphere of 95 % air and 5 % CO_2 at 37 ºC. Saos-2, BJ, and hFOB 1.19 cells were treated with microparticles loaded with vancomycin, AmB, and vancomycin/AmB at a concentration of 60 µg/mL for 24 h, 72 h, and 1 week. The selection of this concentration was based on the maximum drug concentration achieved during the release studies.

Cell viability assay

The effect of microparticles loaded with vancomycin, AmB and vancomycin/AmB, and the corresponding drugs on cell viability was determined using the 3-(4,5-dimethyl-thiazol-2-yl)-2,5-diphenyl-tetrazolium bromide (MTT) method (Mosmann, T., 1983). Briefly, Saos-2 and BJ cells were seeded onto 24-well plates at a density of 10^5 cells per well and hFOB 1.19 cells at a density of 10^6 cells per well. After cell treatments, MTT stock solution (2 mg/mL in PBS) was added and incubated for 1 h. After incubation, the produced formazan crystals were dissolved using 100 µL per well DMSO. The absorbance was finally determined at 550 nm by using a Spectrostar BMG microplate

reader (BMG Labtech Inc., Ortenberg, Germany). Cell viability was expressed as a percentage compared to control cells.

2.18. Evaluation of cell morphology by Scanning Electron Microscopy (SEM)

Saos-2, BJ, and hFOB 1.19 cells were seeded onto collagen-coated (1:10 dilution, *v:v*) dishes. Cells were then treated with microparticles loaded with AmB, vancomycin, and AmB/vancomycin as well as with AmB or vancomycin for 1 week. After the incubation period, cells were washed two times with phosphate-buffered saline (PBS) and with ultrapure water. Then, cells were dehydrated for 10 min with increasing concentrations of ethanol (50 %, 70 %, 80 %, 90 % and 99.9 % concentrations). Critical drying point was then performed using a LeicaEM CPD300 Critical Point Dryer (Leica Mikrosysteme Vertrieb GmbH, Wetzlar, Germany). Samples were sputter-coated with gold and were examined with a scanning electron microscope (JEOL JSM 6400, Tokyo, Japan) with a 20kV acceleration voltage.

2.19 Statistical analysis

Minitab 19 (Minitab Ltd., Coventry, UK) was used for statistical analysis. The one-way ANOVA test was performed for the release, haemolysis, antifungal and antibacterial, and cytotoxicity *in vitro* assays. *p*-values below 0.05 were considered statistically significant differences. The results were plotted using Origin 2021 (OriginLab Corporation, Northampton, MA, USA).

3. Results

3.1. Preliminary screening: Taguchi DoE

The screening of various formulation and process parameters was performed using a Taguchi design for seven factors at two levels each. Implementation of the design is useful for identifying the most significant factors with minimum experimentation and saving time, effort, and materials. This design has the specific advantage of requiring minimal runs for many independent variables (**Table S1**). Preliminary screening embarks upon the phenomenon of the "sparsity effect", in which only a few of the factors among numerous envisioned ones truly explain a large proportion of the experimental variation [29]. In **Figure1**, Pareto charts illustrate the most influential variables during the spray drying process being depicted as orange bars those factors that affect positively the Critical Quality Attributes (CQAs) of the microparticles, and in red those that affect negatively.

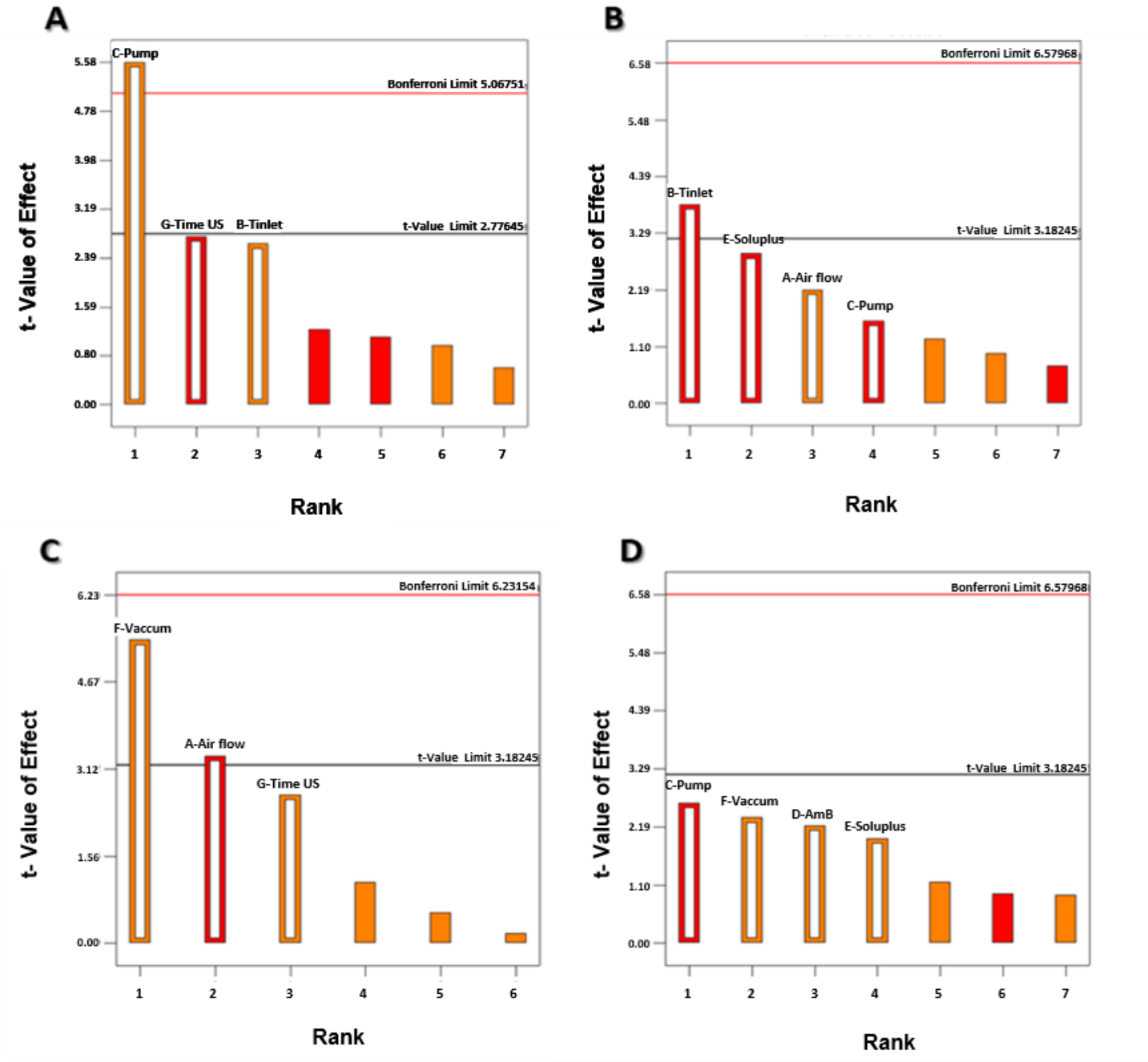

Figure 1. Pareto charts depicting the influence of the seven factors (7 bars) assessed on the Taguchi DOE design. Key: **(A)** Yield (%); **(B)** AmB encapsulation efficiency **(C)** AmB aggregation state; **(D)** AmB efficacy expressed as inhibition halo against *C. albicans*. Orange bars represent a positive effect of the factor on the response while red bars represent a negative effect.

The yield was favored when a higher liquid velocity (pump) was used while the AmB encapsulation efficiency was reduced at higher inlet temperature. Temperature is a critical factor since Soluplus® can increase its stickiness if the working temperature goes above its glass transition temperature. However, the temperature should be kept above the evaporation temperature of the solvent used to ensure suitable drying conditions. Based on this, the inlet temperature was kept at 70 ºC for the Box-Behnken second DoE design. The aggregation state was impacted positively when a high vacuum was used being opposite for the airflow. At higher airflows, the solvent evaporates faster, and particles tend to aggregate less. Regarding, the efficacy against *C. Albicans*, no significant factors were found in the Taguchi design as all formulations exhibited halos above 15 mm in diameter.

3.2. QbD-based model development and response surface analysis

Polynomial analysis was carried out by a multilinear regression analysis method suggesting that the linear model was the best fit for the yield and drug encapsulation responses. The coefficients of the model equations generated for each CQA revealed the goodness of fit of the experimental data to the selected model with high values of R^2 and low *p*-values < 0.05 for the latter responses while no significant differences were observed for the AmB aggregation state.

The yield of the process increased significantly when lower amounts of Soluplus® were used which can be related to the low T_g of the excipient impacting its processability during spray drying. However, higher liquid velocity rates increased the yield while AmB content had no significant impact. The encapsulation efficiency was drastically reduced when greater amounts of AmB were used. The amount of Soluplus® and the liquid velocity did not impact significantly on drug encapsulation (**Figure 2**).

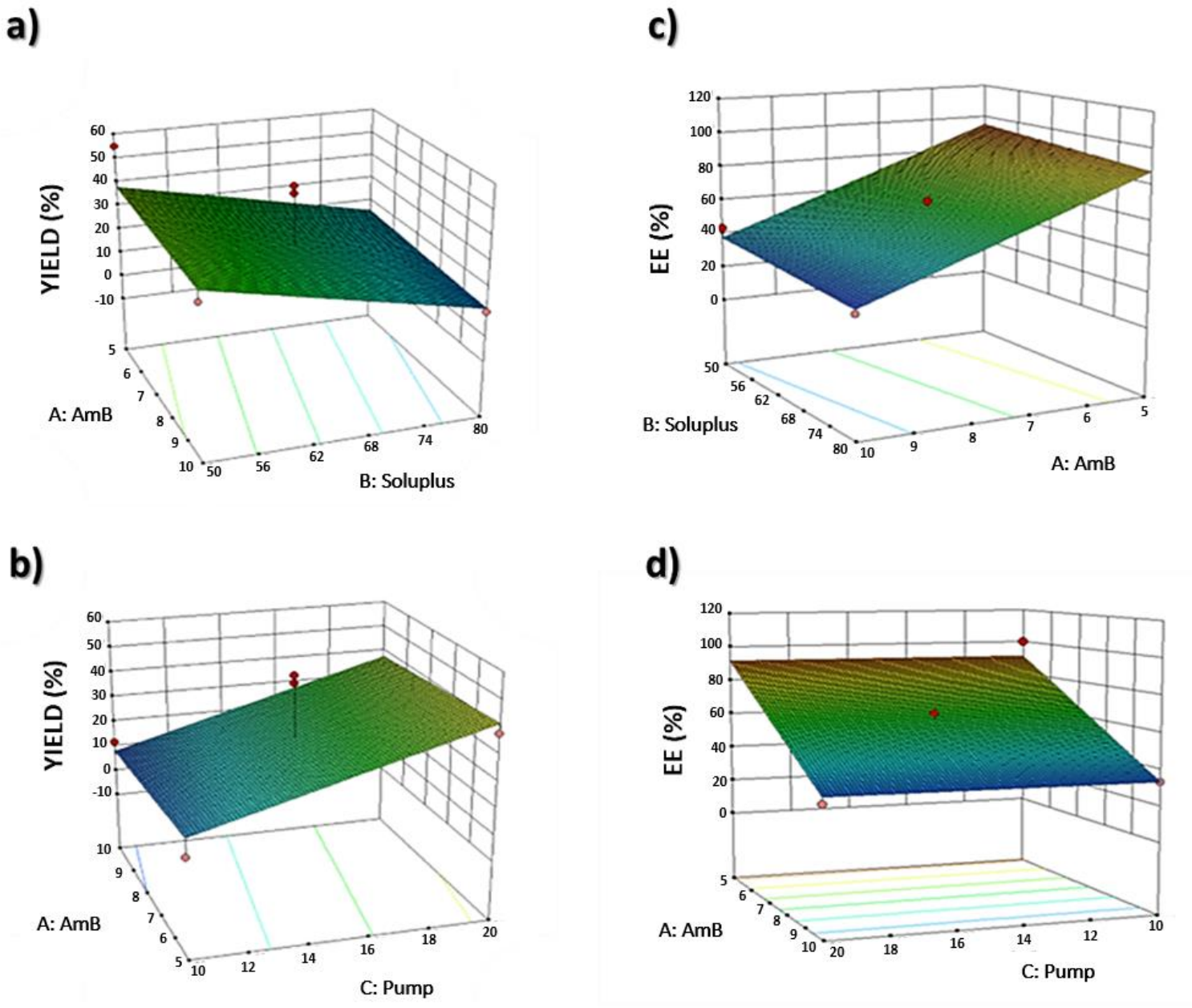

Figure 2. 3D response surface showing the influence of the amount of AmB, the amount of Soluplus, and the liquid velocity on the yield **(a,b)** and AmB encapsulation efficiency **(c,d)**.

3.3. Search for the optimum formulation and validation of QbD

The search for an optimum formulation was performed by trading- off various CQAs to attain the desired objectives giving priority to the maximization of AmB encapsulation efficiency and yield. Based on the aforesaid objectives, the optimized formulation was 5 % of AmB and 50 % of Soluplus®. The remaining formulation consisted of 45 % of Eudragit RL100. The following optimized processing factors were: 20 % liquid velocity equivalent to 12 mL/min, 70 ºC T inlet, 100 % vacuum, and 700 NL/h airflow. Validation of the QbD methodology revealed proximity between the predicted values of the responses (90 % confidence intervals) with observed ones for prepared check-point formulations: 52.86 % yield (51.8 % – 54.89 %), 95.6 % drug encapsulation (7 4 % - 100 %) and 0.79 aggregation rate (0.78 - 0.81).

After carrying out a preliminary set of drug release studies (data not shown), the release was too prolonged (> 7 days), and hence, the optimized formulation was modified by reducing the EudragitRL100 amount to 27.5 % and including 17.5 % of Kollicoat IR to accelerate the drug release profile. The same microparticle formulation was prepared replacing the amount of AmB with vancomycin. A combined formulation with 5 % AmB and 5 % vancomycin along with 50 % Soluplus, 22.5 % Eudragit RL100, and 17.5 % Kollicoat IR was also prepared. The yield, drug encapsulation, and aggregation states were within the confidence intervals from the DoE model generated.

3.4. Physicochemical and solid-state characterization

Morphology

SEM micrographs showed microparticles with a particle size ranging from 1 µm – 10 µm (**Figure 3**). No crystals were observed on the surface of the particles. However, the surface of the particles was collapsed with multiple angular faces which may enhance its surface area and points of contact upon reconstitution and spread over the surface of the femoral stem. **Figure 3d** illustrates how the particles upon reconstitution with hyaluronic acid and deionized water maintain intact spherical shape.

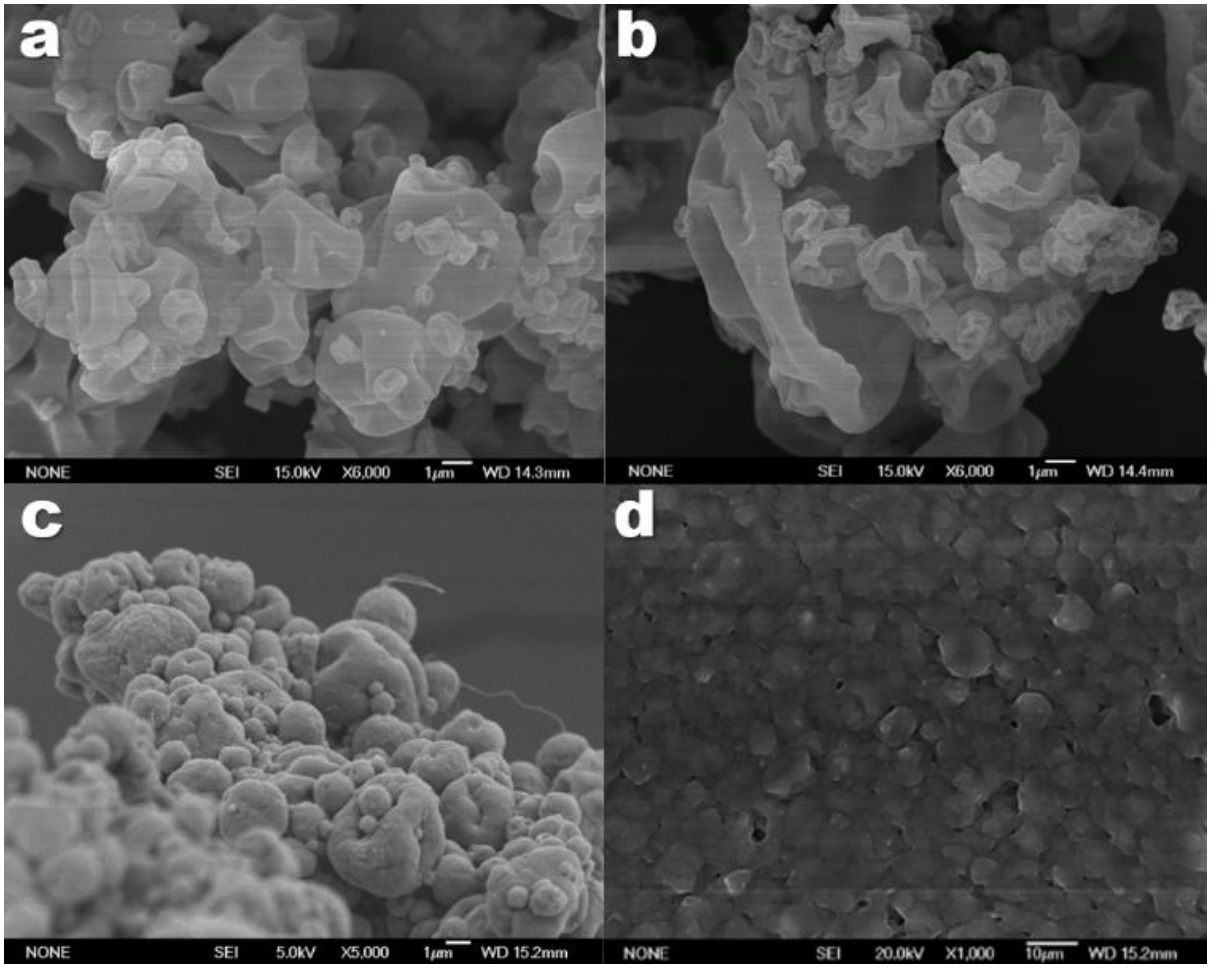

Figure 3. SEM micrographs of spray-dried microparticles. Key: **(a)** AmB microparticles**, (b)** Vancomycin microparticles; **(c)** AmB/vancomycin loaded microparticles; **(d)** AmB/vancomycin microparticles after reconstitution with hyaluronic acid and spread over the prosthesis surface.

X-Ray powder diffraction

pXRD pattern of the loaded microparticles as well as excipients, unprocessed materials, and physical mixtures are illustrated in **Figure 4**. Significant differences were observed between the two APIs, being AmB a crystalline raw powder material while vancomycin was fully amorphous. A characteristic amorphous halo was observed for both microparticulate formulations in contrast to the physical mixture containing AmB in which characteristic Bragg peaks attributed to AmB were observed.

DSC - TGA, and FTIR analysis

Thermal analysis for all the formulations and unprocessed materials is shown in **Figure 4**. In the case of AmB, two endothermic peaks were recorded at around 100 ºC and 200 ºC (**Figure 4**). Similar peaks were found in the physical mixture between AmB and unprocessed excipients (**Figure 4**). However, the endothermic events attributed to AmB were not present in the AmB-loaded microparticulate formulations which align with the pXRD results evidencing its amorphous nature. In the case of vancomycin, the unprocessed material was amorphous and did not show any endothermic event. However, the physical mixture between vancomycin and excipients showed two endothermic events which may be related to the degradation of Eudragit RL100 (~ 200 ºC) and the Soluplus®-hyaluronic acid (~250 ºC – 280 ºC). Only the second thermal events were found in the vancomycin-loaded microparticles which correlates with better thermal stability as indicated in the TGA analysis (**Figure 4**). Similar thermal stability was found for the AmB-loaded microparticles, which was better than the individual components (**Figure 4**).

The FTIR spectra show broad bands for all the components especially those in the amorphous state (**Figure 4**). Characteristic bands were observed at 1732 cm^{-1} and 1629 cm^{-1} in both the AmB and vancomycin microparticulate formulations which are attributed to the C=O stretching for the ester and the tertiary amide of the Soluplus® excipient. Due to the low amount of AmB and vancomycin in the microparticles, specific bands were not observed in the final formulation. However, differences were found between physical mixtures and microparticulate formulations, the latter with broader peaks attributed to its amorphous nature. It is worth highlighting the strong bands at 2853 cm^{-1} and 2929 cm^{-1}, attributed to O-H stretching and the formation of H-bonds between drugs and excipients.

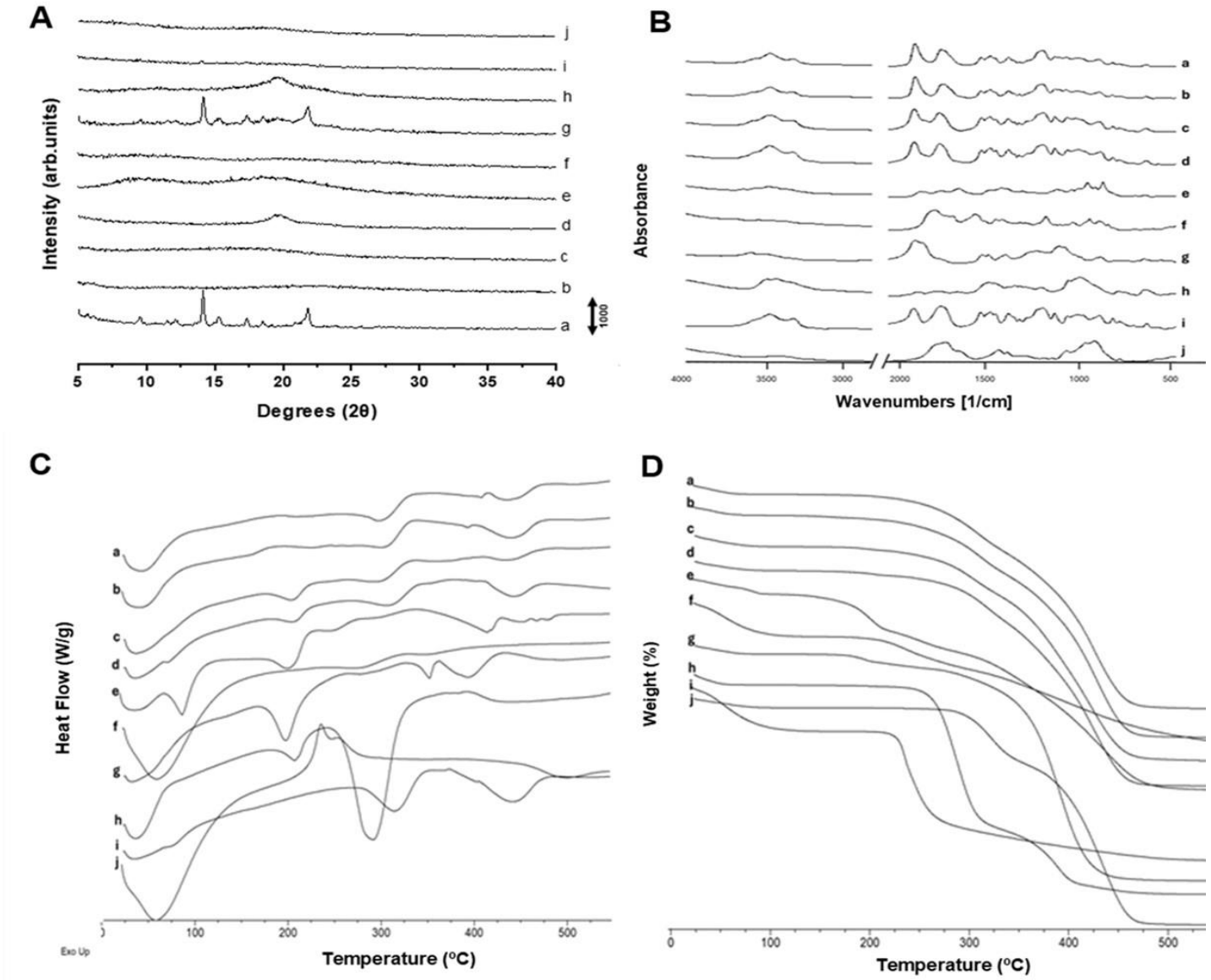

Figure 4. Physicochemical characterization of microparticulate formulations and unprocessed materials.

A. X-ray diffraction of microparticulate formulations. **Key**: **a)** AmB raw material; **b)** Vancomycin raw material; **c)** Eudragit® RL100; **d)** Kollicoat® IR; **e)** Soluplus®; **f)** Hyaluronic acid; **g)** Physical mixture between the excipients and AmB; **h)** Physical mixture between the excipients and vancomycin; **i)** AmB microparticles and **j)** Vancomycin microparticles. **B. FTIR analysis**, **C. DSC analysis** and, **D. TGA analysis** ; **Key**: **a)** Vancomycin loaded microparticles; b**)** AmB loaded microparticles; **c)** Physical mixture between the excipients and vancomycin; **d)** Physical mixture between the excipients and AmB; **e)** AmB raw material; **f)** Vancomycin raw material; **g)** Eudragit® RL100; **h)** Kollicoat® IR; **i)** Hyaluronic acid and **j)** Soluplus®.

3.5. Haemolysis assay

The HC_{50} (haemolytic concentration that produces 50 % haemolysis of exposed red blood cells) for AmB, vancomycin, and AmB/vancomycin microparticles were 99.16 µg/mL, 61.25 µg/mL and, 99.16 µg/mL respectively while the HC_{50} for AmB dissolved in DMSO was 22.55 µg/mL and, for the vancomycin, the toxicity values were above of the highest concentration (50 µg/mL) tested. The encapsulation of AmB in the microparticles showed a significant reduction in the haemolytic toxicity of the drug ($p < 0.05$). HC_{50} was 4.3 times lower after the AmB encapsulation within microparticles. This is a key factor in developing parenteral formulations of AmB, as the main adverse effect limiting therapy along with its nephrotoxicity [20, 34]. The encapsulated AmB showed a sustained drug release profile in an aqueous medium which means that the toxicity is limited upon administration in contact with physiological fluids. The same protective effect was observed for the combined AmB/vancomycin microparticulate formulation. A 5-fold reduction in the HC_{50} was observed. However, this protective effect was not found with vancomycin microparticles considering that this drug is not haemolytic. Vancomycin microparticles were more haematotoxin, due to the combined effect of the excipients that are acting as surfactants on the RBCs (**Figure 5**).

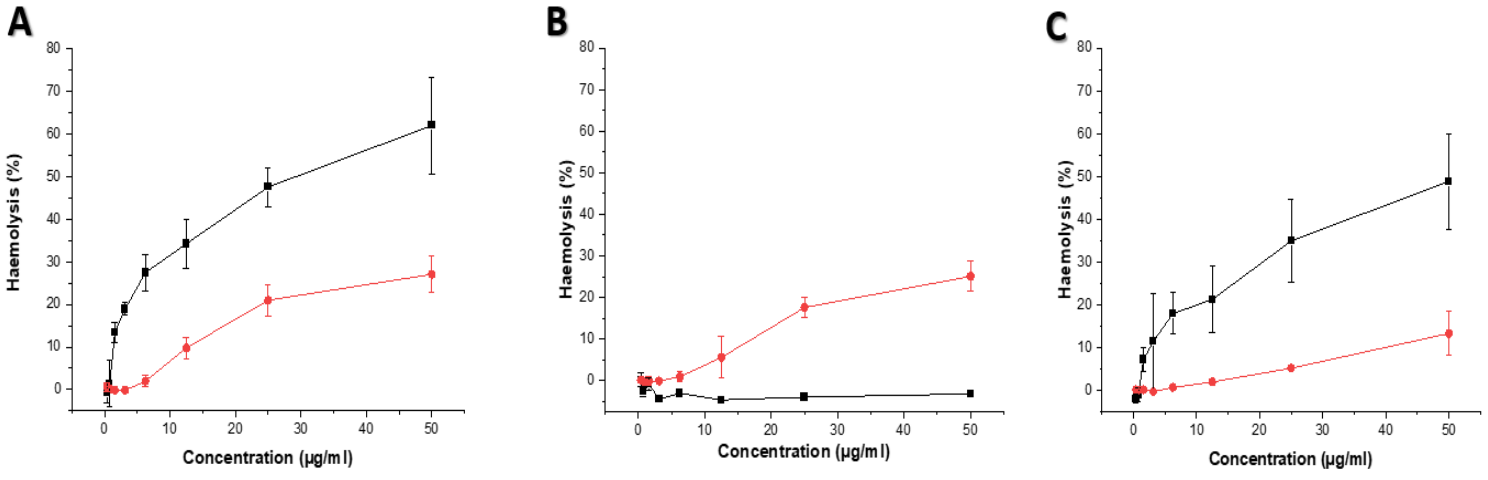

Figure 5. Haemolytic toxicity of microparticulate formulations compared with the active ingredients dissolved in DMSO. Key: **A)** (—■—)AmB (—●—)AmB microparticles; **B)** (—■—)Vancomycin (—●—)Vancomycin microparticles and, **C)** (—■—) AmB and vancomycin (—●—) Combined microparticles with vancomycin and AmB.

3.6. Adhesion and rheological assays

After reconstitution of the microparticles in deionized water and hyaluronic acid, a bioadhesive gel was formed which was easily spread on the surface of the femoral stem. The drying time was below 10 min (n = 3) which facilitates its administration during the surgical procedure.

3.7 Drug release

The three microparticulate formulations showed a sustained release profile marked by a burst release ranging from 40 % to 80 % depending on the drug over the first 10 h followed by a prolonged sustained release over 7 days (**Figure 6**). After 24 h, drug concentration in the medium was reduced which can be due to a parachute effect, especially for AmB whose aqueous solubility is very low. Albumin was added to the medium to compensate for the poor AmB aqueous solubility. In the case of vancomycin, drug stability in aqueous media is poor showing fast degradation (1 % of drug degraded per day). The release profile of a single drug-loaded microparticle was significantly different from those combined ones (p-value < 0.05). AmB-loaded microparticles had a more prolonged release in comparison to the combined-loaded microparticles while the opposite effect was observed for the vancomycin (faster release with the vancomycin-loaded microparticles compared to the dual formulation). This indicates an interaction between both drugs when they are co-formulated together.

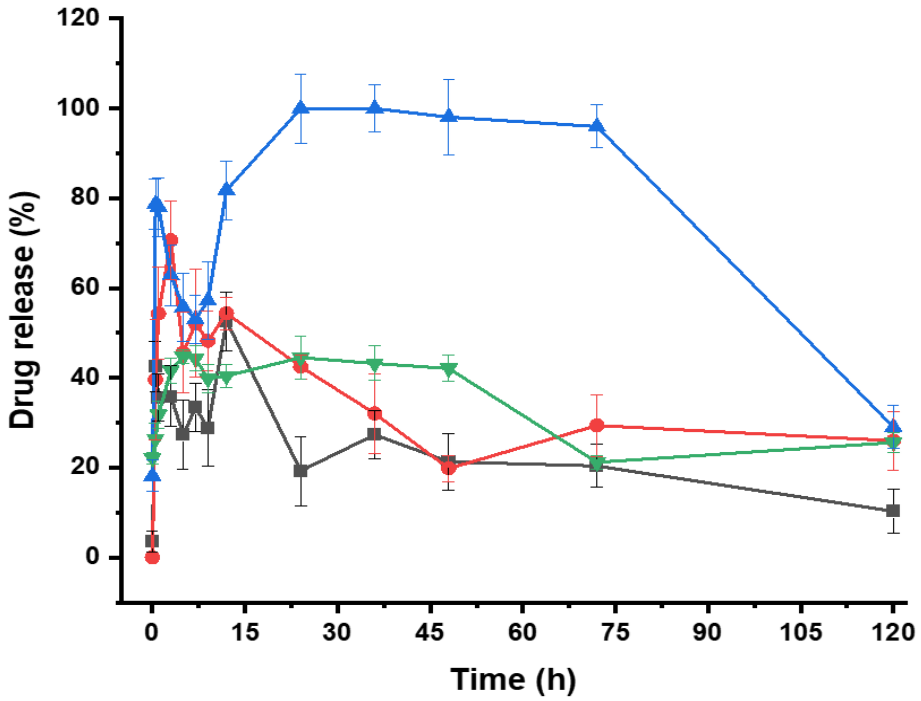

Figure 6. **Drug release after application of the bioadhesive gel on the surface of the femoral stem**. Key: (—■—) Amount of AmB released from microparticles loaded with AmB, **(—●—)** Amount of AmB released from microparticles loaded with vancomycin and AmB; **(—▲—)** Amount of vancomycin released from vancomycin microparticles, and **(—▼—)** Amount of vancomycin released from vancomycin and AmB microparticles.

3.8. Accelerated and long-term drug stability

The kinetic model that showed the best fit for the experimental data points at different conditions for AmB-loaded microparticles was zero-order, while Avrami fitted the degradation profile for vancomycin-loaded microparticles ($R > 0.9$). The degradation rate using either the Avrami or zero-order reaction for both microparticles at different temperatures was employed to extrapolate the activation energy (Ea) from the Arrhenius equation. The activation energy for both formulations was significantly higher in the presence of RH than without RH, indicating better chemical stability (**Table 2**). This can be attributed to a solid-state transition upon exposure to RH, such as a physical transformation from amorphous to crystalline state, which indicates the need for desiccated conditions during storage for both formulations. From the Arrhenius equations, the iso-conversion time considering a specification limit of 10 % degradation at 4 ºC under desiccated conditions for AmB and vancomycin microparticles was 401 days and 214 days, respectively.

Table 2. The correlation coefficient, activation energy, and degradation kinetics of amB and vancomycin microparticulate formulations.

		Correlation coefficient (R)	Ea (kcal/mol)	Degradation kinetic model
Vancomycin microparticles	**RH**	0.9020	14.5134	Avrami
	Without RH	0.9776	9.5878	
AmB microparticles	**RH**	0.8865	14.8176	Zero
	Without RH	0.9936	7.4200	

Long-term stability studies showed that vancomycin-loaded microparticles were chemically stable for at least 100 days at 4 °C/10 % RH and at least 250 days at 25 °C/ 60 % RH (drug content > 90 %). This indicates the susceptibility for crystallization for vancomycin-loaded microparticles which explains the solid-state transformation from amorphous to crystalline and hence, the increase in chemical stability at 25 ºC compared

to refrigerated conditions. AmB microparticles remained stable for more than one year at 4 °C/10 % RH and 25 °C/60 % RH conditions. This indicates that desiccated and refrigerated conditions are necessary to maintain the physicochemical stability of both AmB and vancomycin-loaded microparticles (**Figure 7**). Predicted chemical stability from the Arrhenius equation agreed with the experimental long-term assessment.

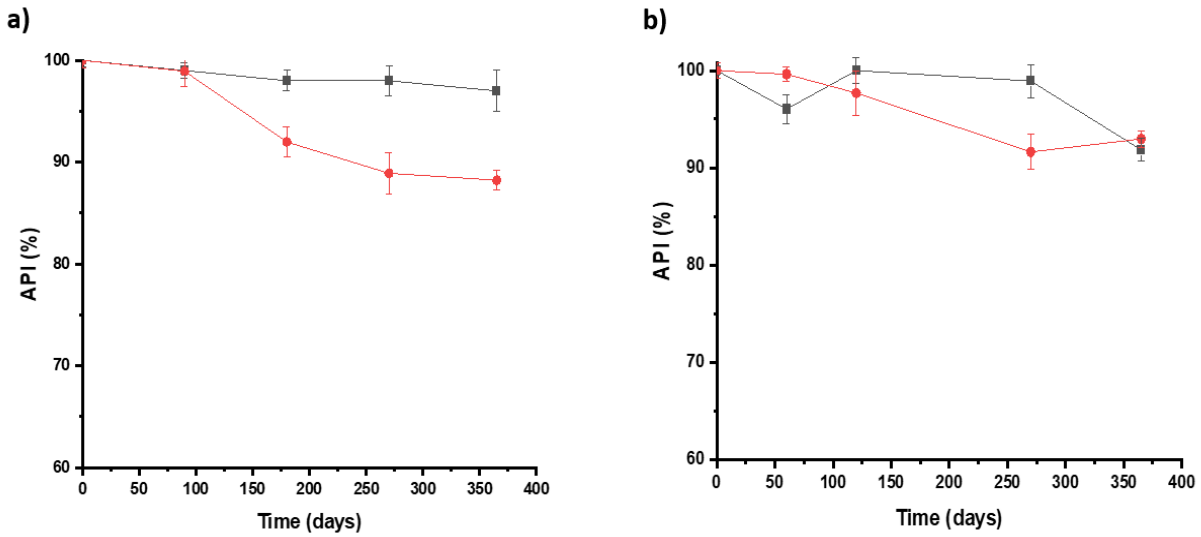

Figure 7. AmB and vancomycin-loaded microparticles long-term chemical stability at different storage conditions. **a)** 5 ± 3 °C/10 % RH and **b)** 25 ± 2 °C/60 % RH ± 5 % RH. Key: (-●-) Vancomycin and (-■-)AmB.

3.10. Antibacterial *in vitro* assay

Antibacterial efficacy studies revealed an inhibition halo above 15 mm for all the formulations tested, including vancomycin-loaded microparticles, the AmB/vancomycin-loaded microparticles, and the drug dissolved in deionized water. This indicates that the drug can freely diffuse across the agar to elicit its antimicrobial effect. However, similarly to the antifungal activity, the sustained drug release profile led to a lower drug concentration in the media resulting in a lower efficacy compared to commercial disks of vancomycin when tested against *S. epidermidis*. For the *S. aureus,* no significant differences (p-value > 0.05) were found between the microparticulate formulations and the Neo-Sensitabs™ discs. For *S. epidermidis,* the Minimum Inhibitory Concentration (MIC) was ≤ 2 µg/mL for vancomycin and vancomycin-loaded microparticles, while for the combined microparticles, the MIC was 8 µg/mL. For *S. aureus*, the MIC was 16 µg/mL for vancomycin dissolved in the agar medium and 32 µg/mL for vancomycin-loaded microparticles as well as the combined microparticles (**Figure 8**).

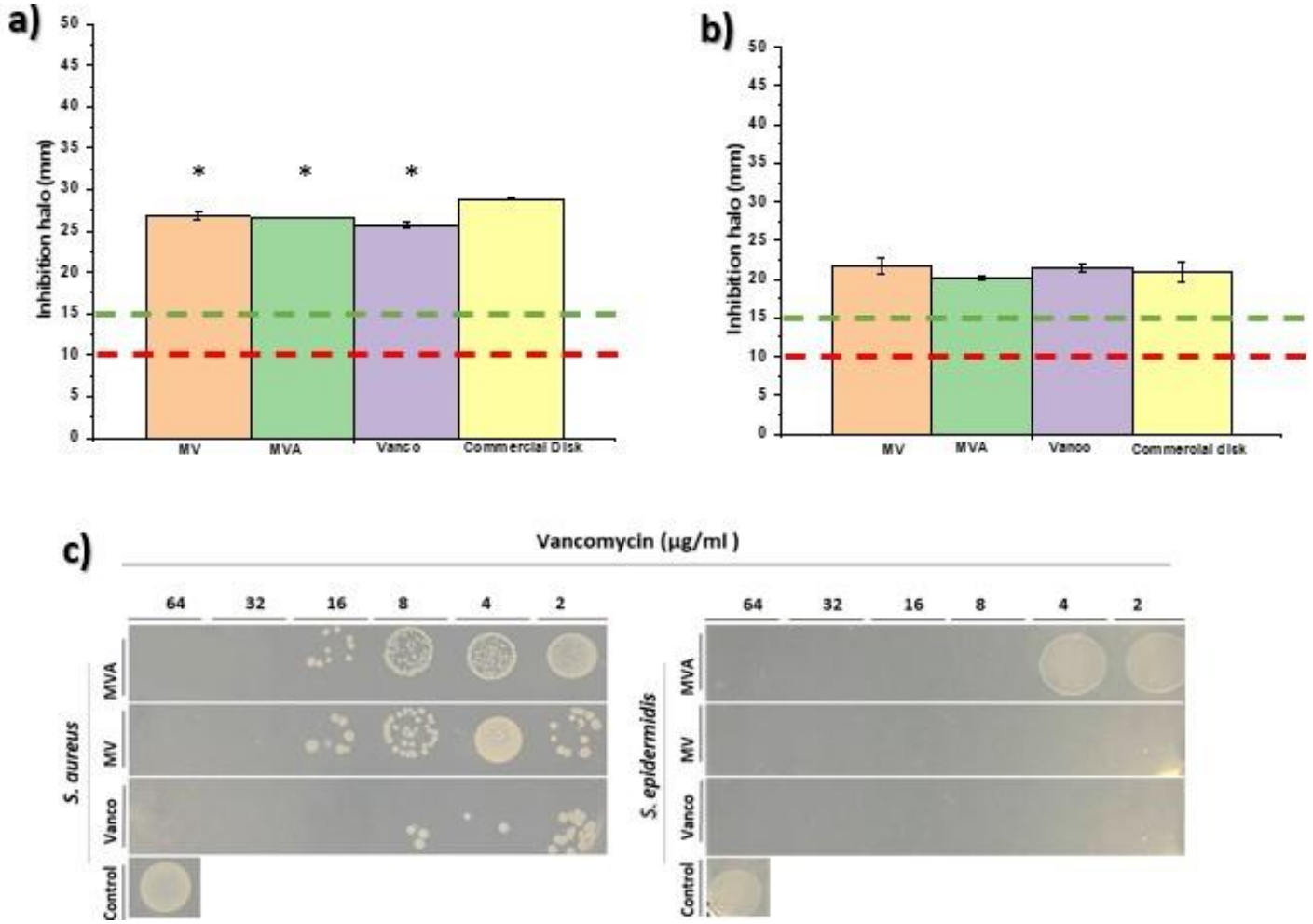

Figure 8. ***In vitro*** **antibacterial efficacy assay against different species of *Staphylococcus* spp**. Key: (**MV**) Vancomycin-loaded microparticles; (**MVA**) AmB/Vancomycin-loaded microparticles and, (**Vanco**) Vancomycin dissolved in DMSO * Statistical differences ($p < 0.05$). Key: (**a**) *S. epidermidis*, (**b**) *S. aureus*. (**c**) Bacterial growth at different concentrations of vancomycin-loaded microparticles alone or in combination with AmB.

3.9. Antifungal in vitro assay

All three strains (*C. albicans, C. glabrata, C. parapsilopsis*) were susceptible to AmB release from microparticles exhibiting a halo above 1.5 cm. However, the halo was below 1.5 cm but above 1.0 cm for *C. Krusei*, as it is well known that this species is more resistant to the effect of the drug. Despite the lower halo for *C. Krusei*, the halo was above 1.0 cm which indicates that the effect is dose-dependent and hence, greater AmB doses will be needed to eradicate a *C. krusei* infection (**Figure 9**). Also, AmB release from microparticles showed a significant lower effect than AmB dissolved in DMSO. This can be linked to the slower release of AmB from the microparticles and hence, the lower drug concentration gradient achieved in the agar plate.

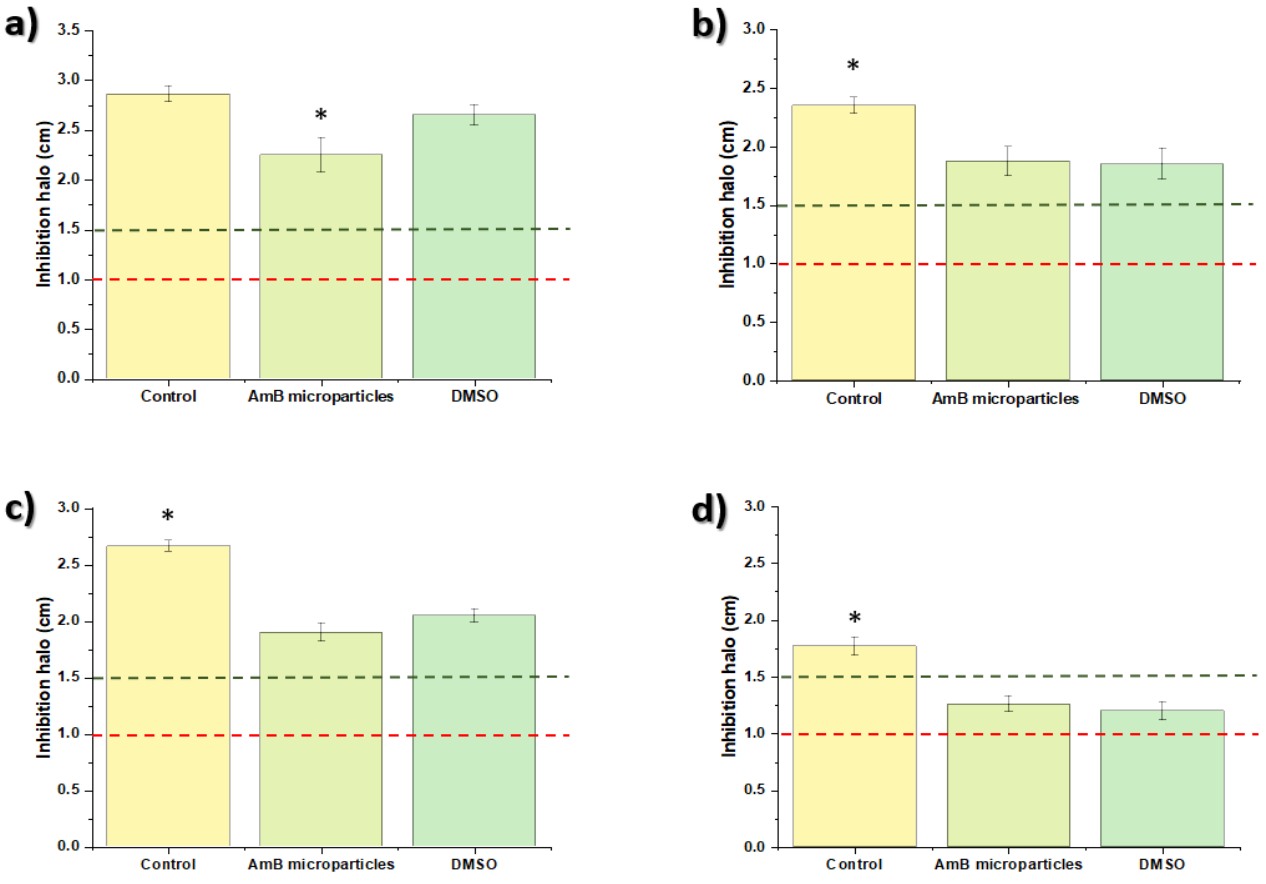

Figure 9. ***In vitro*** **antifungal activity of AmB-loaded microparticles against different** ***Candida*** **spp.** * Statistical differences ($p < 0.05$). Key: **(a)** *C. albicans*, **(b)** *C. parapsilosis*, **(c)** *C. glabrata* and **(d)** *C. krusei.*

Regarding the absence or presence of colonies in Sabouraud agar plates, the Minimum Fungicidal Concentration (MFC) of AmB varied among different *Candida spp*, being the most susceptible species, *C. albicans* and *C. glabrata* (0.25 μg/mL) followed by *C.*

parapsilosis (1 μg/mL), and *C. krusei* (2 μg/mL) to the AmB-loaded microparticles (**Figure 10**). The efficacy of the combined AmB/Vancomycin was superior for *C. albicans* (MFC of 0.125 μg/mL) but lower for the rest of the *Candida* spp. tested. In all the cases, AmB dissolved in DMSO showed a greater activity considering that the sustained drug release from the microparticles reduced the available concentration of the drug at shorter times.

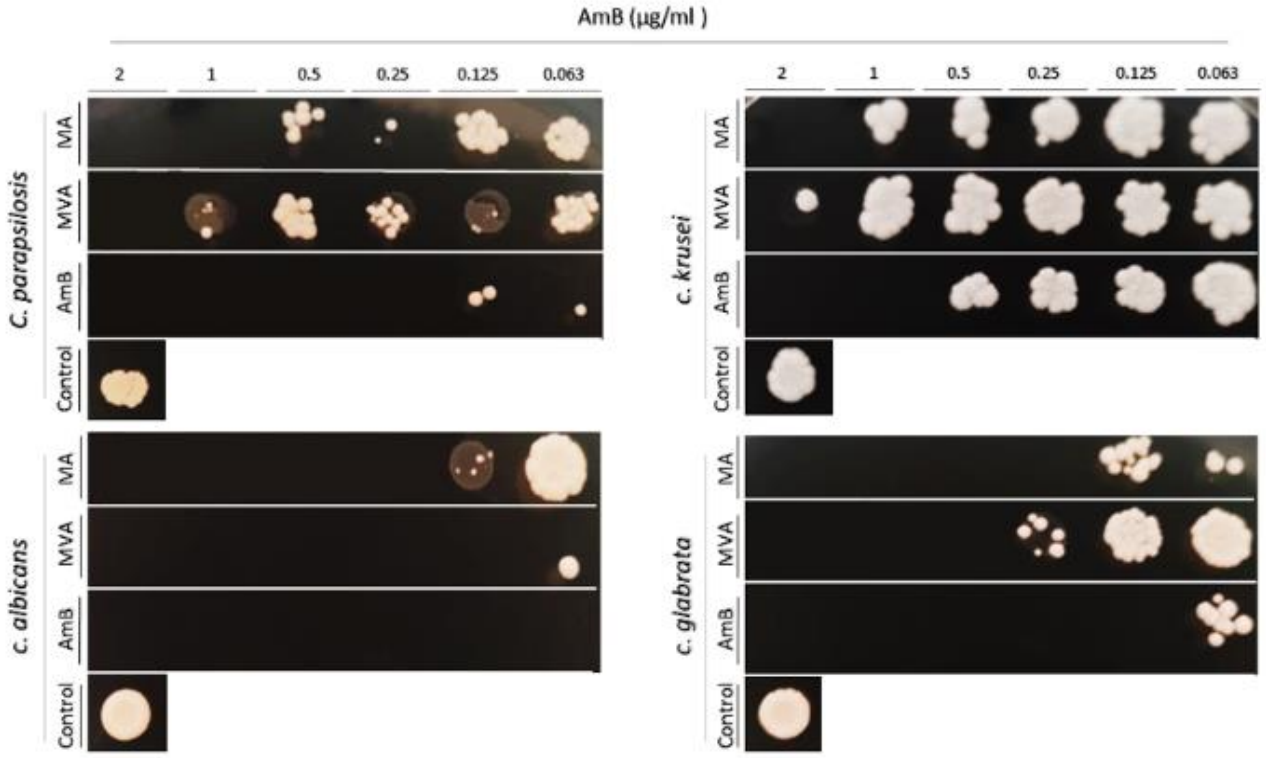

Figure 10. Fungal growth at different concentrations of AmB or AmB/vancomycin microparticles. Key: (**MA**) AmB-loaded microparticles, (**MVA**) AmB/Vancomycin-loaded microparticles, and (**AmB**) Amphotericin B dissolved in DMSO.

3.11. Cytotoxicity assays

The cytotoxic effect of microparticles loaded with vancomycin, AmB, and vancomycin/AmB and the corresponding drugs in solution was evaluated on Saos-2, hFOB, and BJ cells for 24 h, 72 h, and 1 week by the MTT assay (**Figure 11**). For Saos-2 cells, none of the treatments significantly affected the viability of the cells after the 24-h and 72-h incubation periods. However, after 1-week treatment, the results showed that AmB and the combination of AmB and vancomycin significantly reduced the viability of Saos-2 cells by around 40 %. For hFOB cells, after 24 h and 72 h of drug exposure, cell viability was significantly reduced below 40 % when treated with AmB and with AmB/vancomycin compared to the untreated cells. Moreover, after one week of treatment, a significant loss of viability was observed when the hFOB cells were treated with both AmB (0.9 % of cell viability) and AmB/vancomycin (5.9 %), but this cytotoxicity was also observed with the AmB-loaded microparticles (11.4 % viability) and the AmB/vancomycin-loaded microparticles (38.4%). These results evidenced a significant cytoprotective effect when the drug was encapsulated within microparticles along with the AmB/vancomycin combination. Finally, for BJ cells, viability was significantly reduced over time with AmB and with AmB/vancomycin solutions but not when the drugs were encapsulated at all three treatment times. A significant cytoprotective effect was also observed with the microparticulate formulations as well as the AmB/vancomycin combination demonstrating a positive pharmacological interaction between AmB and vancomycin.

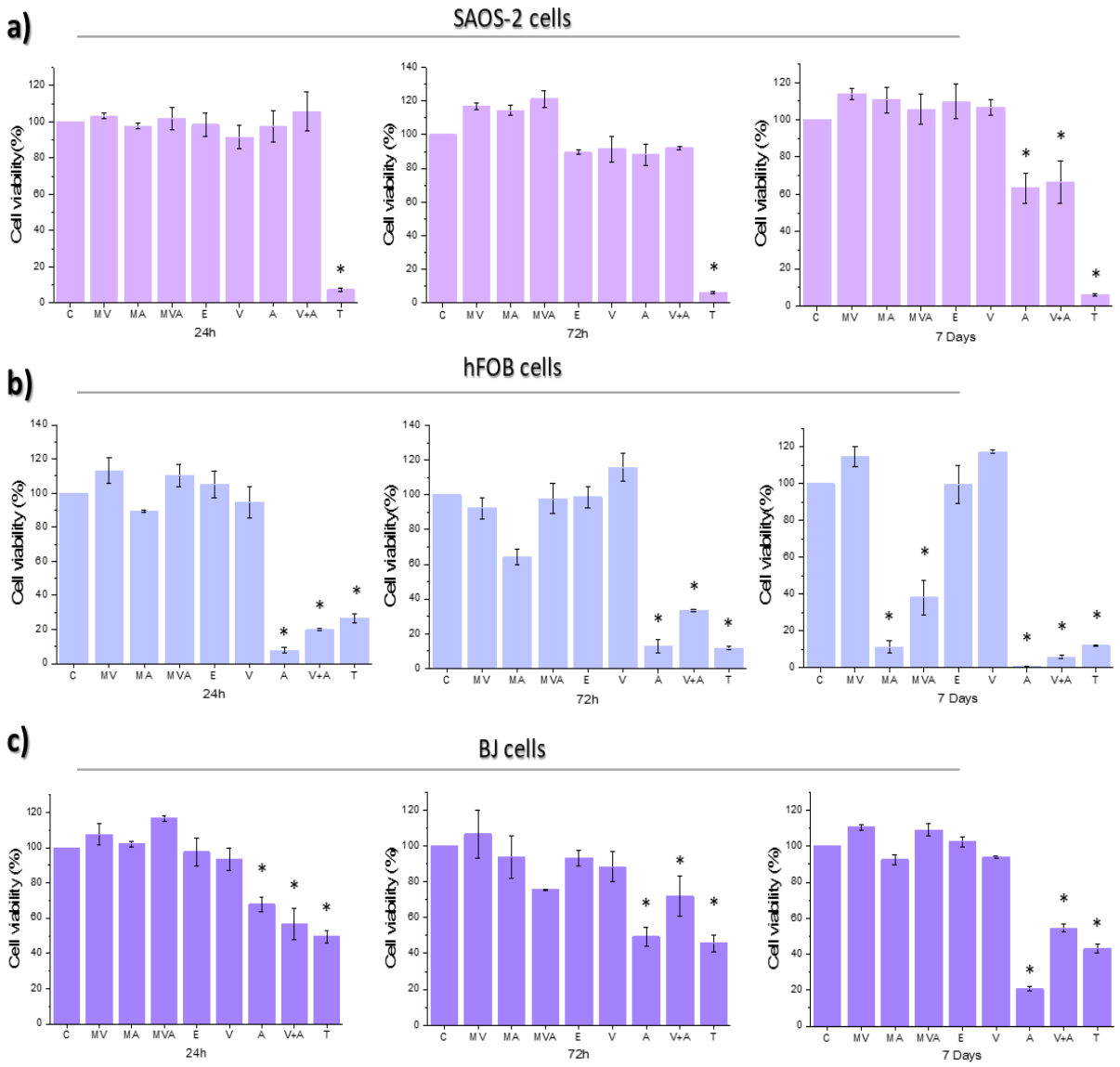

Figure 11. Effect on a) Saos-2, b) hFOB and c) BJ cell viability. Cells were treated with microparticles loaded with vancomycin, AmB and AmB/vancomycin, as well as the drugs as control for 24 h, 72 h and 7 days. Cytotoxicity was analyzed by MTT assay. Key: (**C**) Control; (**MV**) Vancomycin-loaded microparticles; (**MA**) AmB-loaded microparticles; (**MVA**) AmB/vancomycin-loaded microparticles; (**E**) Blank spray dried microparticles; (**V**) Free vancomycin; **(A**) Free AmB; (**V+A**) Free vancomycin and AmB; (**T**) Triton.

Evaluation of cell morphology by SEM

Figure 12 shows the cell morphology of Saos-2, hFOB, and BJ cells after 7 days of exposition to different treatments. In these three cell lines, it is worth noting that the exposition to free AmB or the combination of AmB/vancomycin significantly affects cell morphology, as well as the areas of growing, were sparsely populated with cells. The drug encapsulation in microparticles exerted a protective cell effect, especially from AmB and the combination of both drugs.

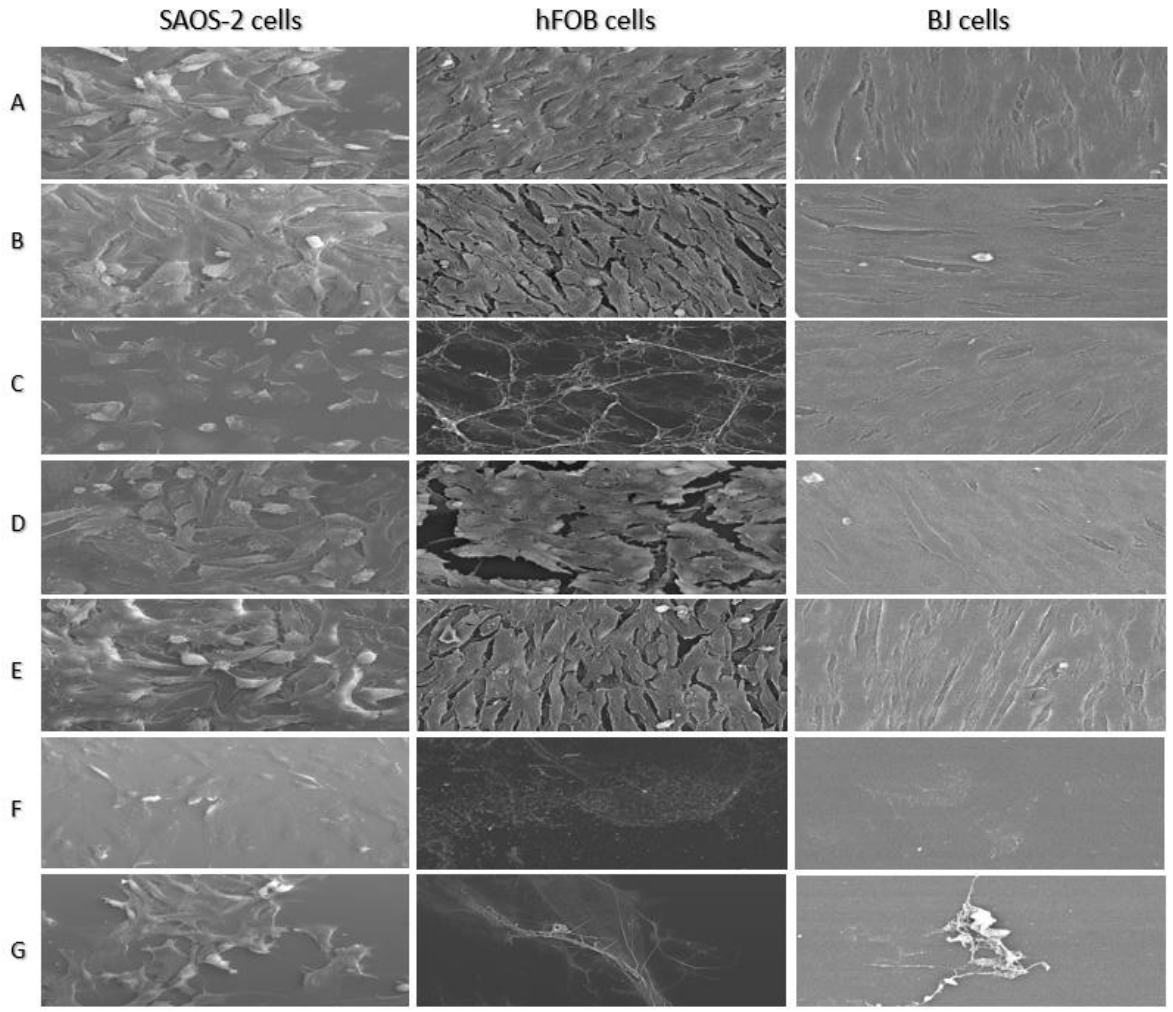

Figure 12. SEM images (magnification x500) of Saos-2 cells, hFOB cells, and BJ cells treated with microparticles loaded with vancomycin, AmB, and vancomycin/AmB and the corresponding drugs for 1 week. Key: (**A**) Control; (**B**) Vancomycin-loaded microparticles; (**C**) AmB-loaded microparticles; (**D**) Combined AmB/vancomycin-loaded microparticles; (**E**) Free vancomycin; **(F)** Free AmB; (**G**) Free vancomycin and AmB.

4. Discussion

PJI is one of the most overwhelming complications after an arthroplasty surgery, increasing the health care system costs, treatment, and the risk of morbidity and mortality significantly. Even though comorbidities such as immunosuppression, diabetes, high body mass index, and others, can elevate the risk of PJI, the related risk with long-lasting operations times is higher [35]. Based on this, prophylaxis is an essential tool against this problem and could reduce significantly the risk of complications [36]. However, limited options are available to surgeons.

Direct administration of antibiotics into the surgical site as powder or solution has been studied as PJI prophylaxis in primary joint replacement. Even though local levels are high during the first h post-surgery, a rapid decline resulting in subtherapeutic concentrations occurs which makes it an easy but with a poor outcome clinical solution [37]. To maintain high local concentration with limited systemic exposure, antimicrobials can be administered via an intra-articular catheter or combined with a carrier to enhance their pharmacokinetic and pharmacological profile [38]. Carrier options include non-resorbable polymethylmethacrylate (PMMA) bone cement and resorbable materials such as calcium sulfate, hydroxyapatite, bioactive glass, and hydrogels. PMMA allows for the formation of structural spacers which is used in multi-stage revision procedures, but it requires subsequent removal and has variable antibiotic compatibility and insufficient drug delivery to reach pharmacological levels [39]. Calcium sulfate is one of the most researched biocompatible carriers for PJIs which can be shaped into beads to suit a variety of clinical applications and releases 100 % of loaded antimicrobial drugs over several weeks [40]. However, it is used is associated with wound leakage, and hypercalcemia, being the clinical evidence for its effectiveness still in the early stages [41]. The use of bacteriophages has attractive inherent properties as are specifically targeted to bacteria with no toxicity on mammalian cells. However, it is required to have phage libraries to target different bacterial species, and its current use for PJIs is limited [42]. Finally, hydrogels offer versatile compatibility with antimicrobials, and elution profiles can be tuned and easily adjusted to patients' needs, but their clinical use is currently unexplored [43, 44]. In this work, we have unraveled the potential of microparticulate hydrogels for the treatment and prophylaxis of PJIs.

Hydrophobic surfaces might be a suitable substrate for bacterial colonization, while hydrophilic surfaces can prevent biofilm formation. Switching towards a hydrophilic microenvironment at the surface of the metallic prosthesis can be an optimal prophylactic approach to prevent bacterial adhesion and consequently biofilm formation. Hyaluronan coating has been demonstrated to change the hydrophobicity of an implant surface into a hydrophilic surface reducing significantly bacterial attachment [45].

Following this premise, we have developed a hyaluronic-based hydrogel that incorporates antimicrobial drugs in microparticulate systems to prolong drug release for one week. The sustained release provided by microparticles resulted in excellent biocompatibility with a significant reduction in haemotoxicity, especially with AmB which is highly haemolytic, but also no signs of toxicity were observed in osteoblasts and fibroblasts. Drug releases were performed mimicking the joint cavity with limited access to physiological fluids. Even though the slower release, the resulting antimicrobial concentration in aqueous media exhibited good antimicrobial activity, which indicated that the release rate was suitable to elicit a pharmacological effect at the joint space. It is worth noting that the combination of AmB and vancomycin within the same microparticulate carrier has shown to be a promising approach for PJIs targeting both bacterial and fungal infections with complementary hydrophilicity, amphiphilic for AmB and hydrophilic for vancomycin. This makes it feasible to prolong the release of vancomycin while enhancing the release of AmB. Even though, further *in vivo* studies need to be performed to confirm the pharmacological-toxicological profile, in this work we have demonstrated for the first time a novel approach to treat and prevent PJIs based on bioadhesive microparticulate hydrogels.

5. Conclusions

The microparticles showed a sustained release profile marked by a burst release followed by a controlled release until 7 days. The excipients were carefully selected, and drug encapsulation resulted in higher biocompatibility against mammalian cells (RBCs, osteoblast, and fibroblasts) and excellent antimicrobial efficacy against bacteria and fungi. The formulation showed optimal adhesion profile to the prosthesis in less than 5 min avoiding extending the surgical procedure. These results show this microparticulate formulation could be a novel and promising approach for the treatment of PJIs. However, further *in vivo* studies need to be performed to confirm the pharmacological-toxicological profile.

Acknowledgments

This study was partially supported by the Complutense University of Madrid Research Group (Innovation in Pharmacology, Nanotechnology, and personalized medicine by 3D printing). Dolores Serrano acknowledges the support received from ESCMID 2021 research grants. This study has been also funded by the Ministry of Science and Innovation (award PID2021-126310OA-I00 to Dolores Serrano.

References

1. A. Hernández-Aceituno, M.R.-Á., R. Llorente-Calderón, P. Portilla-Fernández, A. Figuerola-Tejerina, *Factores de riesgo en artroplastia total y parcial de cadera: infección y mortalidad.* Revista Española de Cirugía Ortopédica y Traumatología, 2021. **65**(4): p. 239-247.
2. Jin, X., et al., *Estimating incidence rates of periprosthetic joint infection after hip and knee arthroplasty for osteoarthritis using linked registry and administrative health data.* Bone Joint J, 2022. **104-B**(9): p. 1060-1066.
3. M.M. Martínez-Suárez, J.C.A.-L., D. Alonso-Álvarez, A.J. López-Díaz, A. Fernández-Somoano, A. Tardón-García,, *Tasas de infección de herida quirúrgica en artroplastia de cadera* Journal of Healthcare Quality Research, 2018. **33**(4): p. 219-224.
4. Franco Arenaz, M., *Epidemiología de la infección de prótesis articular en España en la última década. Análisis de la evolución de la etiologia en el tiempo.* . 2017, Universidad Autonoma de Barcelona Barcelona.
5. Zimmerli W, T.A., Ochsner PE. , *Prosthetic-joint infections.* . N Engl J Med 2004(351): p. 1645-1654.
6. Sambri A, Z.R., Fiore M, Bortoli M, Paolucci A, Filippini M, Zamparini E, Tedeschi S, Viale P, De Paolis M., *Epidemiology of Fungal Periprosthetic Joint Infection: A Systematic Review of the Literature.* doi:10.3390/microorganisms11010084, 2022. **11**(1): p. 84.
7. Chisari E, L.F., Fei J, Parvizi J., *Fungal periprosthetic joint infection: Rare but challenging problem.* Chin J Traumatol., 2022. **25**(2): p. 63-66.
8. Rozis, M., D.S. Evangelopoulos, and S.G. Pneumaticos, *Orthopedic Implant-Related Biofilm Pathophysiology: A Review of the Literature.* Cureus, 2021. **13**(6): p. e15634.
9. Murdoch DR, R.S., Fowler VG, Jr, et al, *Infection of orthopedic prostheses after Staphylococcus aureus bacteremia.* . Clin Infect Dis 2001(32): p. 647-649.
10. Zakovicova P, B.O., Trampuz A. , *Periprosthetic joint infection: current concepts and outlook.* EFORT Open Rev. , 2019. **4**(7): p. 482-494.
11. Li, C., N. Renz, and A. Trampuz, *Management of Periprosthetic Joint Infection.* Hip Pelvis, 2018. **30**(3): p. 138-146.

12. Xu, C., et al., *Is Treatment of Periprosthetic Joint Infection Improving Over Time?* J Arthroplasty, 2020. **35**(6): p. 1696-1702 e1.
13. Taha, M., et al., *New Innovations in the Treatment of PJI and Biofilms-Clinical and Preclinical Topics.* Curr Rev Musculoskelet Med, 2018. **11**(3): p. 380-388.
14. Izakovicova, P., O. Borens, and A. Trampuz, *Periprosthetic joint infection: current concepts and outlook.* EFORT Open Rev, 2019. **4**(7): p. 482-494.
15. Natsuhara, K.M., et al., *Mortality During Total Hip Periprosthetic Joint Infection.* J Arthroplasty, 2019. **34**(7S): p. S337-S342.
16. Lu, J., et al., *Infection after total knee arthroplasty and its gold standard surgical treatment: Spacers used in two-stage revision arthroplasty.* Intractable Rare Dis Res, 2017. **6**(4): p. 256-261.
17. McNally, M., et al., *The EBJIS definition of periprosthetic joint infection.* Bone Joint J, 2021. **103-B**(1): p. 18-25.
18. Blanco, J.F., et al., *Risk factors for periprosthetic joint infection after total knee arthroplasty.* Arch Orthop Trauma Surg, 2020. **140**(2): p. 239-245.
19. Premkumar, A., et al., *Projected Economic Burden of Periprosthetic Joint Infection of the Hip and Knee in the United States.* J Arthroplasty, 2021. **36**(5): p. 1484-1489 e3.
20. Serrano, D.R., et al., *Hemolytic and pharmacokinetic studies of liposomal and particulate amphotericin B formulations.* Int J Pharm, 2013. **447**(1-2): p. 38-46.
21. Ruiz, H.K., et al., *New amphotericin B-gamma cyclodextrin formulation for topical use with synergistic activity against diverse fungal species and Leishmania spp.* Int J Pharm, 2014. **473**(1-2): p. 148-57.
22. Fernandez-Garcia, R., et al., *Self-assembling, supramolecular chemistry and pharmacology of amphotericin B: Poly-aggregates, oligomers and monomers.* J Control Release, 2022. **341**: p. 716-732.
23. Anaya, B.J., et al., *Engineering of 3D printed personalized polypills for the treatment of the metabolic syndrome.* Int J Pharm, 2023. **642**: p. 123194.
24. Pineros, I., et al., *Analgesic and anti-inflammatory controlled-released injectable microemulsion: Pseudo-ternary phase diagrams, in vitro, ex vivo and in vivo evaluation.* Eur J Pharm Sci, 2017. **101**: p. 220-227.

25. Fernandez-Garcia, R., et al., *Ultradeformable Lipid Vesicles Localize Amphotericin B in the Dermis for the Treatment of Infectious Skin Diseases.* ACS Infect Dis, 2020. **6**(10): p. 2647-2660.
26. Serrano DR, L.A., Dea-Ayuela MA, Bilbao-Ramos PE, Garrett NL, Moger J, Guarro J, Capilla J, Ballesteros MP, Schätzlein AG, Bolás F, Torrado JJ, Uchegbu IF. , *Oral particle uptake and organ targeting drives the activity of amphotericin B nanoparticles.* Mol Pharm. , 2015. **12**(2): p. 420-431.
27. Sánchez-Somolinos M, D.-N.M., Benjumea A, Tormo M, Matas J, Vaquero J, Muñoz P, Sanz-Ruíz P, Guembe M. , *Determination of the Elution Capacity of Dalbavancin in Bone Cements: New Alternative for the Treatment of Biofilm-Related Peri-Prosthetic Joint Infections Based on an In Vitro Study.* Antibiotics (Basel). 2022. **11**(10): p. 1300.
28. Serrano, D.R., et al., *Designing Fast-Dissolving Orodispersible Films of Amphotericin B for Oropharyngeal Candidiasis.* Pharmaceutics, 2019. **11**(8).
29. Serrano, D.R., et al., *Optimising the in vitro and in vivo performance of oral cocrystal formulations via spray coating.* Eur J Pharm Biopharm, 2018. **124**: p. 13-27.
30. Waterman, K.C. and R.C. Adami, *Accelerated aging: prediction of chemical stability of pharmaceuticals.* Int J Pharm, 2005. **293**(1-2): p. 101-25.
31. Rolon, M., et al., *Solid Nanomedicines of Nifurtimox and Benznidazole for the Oral Treatment of Chagas Disease.* Pharmaceutics, 2022. **14**(9).
32. Herigstad, B., M. Hamilton, and J. Heersink, *How to optimize the drop plate method for enumerating bacteria.* J Microbiol Methods, 2001. **44**(2): p. 121-9.
33. Serrano, D.R., et al., *A novel formulation of solubilised amphotericin B designed for ophthalmic use.* Int J Pharm, 2012. **437**(1-2): p. 80-2.
34. Torrado, J.J., D.R. Serrano, and I.F. Uchegbu, *The oral delivery of amphotericin B.* Ther Deliv, 2013. **4**(1): p. 9-12.
35. Pablo Sanz-Ruiz, J.A.M.-D., Manuel Villanueva-Martínez, Alex Dos Santos-Vaquinha Blanco, Javier Vaquero., *Is Dual Antibiotic-Loaded Bone Cement More Effective and Cost-Efficient Than a Single Antibiotic-Loaded Bone Cement to Reduce the Risk of Prosthetic Joint Infection in Aseptic Revision Knee Arthroplasty?* The Journal of Arthroplasty

2020. **34**(12): p. 3724-3729.

36. Parvizi J, S.K., Ragland PS, Pour AE, Mont MA., *Efficacy of antibiotic-impregnated cement in total hip replacement.* Acta Orthop., 2008. **79**(3): p. 335-41.
37. Johnson, J.D., et al., *Serum and Wound Vancomycin Levels After Intrawound Administration in Primary Total Joint Arthroplasty.* J Arthroplasty, 2017. **32**(3): p. 924-928.
38. Steadman, W., et al., *Local Antibiotic Delivery Options in Prosthetic Joint Infection.* Antibiotics (Basel), 2023. **12**(4).
39. Anagnostakos, K. and C. Meyer, *Antibiotic Elution from Hip and Knee Acrylic Bone Cement Spacers: A Systematic Review.* Biomed Res Int, 2017. **2017**: p. 4657874.
40. Abosala, A. and M. Ali, *The Use of Calcium Sulphate beads in Periprosthetic Joint Infection, a systematic review.* J Bone Jt Infect, 2020. **5**(1): p. 43-49.
41. Tarar, M.Y., et al., *Wound Leakage With the Use of Calcium Sulphate Beads in Prosthetic Joint Surgeries: A Systematic Review*. Cureus, 2021. **13**(11): p. e19650.
42. Ferry, T., et al., *Past and Future of Phage Therapy and Phage-Derived Proteins in Patients with Bone and Joint Infection.* Viruses, 2021. **13**(12).
43. Yuste, I., et al., *Engineering 3D-Printed Advanced Healthcare Materials for Periprosthetic Joint Infections.* Antibiotics (Basel), 2023. **12**(8).
44. Serrano, D.R., et al., *3D Printing Technologies in Personalized Medicine, Nanomedicines, and Biopharmaceuticals.* Pharmaceutics, 2023. **15**(2).
45. De Meo, D., et al., *Antibiotic-Loaded Hydrogel Coating to Reduce Early Postsurgical Infections in Aseptic Hip Revision Surgery: A Retrospective, Matched Case-Control Study.* Microorganisms, 2020. **8**(4).

Supplementary Material.

Table S1. Matrix Design of Experiment Taguchi

Experiments	Soluplus® (%)	AmB (%)	Air Flow (Nl/h)	Tinlet (ºC)	Aspirator (%)	Inlet liquid velocity (ml/min)	US (min)
1	65	5	600	65	100	5	10
2	65	1	800	65	90	15	10
3	65	1	800	72	100	5	5
4	35	1	600	65	90	5	5
5	35	5	800	65	100	15	5
6	35	5	800	72	90	5	10
7	35	1	600	72	100	15	10
8	65	5	600	72	90	15	5

Table S 2. Matrix Design of Experiment Box- Benhken

Randomization	**Experiments**	**AmB (%)**	**Soluplus® (%)**	**Inlet liquid velocity(ml/min)**
1	**1**	5	50	15
17	**2**	7,5	65	15
8	**3**	10	65	20
3	**4**	5	80	15
9	**5**	7,5	50	10
5	**6**	5	65	10
14	**7**	7,5	65	15
13	**8**	7,5	65	15
12	**9**	7,5	80	20
6	**10**	10	65	10
10	**11**	7,5	80	10
7	**12**	5	65	20
11	**13**	7,5	50	20
16	**14**	7,5	65	15
2	**15**	10	50	15
4	**16**	10	80	15
15	**17**	7,5	65	15

PUBLICACIÓN 3:

Combatting periprosthetic joint infections with 3D-printed antimicrobial EVA-loaded implants

F.C. Luciano, I. Yuste, B.J. Anaya, P. Sanz-Ruiz, A. Ribed-Sánchez, M.P. Ballesteros, M. Tiboni, S. Moroni, G. Maurizii, L. Casettari, and D.R. Serrano.

Pendiente de publicación: Enviado a

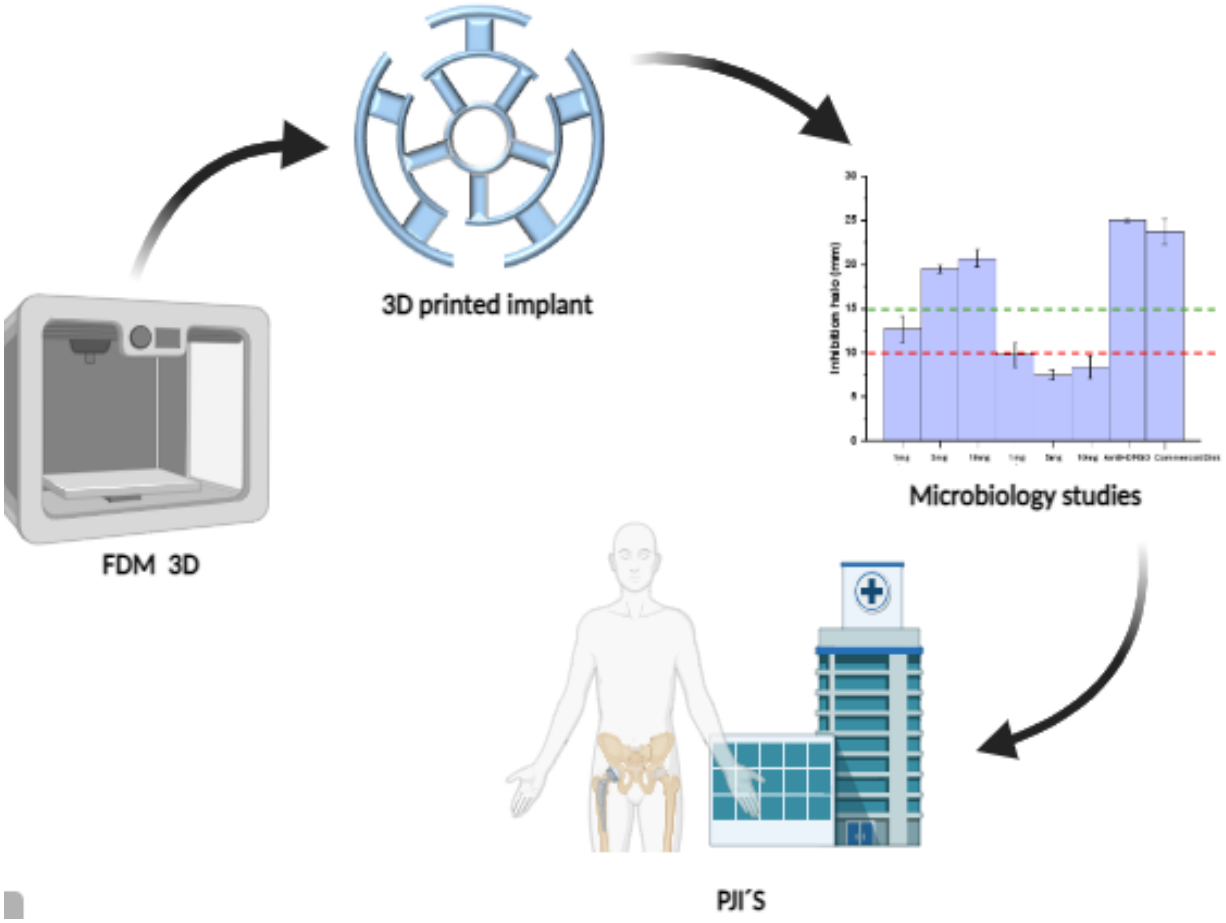

Abstract

Periprosthetic joint infections (PJIs) represent serious complications following hip or knee arthroplasty, leading to significant healthcare challenges and substantially increasing the economic burden. Existing strategies for the prevention and treatment of bacterial PJIs are suboptimal, offering limited antimicrobial efficacy and potentially compromising the biomechanical integrity of the prosthesis. Therapeutic options for fungal infections are particularly limited, and although these infections are less common than those produced by bacteria, they can cause severe health issues in affected patients. PJIs are often associated with biofilms, which are three-dimensional aggregates of diverse microorganisms encased in an extracellular matrix that evades the host's immune system and impedes antibiotic penetration. The aim of this work, as an innovative approach to this healthcare issue, was to develop an implant for the prevention and treatment of fungal PJIs. The manufacturing involved direct powder extrusion (DPE) to print pellets made of EVA and PEG, coated with a broad-spectrum antifungal drug Amphotericin B (AmB). EVA (ethyl-vinyl acetate) and PEG were meticulously chosen to ensure biocompatibility and printability. Implants loaded with AmB demonstrated antifungal efficacy against *Candida albicans*. The drug release profile was rapid within the first 10 hours, releasing 45% of the drug, and continued up to 240 hours, with the 20% of the drug released. These findings suggest a promising, easily tunable solution for PJIs in clinical practice and pharmacy.

Keywords: Additive manufacturing, parenteral implants, personalized medicine, ethyl vinyl acetate (EVA), PJI, prosthetic infections, bone

1. Introduction

Currently, prosthetic joint replacement has markedly enhanced the quality of life for patients suffering from joint injuries. However, the success of these surgeries is increasingly threatened by the rising incidence of periprosthetic joint infections (PJIs), particularly those associated with antimicrobial resistance. Bearing in mind the aging population, increasing obesity rates, and the rise in sports-related injuries, the incidence of knee and hip arthroplasties is expanding at an exponential rate, with the true incidence of PJIs among the most severe and costly complications post-arthroplasty likely being underestimated [1, 2].

The major problem with PJIs is the biofilm formation that occurs all over the prosthesis, hindering an effective antimicrobial treatment [3]. Infections caused by bacteria have a higher incidence than fungal ones (10 % *vs* 1 % of the cases), and 15% of PJIs are caused by multiple microorganisms [4, 5]. However, fungal prosthetic infections are rare complications in this kind of procedure accounting for 1% to 3% of PJI [6, 7]. The *C. Albicans* is the most common cause of PJI infections, even if also non-candida infections are increasing [8]. Despite their rareness, the fungal PJIs translate into higher diagnostic and therapeutical challenges, and the complex structure of fungal biofilms, the presence of comorbidities inducing immunosuppression, the absence of standardized treatment guidelines make the fungal prosthetic infections highly challenging for the healthcare system [9-12]. At present, the main strategies to prevent PJIs include: (i) irrigating the prosthesis with an antibiotic solution, (ii) administering oral and intravenous antibiotics over an extended period, and (iii) using antibiotic-loaded polymethylmethacrylate (PMMA) bone cement after prosthesis removal and tissue debridement. However, when antibiotics are used for irrigation, their local concentration quickly diminishes, making them ineffective for infection prevention. Prolonged oral or intravenous antibiotic therapy can lead to systemic side effects and generally results in low antibiotic concentrations at the joint site. This inadequate local concentration fosters the development of antimicrobial resistance and biofilm formation on the joint surface. [13, 14].

However, for fungal PJIs the two stages exchange with several antifungal drugs seems to be the best option so far, but standardized protocols, clear guidelines about the duration of the antifungal treatment, the drug amount, or the resistance patterns of this therapeutical option are missing [7, 15]. This translates to a very high cost for the health care system and impacts the life quality of patients.

The use of 3D printing as an alternative technology for manufacturing patient-centered treatments for fungal PJIs with cost-effectiveness could open the way to innovative solutions for the problem. 3D printing technologies facilitate the customization of medical solutions to meet individual patient needs. This technology has been utilized across a diverse array of applications, including the development of solid, semi-solid, and locally applied or implanted medications. 3D-printed implants, stents, and medical devices designed for sustained release are considered as treatment in joint replacement therapies, medical prostheses, and cardiovascular interventions [16]. The three-dimensional printing technology presents significant flexibility for transitioning conventional medicine to customized systems and, in the future, hospitals could integrate 3D printing fabrication for manufactured parenteral implants and prostheses [17].

The aim of this work focused on a novel approach for PJIs based on 3D-printed implants loaded with AmB to prevent and treat biofilm formation. Implants were 3D printed using EVA as a biocompatible copolymer loaded with AmB as an antifungal drug using a direct pellet extrusion technique. This technology allows to printing directly the objects starting from a powder mixture of excipients and active ingredients avoiding other laborious steps such as the preparation of the printing filament used in fused deposition modeling 3D printing. A detailed physicochemical characterization was performed followed by drug release studies and *in vitro* antifungal activity against different *Candida spp.*

2. Materials and methods

2.1 Materials

Ethyl-vinyl acetate (EVA) copolymer (Ateva 4030AC) in micronized form was kindly donated by Celanese (Sulzbach, Germany). PEG 10000. AmB (purity > 90 %) was purchased from Kemprotec Limited (Cumbria, UK). Commercial disks of vancomycin and AmB were purchased from Neo-Sensitabs (Rosco, Denmark). Salts and solvents (HPLC-grade) were purchased from Proquinorte (Madrid, Spain). Other reagents used were of ACS Grade and were used without further purification.

2.2 Engineering and design of 3D implants

2.2.1 Implant design

The implant design was made to be adapted to the acetabular component morphology of the hip prosthesis, mimicking the shape with empty spaces to allow screw placement during the surgical procedure. The acetabular surface was carefully measured with a caliper. The implant was circular with a diameter of 64 mm. Tinkercad software (Autodesk, Ohio, USA) was used to design the implant. Afterward, the design was exported into the STL format which was sent for printing to the DPE 3D printer (Tumaker NX PRO PELLETS, Indart3D, Spain). The implant design consisted of three concentric circles with outer diameters of 18, 44, and 66 mm, and 2 mm width for the inner and middle circles (44 and 18 mm) and 3 mm for the outer one (66 mm). The circles in the inside part of the implant were interconnected with branches of 8 x 7 mm for the first circle, while the second and third circles were connected by arms of 11 x 4 mm.

2.2.2 Pellet preparation

Polyethylene glycol (PEG) 10000 (20%) and ethylene-vinyl acetate (EVA) (80%) was mixed using a powder blender (Galena Top, Ataena Srl, Italy) for 30 minutes at 50 rpm and then the mixture was dried in an oven overnight at 40°C before extrusion. PEG 10000 was included as a plasticizer and EVA as a copolymer. The hot melt extrusion of the polymer mixture (40 g, 80°C) was performed with a single-screw extruder (Noztek Pro HT, Shoreham, UK) using a 1.75 mm nozzle. The obtained filament was pelletized (< 2 mm in length) and dried overnight at 40°C before printing to avoid hydration. To ensure

a homogeneous distribution of AmB on the pellets' surface, the oil method was applied [18-20]. Briefly, 5 g of EVA-PEG pellets were placed in a 50 mL conical centrifuge tube and 30 µL of castor oil was added. The tube was vortexed for 5 minutes to spread the oil on the surface of the pellets. The oiled-covered pellets were transferred to a new tube. At this point, a precise amount of AmB (50 mg), to achieve a 1% *w/w* final concentration was added and the tube was vortexed for 5 min to guarantee a homogeneous distribution of the drug on the surface of the pellets.

2.2.3 Implant fabrication using DPE 3D printing

The prepared pellets were directly loaded into the hopper of the 3D printer (NX Pro Pellets, Tumaker, Spain), which featured a single-screw extruder with a 0.4 mm nozzle diameter. Key parameters, including print speed, layer height, and printing temperature, were carefully optimized. The print speed was set to 5 mm/s, the layer height to 0.2 mm, and the infill density to 80%. These settings remained consistent for both blank and AmB-loaded implants. However, the printing temperature varied: for the blank implant, it was set at 80°C, based on DSC analysis of pure EVA and PEG while for the AmB-loaded implant, several trials were conducted, gradually increasing the temperature until optimal extrusion quality was achieved, with the final temperature set at 100°C. Additionally, the build plate was maintained at 60°C and covered with an adhesion sheet (Polypropylene, Ultimaker, The Netherlands) to enhance adhesion.

2.3 Characterization of 3D-printed implants

2.3.1 Implant morphology

The morphology of the optimized implant containing AmB was characterized by Scanning Electron Microscopy (SEM) using a JEOL6335F (Mussashime, Japan) with a voltage of 20 kV. A thin layer coating with gold was sputtered for 120 seconds on microparticles mounted on carbon-coated tubs using a QUORUM Q150R S (Mussashime, Japan) to help conductivity.

2.3.2 FT-IR

The chemical composition of the unprocessed materials and printed devices was investigated using attenuated total reflectance Fourier transformed infrared spectroscopy (ATR-FTIR, Spectrum Two FT-IR spectrometer with ATR accessory, Perkin Elmer, MA,

USA). Measurements were performed at 450–4000 cm^{-1} with a resolution of 4 cm^{-1} and a total of 64 scans. Moreover, to assess the homogeneous distribution of the drug within the implant, FTIR analysis was performed in different regions of the implant. Spectra were normalized with the EVA absorption at 1737 cm^{-1} as a reference.

2.3.3 Thermal analysis

Differential scanning calorimetry (DSC 6000, Perkin Elmer, USA) and thermogravimetric analysis (TGA 4000, Perkin Elmer, USA) were carried out to assess the thermal behavior of unprocessed materials and the printed formulation. For DSC analysis, the samples (~ 5 mg) were placed in aluminum pans and were heated up with a fixed heating rate of 10 °C/min from 30 °C to 180 °C, cooled down to -30°C at a fixed cooling rate of 50 °C/min and heated up again to 180 °C. For TGA measurements, scans were performed from 30 °C to 600 °C at a speed rate of 10 °C/min under a nitrogen flow rate of 30 mL/min. Pyris Manager software (Perkin Elmer, USA) was used for data collection and analysis.

2.3.4 Mechanical analysis

The flexibility of the drug-loaded and blank-printed implants was examined using a texture analyzer (TA. XT plus, Stable Micro Systems, Surrey, UK). For all measurements, the instrument was set in compression mode and the speed of the aluminum probe (20 mm in diameter) was 2 mm/s. The burst strength of the implant was extrapolated from the maximum peak of the force-distance curve. Whereas the degree of flexibility was calculated as the angle (θ) of the device bending upon break. The tangent of the angle was calculated using equation (1), and the bending angle was calculated with the arctangent formula.

$$tan\theta = \frac{b}{a/2} \quad \text{(Eq. 1)}$$

Where a is the initial length of the implant, b is the distance traveled by the probe before the device's breakage and θ is the angle determined at the breakage point.

2.4 *In vitro* drug release studies

The release profile of the 3D-printed implants was evaluated in a 1: 1 (*v:v*) ethanolic-phosphate buffer saline (PBS at pH 7.4) solution [21]. All implants were immersed in beakers containing 100 mL of release medium. The beakers were incubated at 37 ºC under stirring (100 rpm) for 2 weeks. At several time points (1 h, 2 h, 4 h, 6 h, 8 h, 24 h, 48 h, 72 h, 120 h, and 240 h),750 µl of release medium was withdrawn and replaced with an equal volume of fresh media to keep sink conditions. The amount of AmB released from the implants was measured by HPLC in triplicate, the mobile phase consisted of acetonitrile:glacial acetic acid: water (52:4.3:43.7, V:V:V), which was pumped at a flow rate of 1 mL/min, and the sample injection volume was 40 µL with a column Thermo Hypersil-Keystone BDS (200 x 4.6 mm, 5µm). The column temperature was maintained at 25°C and the detector was set at 406 nm [22].

2.5 Antifungal *in vitro* assay

The antifungal activity was evaluated by agar diffusion assay with different *Candida* spp. (*Candida albicans* CECT 1394, *Candida parapsilosis* 57744, and *Candida krusei* 1068) [23, 24]. The 3D AmB-loaded implant was cut in circles with different diameters to have an AmB dose equivalent to 1 mg, 5 mg and 10 mg respectively. The same dimensions were prepared for the blank implants as control. Discs loaded with AmB dissolved in DMSO (10 µg) and commercial discs of AmB (10 µg, Neo-Sensitabs, Rosco, Denmark) were used as a positive control. After 48 h, inhibition zone diameters were measured at points where complete inhibition of fungal growth was observed. Isolates were classified according to the Clinical & Laboratory Standards Institute (CLSI) as AmB susceptible (S) when the zone of inhibition was greater than 15 mm; resistant (R), if the zone of inhibition was greater than 10 mm; and intermediate (or dose-dependent) (I) if the zone of inhibition was between 11 and 14 mm.

3. Results and discussion

3.1 Engineering and design of the 3D-printed implant

The implant geometry was designed to be placed over the acetabular component of the prosthesis respecting the exact dimensions as reported in Figure 1a. The design was not a flat disc to allow the surgeon to place the appropriate screws during the implantation of the prosthesis. Figure 1b-c shows the printed implant without and with the AmB. The presence of the drug was visible due to its characteristic yellowish color. All the computational designed measurements were respected in the printed implants confirming the accuracy of the DPE 3D printing technology.

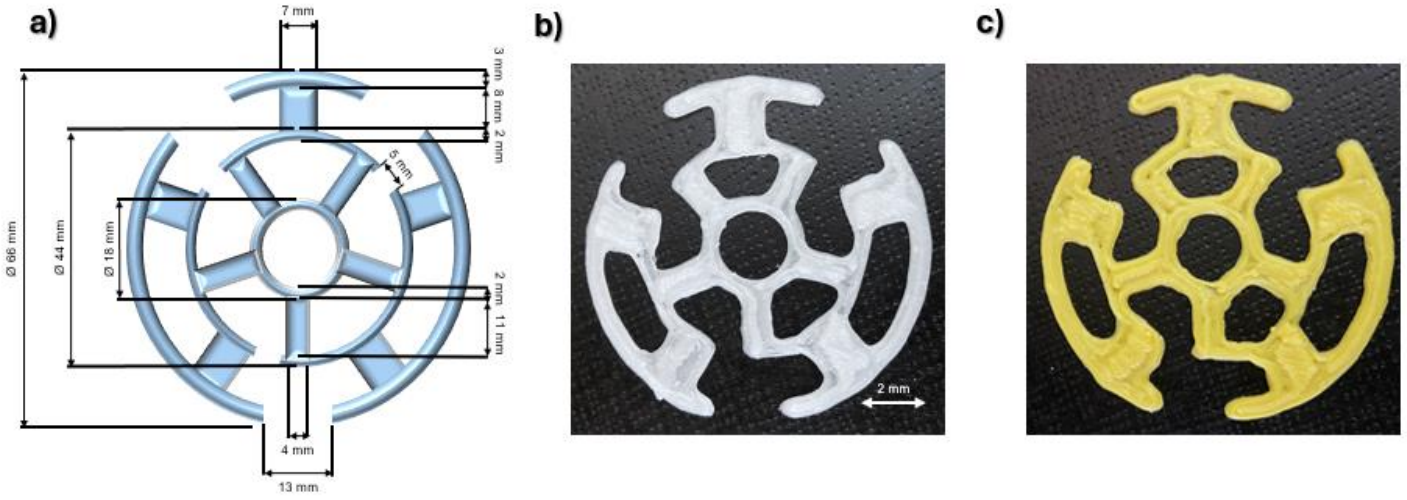

Figure 1. Dimensions of the 3D-printed implant. **Key**: **a)** Implant design; b) 3D printed blank implant; **c)** 3D printed AmB-loaded implant.

3.2 Implant morphology

Figure 2 shows SEM images of the 3D-printed implants both unloaded and loaded with AmB. No porosity was detected by SEM on the surface of the implants matching the combined slow - prolonged drug release. The drug was well mixed with the polymer and uniformly distributed in the implant as no drug crystals were observed on the surface.

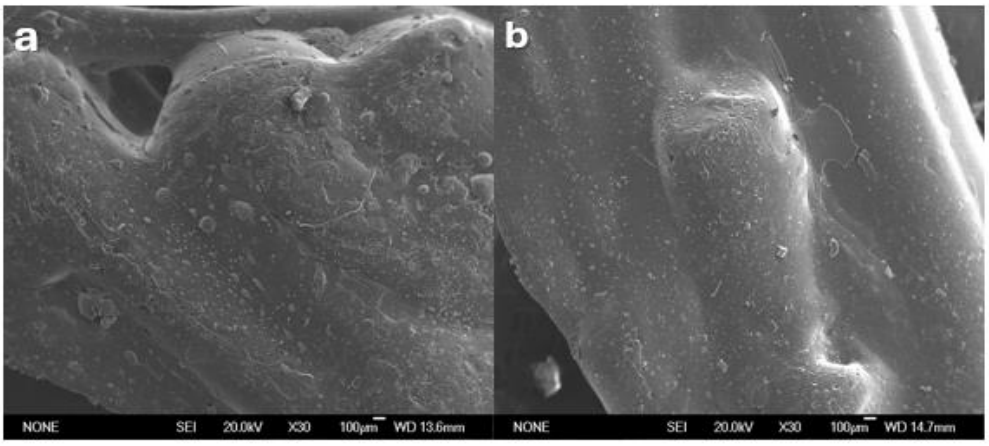

Figure 2. SEM micrographs. **Key**: **a)** 3D printed blank implant; **b)** 3D printed AmB-loaded implant.

3.3. Physicochemical characterization

3.3.1 FT-IR

The chemical composition of the printed implants was further investigated using FTIR to evaluate also possible interactions between the polymers and the drug. Figure 2 shows the FTIR spectra of the pure materials and the 3D-printed implant. The printed implant (a, b) showed the typical peaks of the unprocessed EVA 4030AC (e). Specifically, 1243 cm^{-1} caused by the C-H vibration, 1737 cm^{-1} related to a carbonyl C=O stretching, 2980 cm^{-1} due to absorbance associated with hydroxyl groups vibration, and bands at 1117 and 710 cm^{-1} reflecting vibrations of C-O and O-C-O groups, respectively. Moreover, a similar pattern is observed when comparing the spectra of the 3D-printed implants (a, b). Nevertheless, a new peak at 1640 cm^{-1} emerges in the AmB-implant spectrum (Box Fig. 3), which may be attributed to the C=O stretching vibration of AmB confirming its existence within the implant [25]. Due to the low AmB percentage, peak shifts attributed to H-bond formation were not observed for the EVA or the PEG.

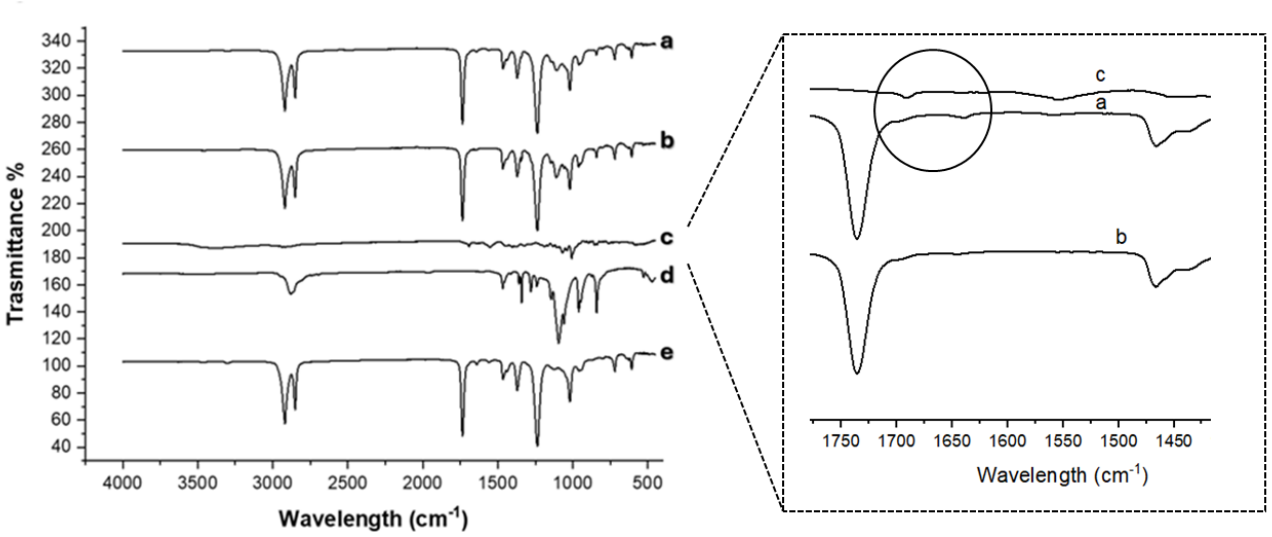

Figure 3. FTIR analysis; Key: a) 3D-printed AmB-loaded implant; **b)** 3D-printed blank implant; **c)** unprocessed AmB raw; **d)** unprocessed PEG and **e)** Unprocessed EVA 4030AC.

3.3.2 Thermal analysis

The DSC thermograms of the printed implants and starting materials are shown in Fig. 4. EVA and PEG present characteristic melting peaks at 52 °C and 75 °C, respectively (Fig. 4A). The endothermic event observed at 106 °C in the AmB thermogram (Fig. 4A) presumably corresponds to water loss, as its reported melting temperature is higher than 170 °C [26]. Moreover, the absence of this peak it could be because AmB degrades before 170 degrees, basically before melting (Fig 4B). Although PEG fully melted during the HME and 3D printing (extrusion and printing temperature: 80 °C and 100 °C respectively), it recrystallized upon cooling to room temperature, as can be seen in the thermograms of the printed devices [27] (Fig. 4A). However, the PEG melting peak shifts to a lower temperature, probably due to the formation of thinner crystals during thermal treatment followed by cooling during the printing process [21]. This hypothesis is reinforced by the shift to 69 °C of PEG melting peak observed in the second heating scan conducted after controlled cooling (Fig. 4B). Additionally, the merging of PEG and EVA melting events may also contribute to the shift of the PEG melting peak to a lower temperature post-printing process.

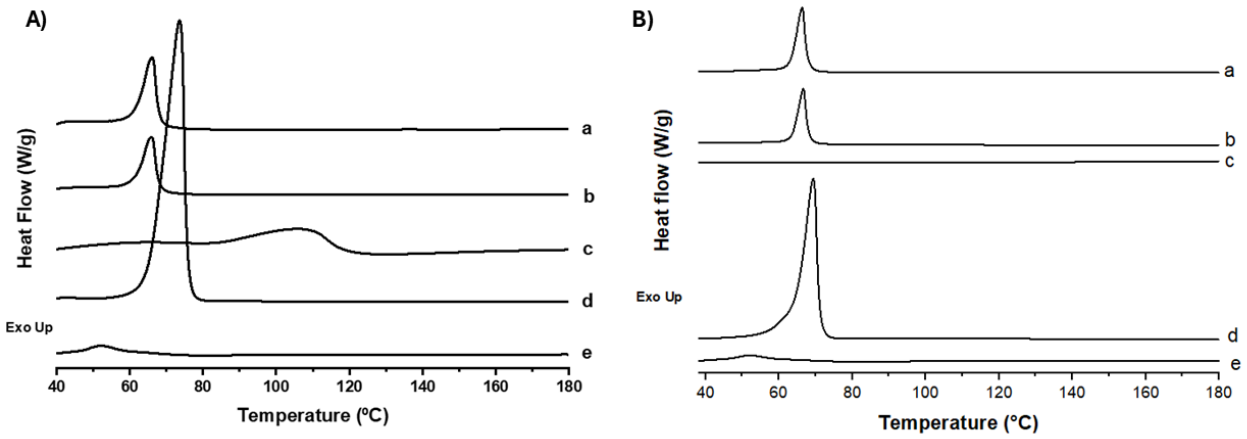

Figure 4. **DSC analysis**: **A**) first scan, and **B**) second scan; **Key**: a) 3D-printed AmB-loaded implant; b) 3D-printed blank implant; c) unprocessed AmB raw; d) unprocessed PEG and e) Unprocessed EVA 4030AC.

Furthermore, given the requirement of two thermal processes in the production of the implants, the thermal stability of the pure materials was evaluated using TGA (Fig. 5). For PEG, degradation begins at 367 °C, with an initial weight loss of approximately 4%, continuing up to 445 °C. EVA, on the other hand, exhibits two distinct degradation phases: the first at around 337 °C with a 5% weight loss, due to acetic acid release, and the second at 427 °C, with an additional 27% weight loss attributed to polymer backbone fragmentation [21]. Regarding AmB, an initial weight loss of about 3–5% up to 104°C is probably due to dehydration, as moisture trapped within the AmB structure was released [28]. After this, the mass loss is stabilized until 175 °C, followed by a 10% loss associated with the onset of AmB decomposition, which continues up to 500 °C. Thus, AmB demonstrated thermal stability at the printing temperature (100 °C). Additionally, incorporating AmB into the EVA-PEG matrix further enhances drug stabilization. Notably, the initial degradation temperature of the printed implants is higher than that of pure AmB in which degradation starts at 333 °C with a weight loss of 5–7%, continuing up to 500 °C. This suggests that the EVA/PEG matrix provides a protective effect against AmB's thermal degradation [25].

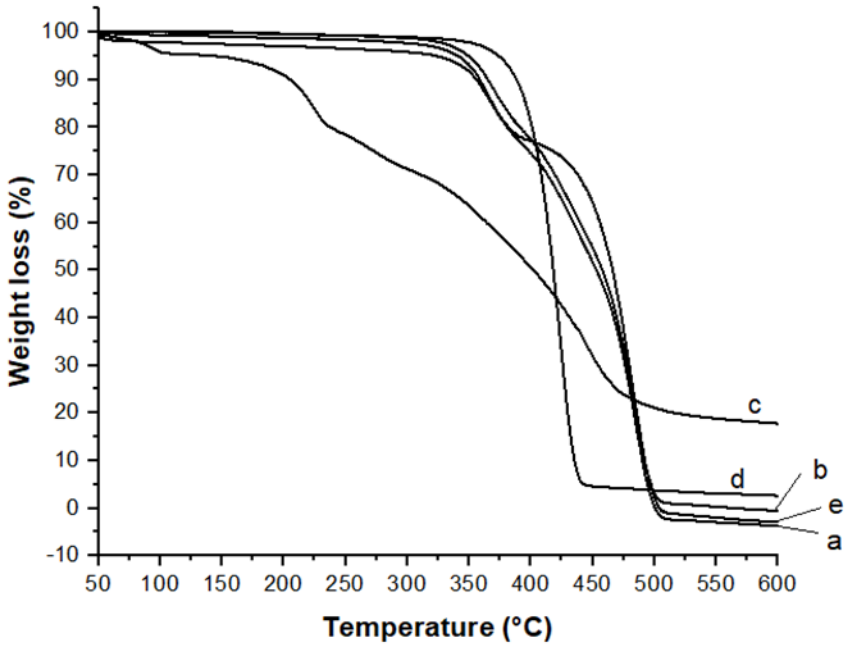

Figure 5. TGA analysis; Key: a) 3D-printed AmB-loaded implant; b) 3D-printed blank implant; c) unprocessed AmB raw; d) unprocessed PEG and e) Unprocessed EVA 4030AC.

3.4 Burst strength and flexibility

The flexibility tests were made to ensure that implants support the manipulation during storage and implantation in the body. The degree of flexibility was considered as the angle (θ) of the implant bending upon break, while the value of burst strength was extrapolated from the maximum peak of the force-distance curve (Table 1). The loaded implant with AmB increased the flexibility by 20% and increased the burst strength by 36% [29]. The increase in flexibility could allow better placement of the implant during surgical operations enhancing patient comfort.

Table 1. Maximum bending angles and burst strengths of 3D-printed implants.

Sample	Burst strength (N)	Degree of flexibility (θ °)
Blank implant	10.5 ± 0.4	48.7± 0.2
AmB-loaded implant	14.3± 0.1	57.3± 0.3

3.5 *In vitro* drug release studies

Considering the low solubility of the drug in water, the release test was carried out in a 1:1 *v:v* mixture of PBS (pH 7,4) and ethanol as previously described by other authors with poorly water-soluble antifungals to keep sink conditions [30]. The drug exhibited an initial burst release in the first 10 h achieving a 45% release followed by a sustained release phase until 120 h achieving a 60% release. Afterward, the AmB concentration in the solution was decreased which can be attributed to drug degradation in aqueous media [31]. Despite the presence of ethanol in the dissolution medium, the release rate of AmB from the implant was incomplete which was probably due to the hydrophobic and non-swellable nature of EVA polymer and the interactions occurring with the AmB.

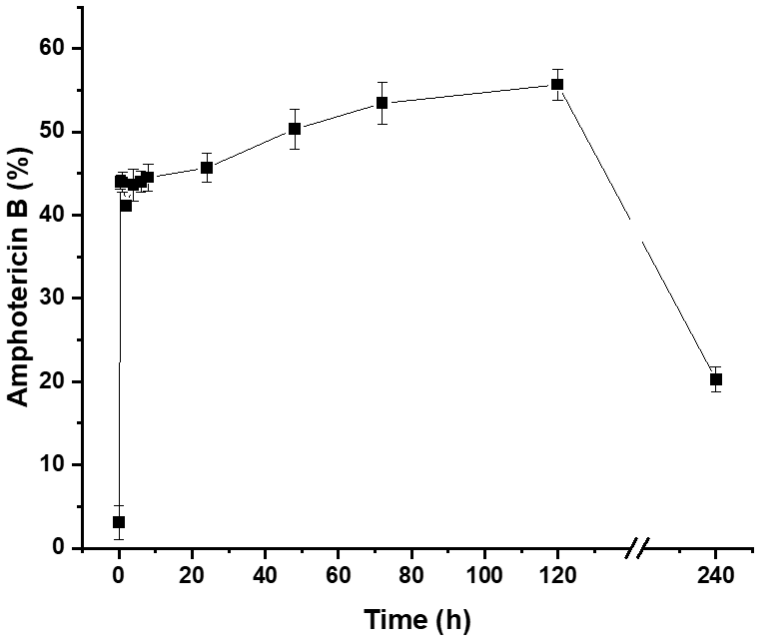

Figure 5. *In vitro* release profiles of 3D-printed AmB-loaded implant.

3.6 Antifungal *in vitro* assay

Despite the incomplete drug release from the implant, *C. albicans* and *C. parapsilosis*, were susceptible to AmB. The greatest efficacy was observed for *C.albicans,* with inhibition halos above 15 mm, and even at low doses of 1 mg, the AmB-loaded implant showed an intermediate dose-response pattern (>10 mm). Interestingly, blank implants also showed an inhibition halo for *C.albicans*, but this was below 10 mm in diameter. In the case of *C.parapsilosis,* only the highest dose tested (15 mg) showed a dose-dependent profile, while *C. krusei* was resistant to all AmB doses even from AmB dissolved in DMSO. *C. albicans* in all the doses tested showed statistical differences with the AmB+ DMSO control, and between the Commercial disk and the 1mg AmB-loaded implant and all blank implants. (**Figure 6**).

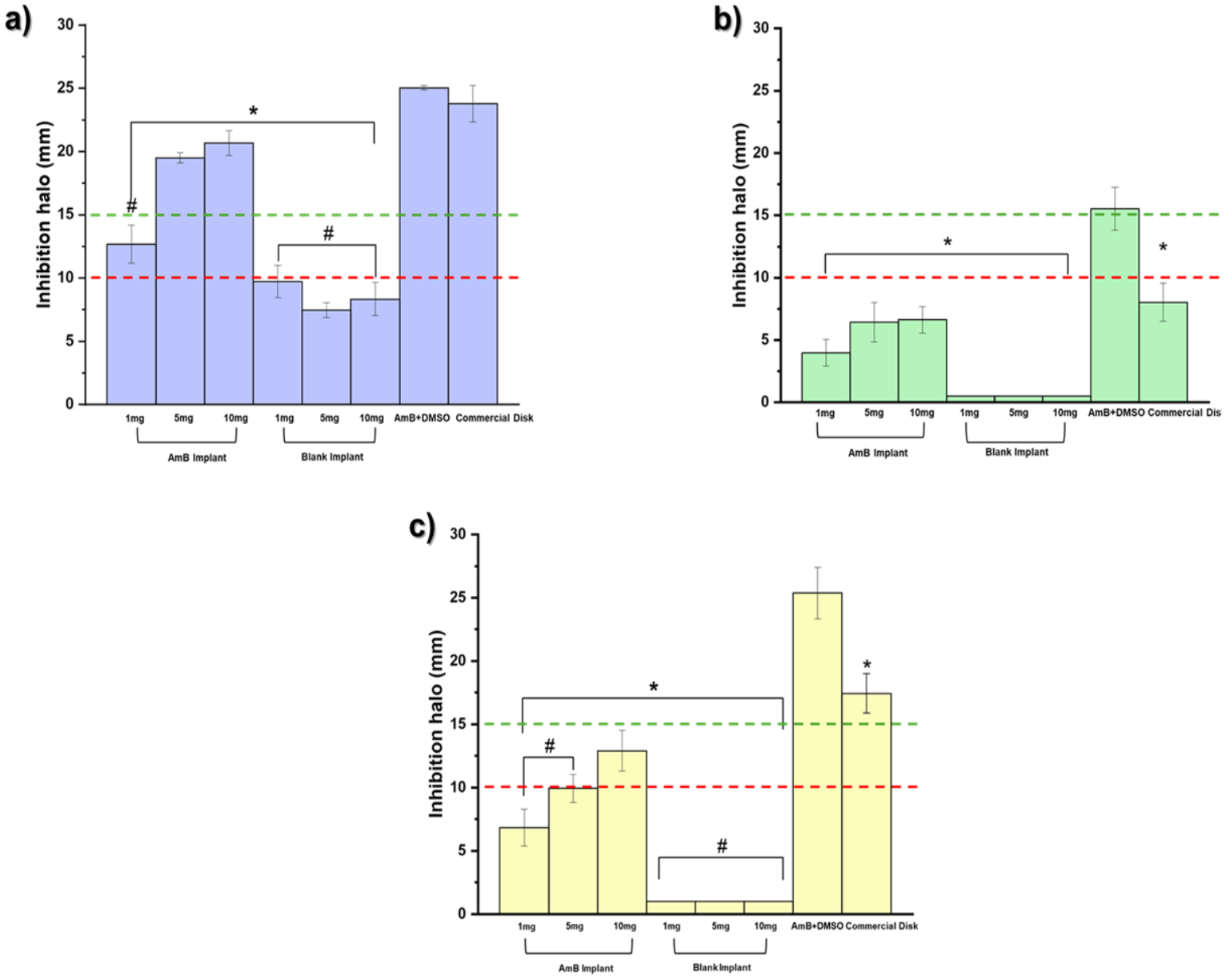

Figure 6. ***In vitro*** **antifungal activity of 3D printed implants against different Candida spp.** Key: **(a)** *C. albicans*, **(b)** *C. krusei* and **(c)** *C. parapsilosis*. ***** Statistical differences ($p < 0.05$).

4. Discussion

Periprosthetic joint infection (PJIs) represents a significant complication for arthroplasty surgeries characterized by high treatment healthcare costs and associated morbidity and mortality. In orthopedic practice, the primary focus is on the prophylaxis of these infections. Population patterns in developed nations indicate a projected rise in the incidence of joint replacement surgical procedures, particularly among patients with various comorbidities. This underscores the urgent need to develop novel strategies for addressing PJIs [32].

The most common treatment for this complication is the application of commercial antibiotic-loaded polymethyl methacrylate (PMMA) cement utilized for prosthesis fixation. This antibiotic-loaded cement initially produces a high local antibiotic concentration, followed by a prolonged release phase that can extend over several months to years, potentially leading to microbial resistance. There is currently no consensus regarding the optimal dose of AmB to be combined with PMMAs for effective local treatment of PJIs. Given that most PJIs are caused by bacteria, there is limited experience with antifungal agents in this context. AmB exerts its antifungal effect by binding it to ergosterol in the plasma membrane of fungal cells, inducing apoptosis. While it is a highly effective agent, the recommended systemic intravenous dosage is constrained to 1 mg/kg when using Fungizone® and 5 mg/kg for AmBisome AmB commercials formulations. A notably low release of AmB from bone cement has been reported being released at only 0.03% after one-week post-implantation [33-35].

To the best of our knowledge, this work presents, for the first time, a personalized 3D-printed implant fabricated using direct pellet 3D printing extrusion technology, specifically designed to conform to the convex geometry of the acetabular component. This implant can incorporate two distinct polymers in combination, as well as an antifungal agent, providing additional functional properties. The design of this 3D-printed implant was meticulously developed to promote osteointegration, a critical process for ensuring the effective union between the implant and surrounding bone. In this regard, the preservation of large gaps between the arms of the implant was prioritized to facilitate biological ingrowth and bone regeneration.

Instead of employing a full coverage of the acetabular surface, a bioinspired "web" or mesh architecture was chosen, which allows for structural stability while facilitating fluid exchange and the cellular penetration required for osteointegration. This innovative design takes advantage of the benefits of customization, ensuring that the implant can be specifically tailored to the anatomical variations of the patient, thereby optimizing the rehabilitation process.

The applicability of this approach is not limited to hip replacement surgery but could be extrapolated to other arthroplastic interventions where implant conformation precision is critical for clinical success. In this context, 3D printing technology, with its ability to manufacture implants of complex geometry, offers significant potential for the development of highly personalized prostheses. This customization capability could lead to innovative designs tailored specifically to the morphology of each patient, enabling their fabrication and adjustment by trained healthcare professionals proficient in advanced additive manufacturing techniques.

The composition of the implant with EVA-PEG as excipients was carefully selected to ensure the biocompatibility of the formulation with the human body. EVA as a copolymer for 3D printing formulations possesses ideal polymer characteristics such as easy extrudability, low melting point, high versatility, and low glass transition temperature required to prevent AmB degradation. The application of EVA polymer encompasses various uses in the pharmaceutical field, such as and subcutaneous implants, transdermal patches and, intrauterine devices [36-38]. However, previous studies showed that the EVA co-polymer composition affected the drug release rate so, this parameter could be tuned by the choice of different polymer grades available in the market [39, 40].

Furthermore, the drug-loaded AmB was superior to other implants developed by 3D printed technique, loaded by other methods such as passive diffusion. Although the AmB release profile was incomplete, due in part to drug release hindering from the EVA-PEG matrix, the efficacy against *C.albicans*, the most predominantly pathogen responsible for fungal PJIs, remained high, showing an interesting therapeutic potential for clinical practice [41-43]**.**

6. Conclusions

The development of a 3D-printed implant loaded with AmB represents an innovative strategy for both the treatment and prevention of PJIs, leveraging AmB's potent antifungal activity. The selection of EVA and PEG as excipients for the implant was meticulously optimized to ensure printability as well as compatibility with human tissues. The AmB-loaded implants demonstrated robust antifungal activity, effectively inhibiting *C. albicans*. Drug release studies revealed a biphasic release profile: an initial burst release of approximately 45% of the drug within the first 10 hours required to prevent early infections, followed by a sustained release phase over 5 days. These promising findings suggest that the 3D-printed AmB-loaded implant has significant potential as a therapeutic and prophylactic solution for managing PJIs. Its design aligns well with the requirements of clinical and pharmaceutical applications, offering a feasible alternative to conventional approaches. However, further comprehensive studies are essential to fully characterize the pharmacological efficacy, long-term safety, and toxicological profile of the implant. These investigations should include rigorous *in vitro* assessments and *in vivo* validations to ensure its readiness for clinical implementation and to establish its superiority or complementary role in existing treatment paradigms.

Acknowledgments

This study was partially supported by the Complutense University of Madrid Research Group (Innovation in Pharmacology, Nanotechnology, and personalized medicine by 3D printing). This study has been also funded by the Ministry of Science and Innovation (award PID2021-126310OA-I00 to Dolores Serrano.

References

1. Jin, X., et al., *Estimating incidence rates of periprosthetic joint infection after hip and knee arthroplasty for osteoarthritis using linked registry and administrative health data.* Bone Joint J, 2022. **104-b**(9): p. 1060-1066.
2. Hernández-Aceituno, A., et al., *Factores de riesgo en artroplastia total y parcial de cadera: infección y mortalidad.* Revista Española de Cirugía Ortopédica y Traumatología, 2021. **65**.
3. Li, C., N. Renz, and A. Trampuz, *Management of Periprosthetic Joint Infection.* Hip Pelvis, 2018. **30**(3): p. 138-146.
4. Sambri, A., et al., *Epidemiology of Fungal Periprosthetic Joint Infection: A Systematic Review of the Literature.* Microorganisms, 2022. **11**(1).
5. Chisari, E., et al., *Fungal periprosthetic joint infection: Rare but challenging problem.* Chin J Traumatol, 2022. **25**(2): p. 63-66.
6. Azzam, K., et al., *Microbiological, Clinical, and Surgical Features of Fungal Prosthetic Joint Infections: A Multi-Institutional Experience.* JBJS, 2009. **91**(Supplement_6).
7. Kuo, F.-C., et al., *Two-Stage Exchange Arthroplasty Is a Favorable Treatment Option Upon Diagnosis of a Fungal Periprosthetic Joint Infection.* The Journal of Arthroplasty, 2018. **33**(11): p. 3555-3560.
8. Koutserimpas, C., et al., *Non-albicans Candida prosthetic joint infections: A systematic review of treatment.* (2307-8960 (Print)).
9. Brown, T.S., et al., *Periprosthetic Joint Infection With Fungal Pathogens.* Journal of Arthroplasty, 2018. **33**(8): p. 2605-2612.
10. Karczewski, D., et al., *Candida periprosthetic joint infections — risk factors and outcome between albicans and non-albicans strains.* International Orthopaedics, 2022. **46**(3): p. 449-456.
11. Kuo, F.-C., et al., *Two-stage exchange arthroplasty is a favorable treatment option upon diagnosis of a fungal periprosthetic joint infection.* The Journal of Arthroplasty, 2018. **33**(11): p. 3555-3560.
12. Chandra, J., et al., *Biofilm formation by the fungal pathogen Candida albicans: development, architecture, and drug resistance.* Journal of bacteriology, 2001. **183**(18): p. 5385-5394.

13. Argenson, J.N., et al., *Hip and Knee Section, Treatment, Debridement and Retention of Implant: Proceedings of International Consensus on Orthopedic Infections.* J Arthroplasty, 2019. **34**(2s): p. S399-s419.
14. Wall, V., et al., *Controlling Antibiotic Release from Polymethylmethacrylate Bone Cement.* Biomedicines, 2021. **9**(1).
15. Gross, C.E., et al., *Fungal Periprosthetic Joint Infection: A Review of Demographics and Management.* The Journal of Arthroplasty, 2021. **36**(5): p. 1758-1764.
16. Serrano, D.A.-O., et al., *3D Printing Technologies in Personalized Medicine, Nanomedicines, and Biopharmaceuticals. LID - 10.3390/pharmaceutics15020313 [doi] LID - 313.* (1999-4923 (Print)).
17. Yuste, I., et al., *Engineering 3D-Printed Advanced Healthcare Materials for Periprosthetic Joint Infections.* Antibiotics, 2023. **12**: p. 1229.
18. Tiboni, M., et al., *3D printed clotrimazole intravaginal ring for the treatment of recurrent vaginal candidiasis.* International Journal of Pharmaceutics, 2021. **596**: p. 120290.
19. Domínguez-Robles, J., et al., *3D Printing of Drug-Loaded Thermoplastic Polyurethane Meshes: A Potential Material for Soft Tissue Reinforcement in Vaginal Surgery.* Pharmaceutics, 2020. **12**(1): p. 63.
20. Mills, D.K., et al., *Studies on the cytocompatibility, mechanical and antimicrobial properties of 3D printed poly(methyl methacrylate) beads.* Bioactive Materials, 2018. **3**(2): p. 157-166.
21. Maurizii, G., et al., *3D-printed EVA-based patches manufactured by direct powder extrusion for personalized transdermal therapies.* International Journal of Pharmaceutics, 2023. **635**: p. 122720.
22. Serrano, D.R., et al., *Hemolytic and pharmacokinetic studies of liposomal and particulate amphotericin B formulations.* International Journal of Pharmaceutics, 2013. **447**(1): p. 38-46.
23. Ruiz HK, S.D., Dea-Ayuela MA, Bilbao-Ramos PE, Bolas-Fernandez F, Torrado JJ, et al., *New amphotericin B-gamma cyclodextrin formulation for topical use with synergistic activity against diverse fungal species and Leishmania spp.* Int J Pharm., 2014. **473(1-2)**: p. 148-57.

24. Serrano, D.R., et al., *A novel formulation of solubilised amphotericin B designed for ophthalmic use.* Int J Pharm, 2012(437 (1-2)): p. 80-2.
25. Moroni, S., et al., *3D printing fabrication of Ethylene-Vinyl Acetate (EVA) based intravaginal rings for antifungal therapy.* Journal of Drug Delivery Science and Technology, 2023. **84**: p. 104469.
26. Zu, Y., et al., *Preparation and characterization of amorphous amphotericin B nanoparticles for oral administration through liquid antisolvent precipitation.* European Journal of Pharmaceutical Sciences, 2014. **53**: p. 109-117.
27. Almeida, A., et al., *Sustained release from hot-melt extruded matrices based on ethylene vinyl acetate and polyethylene oxide.* European Journal of Pharmaceutics and Biopharmaceutics, 2012. **82**(3): p. 526-533.
28. Soto, R., et al., *Solubility, aggregation and stability of Amphotericin B drug in pure organic solvents: Thermodynamic analysis and solid form characterization.* Journal of Molecular Liquids, 2022. **366**: p. 120276.
29. Azizoğlu, E. and Ö. Özer, *Fabrication of Montelukast sodium loaded filaments and 3D printing transdermal patches onto packaging material.* International Journal of Pharmaceutics, 2020. **587**: p. 119588.
30. Friuli, V., et al., *Influence of Dissolution Media and Presence of Alcohol on the In Vitro Performance of Pharmaceutical Products Containing an Insoluble Drug.* Journal of Pharmaceutical Sciences, 2018. **107**(1): p. 507-511.
31. Alencar, É.N., et al., *Unveiling the Amphotericin B Degradation Pathway and Its Kinetics in Lipid-Based Solutions.* Journal of Pharmaceutical Sciences, 2021. **110**(3): p. 1248-1258.
32. Sanz-Ruiz, P., et al., *Is Dual Antibiotic-Loaded Bone Cement More Effective and Cost-Efficient Than a Single Antibiotic-Loaded Bone Cement to Reduce the Risk of Prosthetic Joint Infection in Aseptic Revision Knee Arthroplasty?* J Arthroplasty, 2020. **35**(12): p. 3724-3729.
33. Torrado, J.J., D.R. Serrano, and I.F. Uchegbu, *The oral delivery of amphotericin B.* Ther Deliv, 2013. **4**(1): p. 9-12.
34. Serrano, D. and A. Lalatsa, *Oral amphotericin B: The journey from bench to market.* Journal of Drug Delivery Science and Technology, 2017. **42**.
35. Goss, B., et al., *Elution and Mechanical Properties of Antifungal Bone Cement.* The Journal of arthroplasty, 2007. **22**: p. 902-8.

36. Zhang, B. and S. CHEMIST, *Potential Use of Ethylene Vinyl Acetate Copolymer Excipient in Oral Controlled Release Applications: A Literature Review.* 2015.
37. Samaro, A., et al., *Can filaments, pellets and powder be used as feedstock to produce highly drug-loaded ethylene-vinyl acetate 3D printed tablets using extrusion-based additive manufacturing?* International Journal of Pharmaceutics, 2021. **607**: p. 120922.
38. Schneider, C., et al., *Applications of ethylene vinyl acetate copolymers (EVA) in drug delivery systems.* Journal of Controlled Release, 2017. **262**: p. 284-295.
39. Tallury, P., N. Alimohammadi, and S. Kalachandra, *Poly(ethylene-co-vinyl acetate) copolymer matrix for delivery of chlorhexidine and acyclovir drugs for use in the oral environment: Effect of drug combination, copolymer composition and coating on the drug release rate.* Dental Materials, 2007. **23**(4): p. 404-409.
40. Shin, S.-C. and H.-J. Lee, *Controlled release of triprolidine using ethylene-vinyl acetate membrane and matrix systems.* European Journal of Pharmaceutics and Biopharmaceutics, 2002. **54**(2): p. 201-206.
41. Lalremruata, R., *Prosthetic joint infection: A microbiological review.* 2015. **29**(3): p. 120-128.
42. Merrer, J., et al., *Candida albicans Prosthetic Arthritis Treated with Fluconazole Alone.* Journal of Infection, 2001. **42**(3): p. 208-209.
43. Grzelecki, D., et al., *Periprosthetic Joint Infections Caused by Candida Species-A Single-Center Experience and Systematic Review of the Literature.* J Fungi (Basel), 2022. **8**(8).

Discusión

Discussion

The aim of this Doctoral Thesis has been the development and optimization of innovative drug delivery systems that offer controlled or sustained release properties, with a specific focus on addressing unmet clinical needs in the management of PJIs. These infections are severe complications in orthopedic surgeries, often leading to prolonged treatment times, increased patient morbidity, and higher healthcare costs. To this end, the work concentrated on two distinct delivery platforms: (i) microparticles encapsulating active pharmaceutical ingredients, engineered to form a bioadhesive gel upon application, and (ii) a 3D-printed parenteral implant, also loaded with antimicrobial agents, such as AmB and vancomycin. Both systems are intended for localized, *in situ* application during surgical procedures to provide targeted treatment and prophylaxis for PJIs.

The design and optimization of these delivery systems were guided by several critical factors inherent to the challenges of PJI management. Conventional systemic treatments often fail to achieve therapeutic concentrations at the infection site, and they are associated with systemic toxicity and other side effects. Furthermore, the ability to prevent or disrupt microbial biofilms, a key contributor to the chronicity and resistance of PJIs, requires localized, high-concentration delivery of antimicrobial agents in a controlled manner. Therefore, the developed systems were designed with key attributes such as compatibility with host tissues; biodegradability, to avoid the need for surgical removal after drug release; and precise control over the release kinetics to ensure a sustained therapeutic effect while minimizing potential drug-related toxicity.

In the first chapter, microparticles forming a bioadhesive gel were developed to provide a flexible and adaptable means of delivering antimicrobials directly to the affected joint site. The bioadhesive properties of the gel ensure prolonged retention at the application site, enhancing local drug concentrations over an extended period. In the second chapter, a 3D-printed implant, represented a cutting-edge approach to drug delivery, offering the potential for customization in terms of implant geometry, drug loading, and release profiles. This implant was specifically designed to deliver antimicrobials in a sustained and localized manner, reducing the risk of infection recurrence while providing a scaffold that can integrate into the surgical environment.

In developing these systems, considerable attention was given to optimizing their physical, chemical, and biological properties to ensure clinical efficacy and safety. This

included extensive *in vitro* characterization of drug release profiles, antimicrobial activity assays to confirm efficacy against relevant pathogens, and preliminary biocompatibility testing.

The results of this Thesis, as detailed in the corresponding publications, demonstrate significant promise for their application in clinical settings. These findings, along with their implications for the future of PJI treatment and the broader field of localized drug delivery, will be discussed in detail in the following sections of this thesis.

Periprosthetic joint infection is one of the most overwhelming complications after an arthroplasty surgery, increasing the health care system costs, treatment, and the risk of morbidity and mortality significantly. Even though comorbidities such as immunosuppression, diabetes, high body mass index, and others, can elevate the risk of PJI, the related risk with long-lasting operations times is higher [1]. Based on this, prophylaxis is an essential tool against this problem and could reduce significantly the risk of complications [2]. Population patterns in developed nations indicate a projected rise in the incidence of joint replacement surgical procedures, particularly among patients with various comorbidities. This underscores the urgent need to develop novel strategies for addressing PJIs [3]. However, limited options are available to surgeons.

Direct administration of antibiotics into the surgical site as powder or solution has been studied as PJI prophylaxis in primary joint replacement. Even though local levels are high during the first-hour post-surgery, a rapid decline resulting in subtherapeutic concentrations occurs which makes it an easy but with a poor outcome clinical solution [4]. To maintain high local concentration with limited systemic exposure, antimicrobials can be administered via an intra-articular catheter or combined with a carrier to enhance their pharmacokinetic and pharmacological profile [5]. Carrier options include non-resorbable polymethylmethacrylate (PMMA) bone cement and resorbable materials such as calcium sulfate, hydroxyapatite, bioactive glass, and hydrogels. PMMA allows for the formation of structural spacers which is used in multi-stage revision procedures, but it requires subsequent removal and has variable antibiotic compatibility and insufficient drug delivery to reach pharmacological levels, and that prolonged release phase can extend over several months to years, potentially leading to microbial resistance [6]. Calcium sulfate is one of the most researched biocompatible carriers for PJIs which can be shaped into beads to suit a variety of clinical applications and releases 100 % of loaded

antimicrobial drugs over several weeks [7]. However, it is used is associated with wound leakage, and hypercalcemia, being the clinical evidence for its effectiveness still in the early stages [8].

Currently, there is a lack of consensus in the literature regarding the optimal dosage of Amphotericin B (AmB) to be combined with polymethylmethacrylate (PMMA) for the effective local treatment of prosthetic joint infections (PJIs). This is partly due to the fact that most PJIs are primarily caused by bacterial pathogens, leading to relatively limited clinical experience with antifungal agents in this particular context. Nonetheless, given the growing concern for fungal infections in joint prostheses, especially in immunocompromised or high-risk patient populations, there is an increasing interest in the potential role of antifungal therapies in the management of PJIs.AmB exerts its antifungal activity through a well-characterized mechanism of action, which involves binding to ergosterol, a key component of the plasma membrane in fungal cells. This interaction disrupts the membrane's integrity, leading to membrane destabilization, leakage of cellular contents, and ultimately, induction of apoptosis in fungal cells. Despite its potent antifungal properties, AmB has limitations, particularly in terms of its systemic administration, which is typically constrained to doses of 1 mg/kg when using the conventional formulation, Fungizone®, and up to 5 mg/kg for the liposomal formulation, AmBisome®. These dose limitations are primarily due to the potential for nephrotoxicity and other systemic side effects associated with AmB administration, thereby restricting its systemic use in clinical practice. In the context of local delivery, particularly when incorporated into bone cement such as PMMA, the release kinetics of AmB are a critical factor in determining its efficacy. Studies have shown that, after implantation of AmB-loaded bone cement, the drug is released at notably low concentrations. For instance, one week post-implantation, the release rate is reported to be as low as 0.03%. This limited release, though sustained, may be insufficient to achieve the desired therapeutic concentrations in the peri-implant environment, potentially limiting the effectiveness of local antifungal treatment. Therefore, optimizing the release profiles of AmB from bone cement formulations remains an important area of research, with the goal of enhancing antifungal efficacy while minimizing systemic exposure and associated toxicity [9-11].

The use of bacteriophages has attractive inherent properties as are specifically targeted to bacteria with no toxicity on mammalian cells. However, it is required to have phage

libraries to target different bacterial species, and its current use for PJIs is limited [12]. Finally, hydrogels offer versatile compatibility with antimicrobials, and elution profiles can be tuned and easily adjusted to patients' needs, but their clinical use is currently unexplored [13, 14]. In this work, we have unraveled the potential of microparticulate hydrogels for the treatment and prophylaxis of PJIs.

Hydrophobic surfaces might be a suitable substrate for bacterial colonization, while hydrophilic surfaces can prevent biofilm formation. Switching towards a hydrophilic microenvironment at the surface of the metallic prosthesis can be an optimal prophylactic approach to prevent bacterial adhesion and consequently biofilm formation. Hyaluronan coating has been demonstrated to change the hydrophobicity of an implant surface into a hydrophilic surface reducing significantly bacterial attachment [15].

Following this premise, we have developed a hyaluronic-based hydrogel that incorporates antimicrobial drugs in microparticulate systems to prolong drug release for one week. The sustained release provided by microparticles resulted in excellent biocompatibility with a significant reduction in haemotoxicity, especially with AmB which is highly haemolytic, but also no signs of toxicity were observed in osteoblasts and fibroblasts. Drug releases were performed mimicking the joint cavity with limited access to physiological fluids. Even with the slower release, the resulting antimicrobial concentration in aqueous media exhibited good antimicrobial activity, which indicated that the release rate was suitable to elicit a pharmacological effect at the joint space. It is worth noting that the combination of AmB and vancomycin within the same microparticulate carrier has shown to be a promising approach for PJIs targeting both bacterial and fungal infections with complementary hydrophilicity, amphiphilic for AmB and hydrophilic for vancomycin. This makes it feasible to prolong the release of vancomycin while enhancing the release of AmB. Even though further *in vivo* studies need to be performed to confirm the pharmacological-toxicological profile, in this work we have demonstrated for the first time a novel approach to treat and prevent PJIs. Currently, a variety of strategies for the treatment of periprosthetic joint infections (PJIs) are being actively developed, reflecting the growing need for innovative approaches to address this challenging clinical condition. Among these, 3D printing has garnered significant attention as an advanced fabrication technique due to its unparalleled ability to create highly customizable drug delivery systems tailored to individual patient needs. This technology allows for precise control over implant geometry, material composition, and drug loading, enabling the

development of solutions that are specifically designed to optimize therapeutic outcomes in diverse clinical scenarios.

To complement the goals of this research, a 3D-printed implant was developed as part of a multifaceted strategy for the treatment of prosthetic joint infections. The implant was specifically designed to serve as a localized drug delivery platform, capable of targeting the infection site with high precision while minimizing systemic exposure and associated side effects. AmB, as an antifungal agent, was selected for incorporation into the implant due to its broad-spectrum activity against fungal pathogens commonly implicated in PJIs, such as *Candida spp*. This choice reflects the increasing recognition of fungal infections as a complicating factor in PJIs, which can exacerbate treatment challenges and prolong recovery.

A critical aspect of the implant's design involved the selection of suitable polymeric materials. These materials were carefully chosen to meet stringent requirements for biodegradability and biocompatibility, ensuring that the implant would not only release the antifungal agent in a controlled and sustained manner but also degrade safely within the body without the need for surgical removal. This approach reduces the risk of additional surgical interventions and enhances patient comfort and compliance. Furthermore, the polymers have been chosen to provide mechanical stability, ensuring that the implant could integrate effectively into the surgical site while maintaining its structural integrity during the drug release period. The use of 3D printing in this context offers several additional advantages, including the potential to fabricate implants that are patient-specific, and tailored to the unique anatomical and pathological characteristics of the affected joint. This customization can improve the accuracy of drug delivery, enhance therapeutic efficacy, and reduce the likelihood of adverse effects. The versatility of 3D printing also allows for rapid prototyping and iteration, facilitating the optimization of implant designs based on experimental findings and clinical feedback.

Overall, the integration of 3D printing technology with advanced materials science and pharmacological expertise represents a cutting-edge approach to addressing the multifactorial challenges associated with PJIs. This research highlights the potential of 3D-printed implants not only as a treatment modality for existing infections but also as a prophylactic measure to prevent recurrence or microbial resistance, offering a significant step forward in the management of this kind of disease.

To our work, this represents the inaugural report of a 3D-printed personalized implant specifically designed to conform to the convex geometry of the acetabular component, capable of accommodating one or two combined different polymers and an antifungal agent. The 3D-printed implant was meticulously designed to promote osteointegration; thus, a bioinspired architecture was chosen instead of fully covering the acetabular surface. The applicability could be extrapolated to other arthroplasties. Considering the potential of 3D printing technology, innovative designs tailored to prosthesis morphology could be developed and fabricated by trained healthcare professionals.

The composition of the implant with EVA-PEG as excipients was carefully selected to ensure the biocompatibility of the formulation with the human body. EVA as a copolymer for 3D printing formulations is an interesting excipient, due to the characteristics it has such as easy extrudability and printability, versatility, and low glass transition temperature required to avoid AmB degradation temperature. In the pharmaceutical sector, the application of ethylene-vinyl acetate (EVA) polymer encompasses various uses, such as and subcutaneous implants, transdermal patches and, intrauterine devices [16-18]. However, previous studies showed that the EVA co-polymer composition affected the drug release rate so, this parameter could be tuned by the choice of different polymer grades available in the market [19, 20].

Furthermore, the AmB loading was superior to other implants developed with the 3D printed technique, loaded by other methods such as passive diffusion and different printing techniques [21, 22]

Although the release profile is incomplete, this may be due in part to the partial retention of amphotericin B (AmB) within the implant, as well as its degradation in aqueous environments. Nevertheless, it retains the efficacy, particularly against *C. albicans*, which is one of the primary strains responsible for fungal periprosthetic joint infections (PJIs) [23-25]**.**

References

1. Pablo Sanz-Ruiz, J.A.M.-D., Manuel Villanueva-Martínez, Alex Dos Santos-Vaquinha Blanco, Javier Vaquero., *Is Dual Antibiotic-Loaded Bone Cement More Effective and Cost-Efficient Than a Single Antibiotic-Loaded Bone Cement to Reduce the Risk of Prosthetic Joint Infection in Aseptic Revision Knee Arthroplasty?* The Journal of Arthroplasty 2020. **34**(12): p. 3724-3729.
2. Parvizi J, S.K., Ragland PS, Pour AE, Mont MA., *Efficacy of antibiotic-impregnated cement in total hip replacement.* Acta Orthop., 2008. **79**(3): p. 335-41.
3. Sanz-Ruiz, P., et al., *Is Dual Antibiotic-Loaded Bone Cement More Effective and Cost-Efficient Than a Single Antibiotic-Loaded Bone Cement to Reduce the Risk of Prosthetic Joint Infection in Aseptic Revision Knee Arthroplasty?* J Arthroplasty, 2020. **35**(12): p. 3724-3729.
4. Johnson, J.D., et al., *Serum and Wound Vancomycin Levels After Intrawound Administration in Primary Total Joint Arthroplasty.* J Arthroplasty, 2017. **32**(3): p. 924-928.
5. Steadman, W., et al., *Local Antibiotic Delivery Options in Prosthetic Joint Infection.* Antibiotics (Basel), 2023. **12**(4).
6. Anagnostakos, K. and C. Meyer, *Antibiotic Elution from Hip and Knee Acrylic Bone Cement Spacers: A Systematic Review.* Biomed Res Int, 2017. **2017**: p. 4657874.
7. Abosala, A. and M. Ali, *The Use of Calcium Sulphate beads in Periprosthetic Joint Infection, a systematic review.* J Bone Jt Infect, 2020. **5**(1): p. 43-49.
8. Tarar, M.Y., et al., *Wound Leakage With the Use of Calcium Sulphate Beads in Prosthetic Joint Surgeries: A Systematic Review*. Cureus, 2021. **13**(11): p. e19650.
9. Torrado, J.J., D.R. Serrano, and I.F. Uchegbu, *The oral delivery of amphotericin B.* Ther Deliv, 2013. **4**(1): p. 9-12.
10. Serrano, D. and A. Lalatsa, *Oral amphotericin B: The journey from bench to market.* Journal of Drug Delivery Science and Technology, 2017. **42**.
11. Goss, B., et al., *Elution and Mechanical Properties of Antifungal Bone Cement.* The Journal of arthroplasty, 2007. **22**: p. 902-8.

12. Ferry, T., et al., *Past and Future of Phage Therapy and Phage-Derived Proteins in Patients with Bone and Joint Infection.* Viruses, 2021. **13**(12).
13. Yuste, I., et al., *Engineering 3D-Printed Advanced Healthcare Materials for Periprosthetic Joint Infections.* Antibiotics (Basel), 2023. **12**(8).
14. Serrano, D.R., et al., *3D Printing Technologies in Personalized Medicine, Nanomedicines, and Biopharmaceuticals.* Pharmaceutics, 2023. **15**(2).
15. De Meo, D., et al., *Antibiotic-Loaded Hydrogel Coating to Reduce Early Postsurgical Infections in Aseptic Hip Revision Surgery: A Retrospective, Matched Case-Control Study.* Microorganisms, 2020. **8**(4).
16. Zhang, B. and S. CHEMIST, *Potential Use of Ethylene Vinyl Acetate Copolymer Excipient in Oral Controlled Release Applications: A Literature Review.* 2015.
17. Samaro, A., et al., *Can filaments, pellets and powder be used as feedstock to produce highly drug-loaded ethylene-vinyl acetate 3D printed tablets using extrusion-based additive manufacturing?* International Journal of Pharmaceutics, 2021. **607**: p. 120922.
18. Schneider, C., et al., *Applications of ethylene vinyl acetate copolymers (EVA) in drug delivery systems.* Journal of Controlled Release, 2017. **262**: p. 284-295.
19. Tallury, P., N. Alimohammadi, and S. Kalachandra, *Poly(ethylene-co-vinyl acetate) copolymer matrix for delivery of chlorhexidine and acyclovir drugs for use in the oral environment: Effect of drug combination, copolymer composition and coating on the drug release rate.* Dental Materials, 2007. **23**(4): p. 404-409.
20. Shin, S.-C. and H.-J. Lee, *Controlled release of triprolidine using ethylene-vinyl acetate membrane and matrix systems.* European Journal of Pharmaceutics and Biopharmaceutics, 2002. **54**(2): p. 201-206.
21. Yuste, I., et al., *Engineering 3D-Printed Advanced Healthcare Materials for Periprosthetic Joint Infections.* 2023. **12**(8): p. 1229.
22. Domsta, V. and A. Seidlitz, *3D-Printing of Drug-Eluting Implants: An Overview of the Current Developments Described in the Literature.* Molecules, 2021. **26**(13).
23. Lalremruata, R., *Prosthetic joint infection: A microbiological review.* 2015. **29**(3): p. 120-128.
24. Merrer, J., et al., *Candida albicans Prosthetic Arthritis Treated with Fluconazole Alone.* Journal of Infection, 2001. **42**(3): p. 208-209.

25. Grzelecki, D., et al., *Periprosthetic Joint Infections Caused by Candida Species-A Single-Center Experience and Systematic Review of the Literature.* J Fungi (Basel), 2022. **8**(8).

Discusión

El objetivo de esta Tesis Doctoral ha sido el desarrollo y la optimización de sistemas de liberación de fármacos que ofrezcan propiedades de liberación controlada o sostenida, con un enfoque específico en abordar necesidades clínicas no satisfechas en el manejo de las infecciones articulares periprotésicas (PJIs). Estas infecciones representan una complicación grave en las cirugías ortopédicas, que a menudo conllevan tiempos prolongados de tratamiento, mayor morbilidad en los pacientes y un incremento significativo en los costes de atención médica. Para abordar esta problemática, el trabajo se centró en dos sistemas de liberación de fármacos distintos: (i) micropartículas que encapsulan principios activos diseñadas para formar un gel bioadhesivo y su posterior aplicación sobre las prótesis y (ii) un implante parenteral impreso en 3D, también cargado con un agente antimicrobiano, como anfotericina B (AmB) como antifúngico. Ambos sistemas están diseñados para su aplicación directa, *in situ*, durante los procedimientos quirúrgicos, teniendo como principal objetivo el tratamiento y la profilaxis de las infecciones de prótesis articulares.

El diseño y la optimización de estos sistemas de liberación controlada se realizaron en base a varios factores críticos inherentes a los desafíos del manejo de las infecciones articulares periprotésicas. Los tratamientos sistémicos convencionales a menudo no logran alcanzar concentraciones terapéuticas adecuadas en el sitio de infección y, además, están asociados con toxicidad sistémica y otros efectos secundarios. Además, la capacidad de prevenir o eliminar los biofilms microbianos, es un factor clave en el desarrollo y resistencia de las PJIs, requiriendo la administración localizada de agentes antimicrobianos en altas concentraciones y de manera controlada. Por lo tanto, los sistemas desarrollados se diseñaron con características clave como biocompatibilidad, para garantizar la compatibilidad con los tejidos del huésped, biodegradabilidad, para evitar la necesidad de extracción quirúrgica tras la liberación del fármaco; y un control preciso sobre las cinéticas de liberación, asegurando un efecto terapéutico sostenido mientras se minimizan los posibles efectos tóxicos relacionados con el fármaco.

El primer sistema, son unas micropartículas matriciales que encapsulan los principios activos y forman un gel bioadhesivo tras su reconstitución con medio fisiológico. Estas fueron desarrolladas para proporcionar un medio flexible y adaptable para la

administración de antimicrobianos directamente en el sitio afectado de la articulación. Las propiedades bioadhesivas del gel aseguran una retención prolongada en el sitio de aplicación, lo que mejora la concentración local del fármaco durante un período extendido. El segundo sistema, un implante impreso en 3D, representa un enfoque innovador para la liberación de fármacos, ofreciendo personalizar la geometría del implante, la carga de fármaco y los perfiles de liberación. Este implante fue diseñado específicamente para liberar antimicrobianos de manera sostenida y localizada, reduciendo el riesgo de recurrencia de infecciones, mientras proporciona una estructura que puede integrarse en el entorno quirúrgico.

En el desarrollo de estos sistemas, se prestó una considerable atención a la optimización de sus propiedades físicas, químicas y biológicas para garantizar su eficacia y seguridad clínica. Esto incluyó una completa caracterización *in vitro* de los perfiles de liberación de fármacos, la realización tanto de los ensayos de actividad antimicrobiana para confirmar la eficacia frente a patógenos relevantes como las pruebas preliminares de biocompatibilidad. Los resultados de estos sistemas, detallados en las publicaciones correspondientes, demuestran un gran potencial para su aplicación en entornos clínicos. Estos hallazgos, junto con sus implicaciones para el tratamiento futuro de las infecciones de articulaciones prostéticas y el campo más amplio de la liberación localizada de fármacos, serán discutidos en detalle en la presente sección de esta tesis.

La infección periprotésica de la articulación, es una de las complicaciones más abrumadoras tras una cirugía de artroplastia, aumentando significativamente los costes del sistema de salud, el tiempo de tratamiento y el riesgo de morbilidad y mortalidad. Aunque las comorbilidades como la inmunosupresión, la diabetes, el índice de masa corporal elevado, entre otras, pueden aumentar el riesgo de PJI, el riesgo asociado con los tiempos prolongados de operación es el más elevado [1]. Basado en esto, la profilaxis es una herramienta esencial contra este problema y podría reducir significativamente el riesgo de complicaciones [2]. Los patrones poblacionales, en países desarrollados indican un aumento proyectado en la incidencia de procedimientos quirúrgicos de reemplazo articular, particularmente entre pacientes con diversas comorbilidades. Esto subraya la necesidad urgente de desarrollar nuevas estrategias para abordar las infecciones periprotésicas [3].

La administración directa de antibióticos en el sitio quirúrgico en forma de polvo o solución ha sido estudiada como profilaxis para la infección periprotésica de la articulación (PJI) en reemplazos articulares primarios y se ha comprobado que, aunque los niveles locales son elevados durante las primeras horas postquirúrgicas, se produce una rápida disminución de los mismos, que da lugar a concentraciones subterapéuticas, lo que convierte esta solución en una opción clínica sencilla, pero con un resultado poco útil [4]. Para mantener una alta concentración local con exposición sistémica limitada, los antimicrobianos pueden administrarse a través de un catéter intraarticular o combinarse con un transportador para mejorar su perfil farmacocinético y farmacológico [5]. Las opciones de transportadores incluyen cemento óseo no reabsorbible de polimetilmetacrilato (PMMA) y como sulfato de calcio, hidroxiapatita, vidrio bioactivo e hidrogeles. El PMMA permite la formación de espaciadores estructurales utilizados en procedimientos de revisión multietapa, pero requiere una extracción posterior y presenta una compatibilidad variable con antibióticos y una liberación insuficiente de fármacos para alcanzar niveles farmacológicos. Además, la fase de liberación prolongada puede extenderse durante varios meses a años, lo que potencialmente conduce a la resistencia microbiana [6]. El sulfato de calcio es uno de los transportadores más investigados y biocompatibles para las PJI, el cual puede moldearse en esferas para adaptarse a diversas aplicaciones clínicas y libera el 100 % de los fármacos antimicrobianos cargados durante varias semanas [7]. Sin embargo, su uso está asociado con fugas en la herida e hipercalcemia, siendo la evidencia clínica sobre su efectividad aún incipiente [8].

Actualmente, no existe un consenso respecto a la dosificación óptima de AmB que debe combinarse con PMMA para un tratamiento local efectivo de las PJIs. Dado que la mayoría de las PJIs son causadas por bacterias, la experiencia con agentes antifúngicos en este contexto es limitada. La AmB ejerce su efecto antifúngico uniéndose al ergosterol de la membrana plasmática de las células fúngicas, induciendo la apoptosis. Aunque es un agente altamente efectivo, la dosis intravenosa sistémica recomendada se limita a 1 mg/kg cuando se utiliza Fungizona® y a 5 mg/kg para las formulaciones comerciales de AmBisome®. Algunos autores han reportado una liberación notablemente baja de AmB a partir del cemento óseo, siendo sólo liberándose un 0.03% después de una semana [9-11].

El uso de bacteriófagos puede ser un recurso adecuado, ya que están específicamente dirigidos a bacterias sin toxicidad para las células mamíferas. Sin embargo, se requiere

contar con reservas de fagos para dirigirse a diferentes especies bacterianas, y su uso actual para las PJI es limitado [12]. Finalmente, los hidrogeles ofrecen una compatibilidad versátil con antimicrobianos y pueden ajustarse fácilmente a las necesidades de los pacientes, pero su uso clínico aún no ha sido investigado [13, 14]. En este trabajo, hemos desentrañado el potencial de los hidrogeles microparticulados para el tratamiento y la profilaxis de las infecciones periprotésicas de la articulación.

Las superficies hidrófobas podrían ser un sustrato adecuado para la colonización bacteriana, mientras que las superficies hidrofílicas pueden prevenir la formación de biofilm. Cambiar hacia un microentorno hidrofílico en la superficie de la prótesis metálica puede ser un enfoque profiláctico óptimo para prevenir la adhesión bacteriana y, en consecuencia, la formación de biofilm. Se ha demostrado que el recubrimiento de hialuronato cambia la hidrofobicidad de la superficie de un implante a una superficie hidrofílica, reduciendo significativamente la adhesión bacteriana [15].

Siguiendo esta premisa, hemos desarrollado un hidrogel basado en hialuronato que incorpora fármacos antimicrobianos en sistemas de micropartículas para prolongar la liberación del fármaco durante una semana. La liberación sostenida proporcionada por las micropartículas resultó en una excelente biocompatibilidad con una reducción significativa de la hemotoxicidad, especialmente con AmB, que es altamente hemolítica, y tampoco se observaron signos de toxicidad en osteoblastos y fibroblastos. Los estudios de liberación de fármacos se realizaron simulando la cavidad articular y con acceso limitado a fluidos fisiológicos. A pesar de que la liberación es más lenta, la concentración antimicrobiana resultante en medios acuosos se mantuvo por encima de la concentración mínima inhibitoria de las cepas probadas, lo que indicó que la tasa de liberación era adecuada para provocar un efecto farmacológico en el espacio articular. Cabe destacar que la combinación de AmB y vancomicina dentro del mismo transportador (las micropartículas) ha demostrado ser un recurso prometedor para las PJI, dirigido tanto a infecciones bacterianas como fúngicas, con una hidrofobicidad complementaria, anfifílica para AmB e hidrofílica para vancomicina. Esto hace viable prolongar la liberación de vancomicina mientras se mejora la liberación de AmB. Sin embargo, se deben realizar más estudios *in vivo* para confirmar el perfil farmacológico-toxicológico; Actualmente, se están desarrollando estrategias para el tratamiento de las infecciones periprotésicas de

la articulación, lo que refleja la creciente necesidad de enfoques innovadores para abordar esta desafiante condición clínica. Entre éstas, la impresión 3D ha generado una atención significativa como una técnica avanzada de fabricación debido a su capacidad inigualable para crear sistemas de liberación de fármacos altamente personalizables adaptados a las necesidades individuales de los pacientes. Esta tecnología permite un control preciso sobre la geometría del implante, la composición del material y la carga del fármaco, lo que posibilita el desarrollo de soluciones diseñadas específicamente para optimizar los resultados terapéuticos en diversos escenarios clínicos.

Para complementar los objetivos de esta investigación, se desarrolló un implante impreso en 3D como parte de una estrategia innovadora para el tratamiento de las infecciones de articulaciones protésicas. El implante fue diseñado específicamente para servir como un sistema de liberación localizada de fármacos, capaz de dirigirse al sitio de la infección con alta precisión, mientras minimiza la exposición sistémica y los efectos secundarios asociados. Se seleccionó la anfotericina B, como agente antifúngico, para su incorporación en el implante debido a su actividad de amplio espectro contra patógenos fúngicos comúnmente implicados en las PJI, como *Candida spp.* Esta elección refleja el creciente reconocimiento de las infecciones fúngicas como un factor considerable en las PJI, lo que puede agravar los desafíos del tratamiento y prolongar la recuperación.

Un aspecto crítico del diseño del implante es la selección de materiales poliméricos adecuados, elegidos cuidadosamente para cumplir con requisitos estrictos de biodegradabilidad y biocompatibilidad, asegurando que el implante no solo liberará el agente antifúngico de manera controlada y sostenida, sino que también se degradará de forma segura dentro del cuerpo sin necesidad de extracción quirúrgica. Esta opción reduce el riesgo de intervenciones quirúrgicas adicionales y mejora la comodidad y la adherencia del paciente. Además, los polímeros seleccionados proporcionan estabilidad mecánica, asegurando que el implante pueda integrarse eficazmente, en el sitio quirúrgico, mientras mantiene su integridad estructural durante el período de liberación del fármaco. El uso de la impresión 3D en este contexto ofrece varias ventajas adicionales, como la posibilidad de fabricar implantes específicos para cada paciente, adaptados a las características anatómicas y patológicas de la articulación afectada. Esta personalización puede mejorar la precisión de la administración del fármaco, aumentar la eficacia terapéutica y reducir

la probabilidad de efectos adversos. La versatilidad de la impresión 3D también permite la creación rápida de prototipos, facilitando la optimización del diseño de los implantes basado en hallazgos experimentales.

En general, la integración de la tecnología de impresión 3D con la ciencia de materiales avanzados y la experiencia farmacológica representa un recurso de vanguardia para abordar los desafíos multifactoriales asociados con las PJIs. Esta investigación destaca el potencial de los implantes impresos en 3D no solo como una modalidad de tratamiento para infecciones existentes, sino también como una medida profiláctica para prevenir la recurrencia o la resistencia microbiana, lo que representa un avance significativo en el manejo de este tipo de enfermedades. En ella se propone un implante personalizado impreso en 3D, diseñado específicamente para adaptarse a la geometría cóncava del componente acetabular, capaz de contener uno o dos polímeros diferentes combinados y un agente antifúngico. El implante impreso en 3D fue meticulosamente diseñado para promover la osteointegración por lo que, se eligió un diseño con en forma de malla en lugar de cubrir completamente la superficie acetabular. La aplicabilidad de este enfoque podría extrapolarse a otros reemplazos de artroplastia.

Se seleccionó la composición del implante, con EVA-PEG como excipientes, para garantizar la biocompatibilidad de la formulación con el cuerpo humano. El EVA, como copolímero para formulaciones de impresión 3D, es un excipiente interesante debido a sus características, como la facilidad de extrusión e impresión sin necesidad de plastificantes, su versatilidad y su baja temperatura de transición vítrea, lo cual es crucial para no sobrepasar la temperatura de degradación de la AmB. En el sector farmacéutico, la aplicación del polímero etileno-vinil-acetato (EVA) abarca diversos usos, como implantes subcutáneos, parches transdérmicos y dispositivos intrauterinos [16-18]. Sin embargo, estudios previos han demostrado que la composición del copolímero de EVA afecta la tasa de liberación del fármaco, por lo que este parámetro podría ajustarse mediante la elección de diferentes variedades del polímero disponibles en el mercado con diferentes ratios de sus copolímeros [19, 20].

Además, la carga del fármaco de AmB fue superior a la de otros implantes desarrollados con la técnica de impresión 3D, cargados mediante otros métodos como la difusión pasiva y diferentes técnicas de impresión [21, 22]. Aunque el perfil de liberación es incompleto,

esto puede deberse en parte a la retención parcial de la AmB dentro del implante, así como a su degradación en ambientes acuosos. No obstante, sigue siendo efectivo, particularmente contra *C. albicans*, que es una de las cepas principales responsables de las infecciones fúngicas periprotésicas de la articulación (PJI) [23-25]

Referencias

1. Pablo Sanz-Ruiz, J.A.M.-D., Manuel Villanueva-Martínez, Alex Dos Santos-Vaquinha Blanco, Javier Vaquero., *Is Dual Antibiotic-Loaded Bone Cement More Effective and Cost-Efficient Than a Single Antibiotic-Loaded Bone Cement to Reduce the Risk of Prosthetic Joint Infection in Aseptic Revision Knee Arthroplasty?* The Journal of Arthroplasty 2020. **34**(12): p. 3724-3729.
2. Parvizi J, S.K., Ragland PS, Pour AE, Mont MA., *Efficacy of antibiotic-impregnated cement in total hip replacement.* Acta Orthop., 2008. **79**(3): p. 335-41.
3. Sanz-Ruiz, P., et al., *Is Dual Antibiotic-Loaded Bone Cement More Effective and Cost-Efficient Than a Single Antibiotic-Loaded Bone Cement to Reduce the Risk of Prosthetic Joint Infection in Aseptic Revision Knee Arthroplasty?* J Arthroplasty, 2020. **35**(12): p. 3724-3729.
4. Johnson, J.D., et al., *Serum and Wound Vancomycin Levels After Intrawound Administration in Primary Total Joint Arthroplasty.* J Arthroplasty, 2017. **32**(3): p. 924-928.
5. Steadman, W., et al., *Local Antibiotic Delivery Options in Prosthetic Joint Infection.* Antibiotics (Basel), 2023. **12**(4).
6. Anagnostakos, K. and C. Meyer, *Antibiotic Elution from Hip and Knee Acrylic Bone Cement Spacers: A Systematic Review.* Biomed Res Int, 2017. **2017**: p. 4657874.
7. Abosala, A. and M. Ali, *The Use of Calcium Sulphate beads in Periprosthetic Joint Infection, a systematic review.* J Bone Jt Infect, 2020. **5**(1): p. 43-49.
8. Tarar, M.Y., et al., *Wound Leakage With the Use of Calcium Sulphate Beads in Prosthetic Joint Surgeries: A Systematic Review.* Cureus, 2021. **13**(11): p. e19650.
9. Torrado, J.J., D.R. Serrano, and I.F. Uchegbu, *The oral delivery of amphotericin B.* Ther Deliv, 2013. **4**(1): p. 9-12.
10. Serrano, D. and A. Lalatsa, *Oral amphotericin B: The journey from bench to market.* Journal of Drug Delivery Science and Technology, 2017. **42**.
11. Goss, B., et al., *Elution and Mechanical Properties of Antifungal Bone Cement.* The Journal of arthroplasty, 2007. **22**: p. 902-8.
12. Ferry, T., et al., *Past and Future of Phage Therapy and Phage-Derived Proteins in Patients with Bone and Joint Infection.* Viruses, 2021. **13**(12).

13. Yuste, I., et al., *Engineering 3D-Printed Advanced Healthcare Materials for Periprosthetic Joint Infections.* Antibiotics (Basel), 2023. **12**(8).
14. Serrano, D.R., et al., *3D Printing Technologies in Personalized Medicine, Nanomedicines, and Biopharmaceuticals.* Pharmaceutics, 2023. **15**(2).
15. De Meo, D., et al., *Antibiotic-Loaded Hydrogel Coating to Reduce Early Postsurgical Infections in Aseptic Hip Revision Surgery: A Retrospective, Matched Case-Control Study.* Microorganisms, 2020. **8**(4).
16. Zhang, B. and S. CHEMIST, *Potential Use of Ethylene Vinyl Acetate Copolymer Excipient in Oral Controlled Release Applications: A Literature Review.* 2015.
17. Samaro, A., et al., *Can filaments, pellets and powder be used as feedstock to produce highly drug-loaded ethylene-vinyl acetate 3D printed tablets using extrusion-based additive manufacturing?* International Journal of Pharmaceutics, 2021. **607**: p. 120922.
18. Schneider, C., et al., *Applications of ethylene vinyl acetate copolymers (EVA) in drug delivery systems.* Journal of Controlled Release, 2017. **262**: p. 284-295.
19. Tallury, P., N. Alimohammadi, and S. Kalachandra, *Poly(ethylene-co-vinyl acetate) copolymer matrix for delivery of chlorhexidine and acyclovir drugs for use in the oral environment: Effect of drug combination, copolymer composition and coating on the drug release rate.* Dental Materials, 2007. **23**(4): p. 404-409.
20. Shin, S.-C. and H.-J. Lee, *Controlled release of triprolidine using ethylene-vinyl acetate membrane and matrix systems.* European Journal of Pharmaceutics and Biopharmaceutics, 2002. **54**(2): p. 201-206.
21. Yuste, I., et al., *Engineering 3D-Printed Advanced Healthcare Materials for Periprosthetic Joint Infections.* 2023. **12**(8): p. 1229.
22. Domsta, V. and A. Seidlitz, *3D-Printing of Drug-Eluting Implants: An Overview of the Current Developments Described in the Literature.* Molecules, 2021. **26**(13).
23. Lalremruata, R., *Prosthetic joint infection: A microbiological review.* 2015. **29**(3): p. 120-128.
24. Merrer, J., et al., *Candida albicans Prosthetic Arthritis Treated with Fluconazole Alone.* Journal of Infection, 2001. **42**(3): p. 208-209.

25. Grzelecki, D., et al., *Periprosthetic Joint Infections Caused by Candida Species-A Single-Center Experience and Systematic Review of the Literature.* J Fungi (Basel), 2022. **8**(8).

Conclusiones/Conclusions

Conclusiones

1. Las micropartículas cargadas con AmB y vancomicina fueron biocompatibles sin causar toxicidad hemolítica ni en céulas óseas de líneas celulares humanas (Saos-2, hFOBs y BJ) incluso a las dosis más altas y con un efecto antibiótico y antifúngico significativo frente a diversas especies de *Staphylococcus* spp. y *Candida* spp.
2. Las micropartículas mostraron un óptimo perfil de liberación, tanto cargadas con los fármacos de forma individual o combinados, manteniendo la liberación durante 7 días lo que es necesario para el tratamiento de las PJIs.
3. El gel bioadhesivo formado por las micropartículas, mostro una buena adhesión a la superficie protésica, con un tiempo de secado de aproximadamente 5 min, evitando así una prolongación del tiempo quirúrgico.
4. La técnica de impresión 3D de extrusión directa permitió producir implantes con EVA-PEG cargados con AmB de manera reproducible, siendo una técnica extrapolable al uso en hospitales. La composición del implante fue cuidadosamente seleccionada para garantizar la biocompatibilidad en el espacio osteoarticular (glóbulos rojos, osteoblastos y fibroblastos) manteniendo una excelente eficacia antifúngica frente a *C. albicans*.
5. El perfil de liberación del implante impreso en 3D cargado con AmB tuvo una liberación dual caracterizada por presentar un perfil más rápido durante las primeras 10 h seguido de una liberación sostenida durante más de 5 días.

Conclusions

1. The microparticles loaded with AmB and vancomycin were biocompatible, not causing hemolytic toxicity either in human cell lines (Saos-2, hFOBs, and BJ) even at the highest dose tested while exhibiting significant antibiotic and antifungal effects against various species of *Staphylococcus spp.* and *Candida spp*.
2. The microparticles demonstrated an optimal release profile, both when loaded with the drugs individually or in combination, maintaining sustained release for 7 days, which is necessary for the treatment of PJIs.
3. The bioadhesive gel formed by the microparticles showed good adhesion to the prosthetic surface, with a drying time of approximately 5 minutes, thus preventing prolonged surgical time.
4. The direct extrusion 3D printing technique enabled the reproducible production of EVA-PEG implants loaded with AmB, a technique that is clinically transferable for use in hospitals. The implant composition was carefully selected to ensure biocompatibility in the osteoarticular space (red blood cells, osteoblasts, and fibroblasts) while maintaining excellent antifungal efficacy against *C. albicans*.
5. The release profile of the 3D-printed implant loaded with AmB exhibited a dual release pattern, characterized by a faster release during the first 10 hours, followed by a sustained release for more than 5 days